



EST 1892

**London
South Bank
University**

PhD in Electrical & Electronic Engineering

Final Dissertation

School of Engineering and Design

London South Bank University

**Analysing integrated renewable energy and smart-grid
systems to improve voltage quality and harmonic
distortion losses at electric-vehicle charging stations**

By
Asif Khan

February 2019

Abstract

Due to environmental impacts of fossil fuels, a move towards using Electric-Vehicles (EV) to reduce carbon emissions and fossil fuels is regarded as a good solution to the climate change problem. In recent years, a dramatic increase of EV and charging stations has raised voltage quality and harmonic distortion issues that are affecting the electrical grid network. To address these issues there is a need to redesign the integrated renewable energy and smart grid network by applying new methodologies. The aim of this work is to propose an isolated smart micro grid, which connects renewable energy generation units to the electric vehicles charging station without degrading voltage quality or causing harmonic distortion losses. A topology has been identified for the smart grid that is simulated with the intention of implementing it with the integration of modern communication technologies that enables the components to produce and reflect data in an efficient way to assist better regulation in the power flow. The power flow is investigated by simulating unpredictable renewable energy and by using car batteries at the electric vehicle charging station. It is investigated how micro grid parameters are affected in the presence of super capacitors, car batteries and the use of larger power electronic converters. In the simulations, an electrical power control system is implemented at power conversion units which generates the correct duty cycle of the converter switches and controls the power flow operation at the smart grid. Then the proposed electrical power control system is compared with other systems such as maximum power point tracking (MPPT) algorithm and space vector pulse width modulation (SVPWM). A smart sensor system and smart protection are connected to protect the grid and to maintain system stability over a long time. The research focuses on developing a smart grid that performs the communication among the converters, performs power sharing, and does preventive management. It also monitors the energy efficiently and balances the energy in the grid irrespective of load or power generation variations. A mathematical model is developed to predict grid behaviour and is validated via MATLAB simulation of the grid. It is noticed that an improvement is made in the efficiency of renewable energy transmission to the electric-vehicle charging station.

Acknowledgment

It is very difficult to express my feeling in words for everyone who assisted me during the research period and completion of the thesis.

First of all, I want to thank Professor Tariq Sattar, Dr Saim Memon for loads of sincere guidance and help throughout the PhD period and giving me opportunity to conduct the research work in a better environment. You have always guided me appropriately and provided me all the opportunities to improve my research work. I believe that you are the best supervisors/researchers student can ever have and a good person whom everyone can believe and trust. Your nice suggestions have boosted my technical skills and improved the quality of my research work. A big thank to both of you and I wish you a best time for the future and want to continue working with you for many years.

I would like to thank Professor Hari Reehal for accepting me as a PhD student and assistance to complete the PhD. At the same time, I would to thank the research management team John Harper, Louise Thomas, Dr Sandra for processing my reports and guidance to enhance research skill. I specially want to thank John Harper for always replying to my queries in the best manner that saved my time and motivated me towards the research work.

I am thankful to all of you for your suggestions and comments on my reports that helped me to improve my research in general and increased the quality of my research papers. I am looking forward to continue the research cooperation in the future.

I would like thank my research colleagues Ousmane oumar, Riduan, who are conducting the research in the same lab as me T415 for always supporting me and giving the useful information during the three years research period.

Table of contents

Contents

Chapter 1.....	10
1.1 Introduction	10
1.2 Aims and Objectives	11
1.3 Literature Review	11
1.4 Research Methodology.....	16
1.5 Contribution to knowledge.....	23
1.6 Journal and Conference publications	25
1.7 Thesis outline.....	25
Chapter 2 Voltage and frequency instabilities of renewable energy sources	27
2.1 Testing and evaluation of energy generation at changing Pitch Angle.....	28
2.2 Simulation and analysis of doubly fed induction generator.....	30
2.3 System testing by applying permanent magnet synchronous generator	32
2.4 Factors creating instability issues in wind energy generation units	35
2.5 Modern techniques to minimise instability issues.....	40
2.6 Solar Farm.....	42
2.7 Case Study: Solar energy system in Pakistan.....	43
2.7.1 Overview of energy generation system in Pakistan	44
2.7.2 Model of a monocrystalline Photovoltaic (PV) system	46
2.7.3 Temperatures across Pakistan.....	48
2.7.4 Simulation results from the model and discussion.....	50
2.7.5 Comparative analysis of PV integrated buildings in different regions of Pakistan	60
Chapter 3 Architecture of a proposed smart microgrid.....	63
3.1 DC Power implementation with Analysis	64
3.2 Smart grid modelling and validation.....	64
3.3.1 Smart grid system description	65
3.3.2 List of power conversion stations connected to the grid terminals	66
3.3 Risk handling features of the smart grid.....	68
3.4 Modelling of Smart grid decision procedures	69
3.5 DC centralised unit implementation on the smart grid	70
3.6 Smart grid protection system simulation and analysis	71

3.7 Simulation results and transient responses on the smart grid.....	73
Summary	76
Chapter 4 Energy conversion and applied control techniques	77
4.1 MOSFET/IGBT.....	77
4.2 Power conversion system.....	78
4.2.1 Modelling and simulation of Boost Energy Convertors	79
4.2.2 Implementation of buck energy converter	81
4.2.3 Modelling and simulation results of buck-boost energy conversion system	82
4.2.4 AC-DC VSC based energy conversion system	83
4.3 Modelling and validation of voltage regulation and control	84
4.4 Voltage flow stability and control comparison with the other methods	87
4.5 MPPT based Control algorithm	91
4.5.1 Perturb and Observe Method control strategy.....	92
4.5.2 Incremental Conductance based control system implementation.....	96
4.5.3 Fix Duty Cycle (FDC) implementation and analysis	99
4.6 Energy control investigation by using Space Vector Pulse Width Modulation (SVPWM)	101
4.7 Simulation Results and analysis.....	106
Summary	108
Chapter 5 Connection of Electric Vehicle Charging Station and Battery Storage to Smart Grid	110
5.1 Features of implemented electric-vehicle charging terminal	115
5.2 Optimal design and energy management at the electric-vehicle charging station	117
5.2.1 Condition 1 best case scenario.....	117
5.2.2 Condition 2 worst case Scenario.....	118
5.3 Electric-vehicles charging station characteristics	120
5.4 Future implementaiton of ultra/super capacitors in Electric/hybrid vehicles.....	121
Summary	122
Chapter 6 Conclusion and Future Work.....	123
Conclusion.....	124
FUTURE WORK.....	125
References.....	126

Table of Figures

Fig.1-1: The reduction of coal import in the UK. Total demand of importation of coal was reduced by 47 percent in first quarter of 2016 compared to the first quarter of 2015 [16]	12
Fig.1-2: Plug-in electric vehicles, hybrid electric vehicles and probability of the increase in numbers of electric vehicles in the UK from 2010 to 2030 [17].	13
Fig.1-3: The vehicle charging from the AC grid and DC grid. It demonstrates the reduction of charging time from the DC grid compared to AC grid [18].	14
Fig.1-4: The renewable energy flow to the smart micro grid and way of electronic communication between them. It also demonstrates the injection of power on the network from several power generation resources such as wind turbine, photovoltaic panels and energy storage system [20]	15
Fig.1-5: A schematic diagram of the integrated smart model consisting of Wind Generator (WG), Photovoltaic (PV) system, Energy Storage system, Electric Vehicle (EV) charging station, and other micro grid related components	18
Fig.1-6: Block diagram of power conversion system connected to micro grid.....	20
Fig.1-7: The block diagram of applied control system to achieve voltage regulation. Pin is the energy input from the wind and solar energy	21
Fig.1-8: Block diagram shows a programmable power protection system implemented at the micro grid.....	21
Fig.1-9: Charging time reduction between the AC grid (3kWh and 11kWh) and the DC grid.	22
Fig.1-10: Charging station terminal features	23
Fig.2-1: Wind generator with time in second and wind speed m/s	28
Fig.2-2: Simulation of applied wind speed to generate electrical energy.	28
Fig.2-3: Examining of the wind turbine energy generation features by the variation in blade pitch angle. Output values are in degrees and time in second.....	29
Fig.2-4: Simulation of variable blade pitch angle.....	29
Fig.2-5: Wind turbine generator Simulink model and an algorithm to compare the set wind speed with reference rotor speed.....	31
Fig.2-6: DFIG used to generate electrical energy and connected to grid via converters.....	31
Fig.2-7 : Constant and regulated voltage is received from DFIG. The three sinusoidal plots are the three phase voltage.	32
Fig.2-8: PMSG based wind Turbine.....	33
Fig. 2-9: Three phase output voltage at the varying wind speed. Severe variations in voltage are observed.....	34
Fig.2-10: Voltage variations at varying wind speed.....	34
Fig.2-11: Voltage output from three phase power PMSG.....	35
Fig.2-12: Frequency instability creates severe voltage variations in the system.....	37
Fig.2-13: Synchronisation issues between wind turbines.....	37
Fig.2-14: Energy generation produced by the synchronous generator at varying wind speed.	38
Fig.2-15: System Overshoot due to synchronisation and frequency instability	39
Fig.2-16: Rotor angle instability in the wind turbines	40
Fig. 2-17: Instability issues at the start up process of a wind energy generation system due to load variations.....	41
Fig.2-18: Simulation of the solar system that is used to generate electrical energy	42
Fig.2-19: Shows the power generation by the solar system. From 9pm-5am no power is generated therefore a storage system and fuel generator will meet the energy demand at this time	43
Fig.2-20. Pakistan annual direct solar radiations (Abdullah et al. 2017).....	45

Fig.2-21: illustrates the schematic model of the solar system. The measurements are used to examine the output at different temperatures.	47
Fig.2-22: (a) Shows the temperature in Southern region of Pakistan (b) Temperature analysis in North East of Pakistan (c) Temperature found in Eastern areas of Pakistan (d) Temperature analysis in North West Pakistan (e) Temperature forecast in Western region of Pakistan.	49
Fig.2-23: (a) Illustrates temperature effects on the voltage (b) Temperature vs solar system electrical power (c) Output current variations at different temperature.	52
Fig.2-24: Shows the model of the simulated solar system tested at 25°C, this system is also tested at different temperatures. 100Wh resistive/inductive loads are used to measure the efficiency of the system.	53
Fig.2-25: (a) Shows temperature effects on the PV structure in peak winter day in Eastern Pakistan. (b) Peak summer day analysis in eastern Pakistan.	55
Fig.2-26: (a) Temperature effect on the solar power in Quetta on the hottest day, West Pakistan. The voltage/efficiency is reduced during both seasons. (b) Peak winter day power generation	56
Fig.2-27: (a) The efficiency of power/voltage generation at the peak winter day temperature - PV structure in the southern region of Pakistan. (b) Peak hottest day: power drops at the PV module are increased	58
Fig.2-28: (a) Power generation from the solar system in Gilgit, North Pakistan in the winter season. During this time, the PV module is generating power/voltage efficiently and better than the rest of Pakistan. (b) Power analysis on the hottest day of 30 June	59
Fig.2-29: (a) Module efficiency analysis for the peak winter day. (b) Efficiency analysis during the summer day	61
Fig.2-30: Average solar power generation on two days, irradiance of 1000 W/m ² between 5am-9pm and 0 W/m ² for from 9am-5pm. Nominal power generation capacity of the solar panel is 100. It is reduced to (53-56) % due to temperature and irradiance effects	61
Fig.3-1: Block diagram of the integrated smart grid consisting of wind/solar photovoltaic (PV) system, storage system and Electric Vehicle (EV) charging station.	66
Fig.3-2: Voltage regulation on the micro grid.	68
Fig.3-3: The internal structure of the protection used to protect the micro grid	73
Fig.3-4: Voltage transients due switching ON/OFF of the wind turbine and solar units by changes wind and sun light	74
Fig.3-5: Observations of current flow in the micro grid	75
Fig.4-1: Insulated gate bipolar transistor (IGBT) used to convert electrical energy	78
Fig.4-2: Boost Converter used to convert the DC/DC power	80
Fig.4-3: Simulation of Buck converter at the electric-vehicle charging station	81
Fig.4-4: Simulation of Buck-Boost converter at the microgrid station	83
Fig.4-5: Three phase voltage to DC voltage rectification	84
Fig.4-6: Closed loop feedback control system for the converter sections for voltage regulation.	85
Fig.4-7: Grid voltage with several applied control algorithms	90
Fig.4-8: Maximum power point to regulate voltage and extract maximum power from the solar system	91
Fig.4-9: Perturb and observe method to regulate the voltage on the microgrid.	92
Fig.4-10: Perturb and Observe algorithm	93
Fig.4-11: Oscillations in voltage observed by implementing P and O method.....	93
Fig.4-12: Voltage on the smart grid by the implementation of Perturb and Observe method.....	95
Fig.4-13: Simulation of Incremental Conductance with integrator.....	97
Fig.4-14: Incremental Conductance algorithm.	98

Fig.4-15: Voltage output by using the Incremental Conductance technique	99
Fig.4-16: Simulation of Fixed Duty Cycle (FDC) applied to the buck converter system.	100
Fig.4-17: Voltage achieved by using the Fixed Duty Cycle.	100
Fig.4-18: Switching Vectors [115]	102
Fig.4-19: Simulation diagram of space vector pulse width modulation	104
Fig.4-20: Vector rotation for space vector pulse width modulation [117]	105
Fig.4-21. Simulation model to investigate control of the smart grid that connects wind/solar sources to the EV charging station.	107
Fig.4-22: (a) Illustrates voltage regulation on the micro grid (b) Voltage output from the solar system (c) minor oscillations in the desired voltage on the micro grid (d) regulated DC voltage achieved at AC/DC power conversion station from the wind turbines	108
Fig.4-23: (a) Applied duty cycle to stabilise the fluctuating voltage from the wind and solar farms (b) Regulation of current flow in the micro grid	108
Fig.5-1: The system energy management algorithm.	111
Fig.5-2: The energy sources connected to the micro grid	112
Fig.5-3: Energy generated by the solar/wind farms for a 24 hours' period.....	112
Figure 5-4: Microgrid connection with the storage system	113
Fig.5-5: Energy management when EV is charging during the 24 hour period.	114
Fig.5-6: Graph showing that the wind/solar energy generation is capable of running the EV station independently from 5am-9pm.	115
Fig.5-7: The smart vehicle-charging terminal where an electric vehicle is charging up and showing the smart measurement display	116
Fig.5-8: Operating features of the Electric-vehicle charging station.....	116
Fig.5-9: The wind/solar energy generation is capable of running the EV station independently from 5am-9pm.	118
Fig.5-10: Power consumption at the electric-vehicle charging station.....	119
Fig.5-11: Energy sources connected to the micro grid by using power conversion system.....	121

Nomenclature

Nomenclature		Abbreviations	
T_s	Switching frequency	kWh	kilowatt hour
R_p	Resistance on the micro grid (Ω)	VDC	Direct voltage current
I_{scn}	Solar current generation	EV charging station	Electric-vehicle charging station
V_3	Storage terminal voltage		
I_{p3}	Storage current (A)	D	Duty cycle
ΔT	Temperature difference [$^{\circ}$ C]	IGBT	Insulated gate bipolar transistor
V_p	Micro grid voltage (V)	MWh	Megawatt hour
I_p	Micro grid current (A)	VDC	Direct voltage current(DC power)
P_p	Power on micro grid (W)	AK	Azad Kashmir
P_1	Wind/solar terminal power (W)	KP	Khyberpakhtoonkhaw
V_s	AC/DC converter capacitor voltage (V)	PWM	Pulse width modulation
I_1	AC/DC converter inductor current (I)	SVPWM	Space vector pulse width modulation
S	Actual irradiance (W/m^2)	MPPT	Maximum power point tracking
R_p	Solar panel internal resistance (Ω)	P & O	Perturb and observe methods
I_{scn}	Solar current generation	IC	Incremental Conductance
T	Time [s]		
ΔT	Change in temperature difference [$^{\circ}$ C]		
S_n	Nominal irradiance (W/m^2)		
I_{ph}	Photovoltaic current		
K_1	Temperature coefficient [$^{\circ}$ C]		
I_o	Saturation current [A] dependent on temperature [$^{\circ}$ C]		
T	Temperature [$^{\circ}$ C]		
V_{oc}	Open circuit voltage		

Chapter 1

1.1 Introduction

Integration of large scale wind and solar farms into the UK transmission system has raised power quality, system stability and network synchronisation problems [1]. Between 2015 to 2016, wind and solar farms increased by 51.2% with total capacity of 8.1 TWh [2, 3, 4]. In 2016, these renewable energy plants were connected to the UK national transmission system where they created several challenges of voltage quality and harmonic distortions due to variable wind flow/sunlight and variations in the electric load [5]. Investigations have been performed on the isolated micro grid to solve the problems of power flow due to the creation of transients, inrush currents and disturbances in the grid, which can damage grid mechanisms and power generation units. The power flow in this type of micro grid can be via AC (alternating current) or DC (direct current). For DC type loads such as electric and hybrid vehicle charging stations, it is advantageous to develop a DC grid to reduce the charging time by reducing the number of power electronic converters [6]. There is no reactive power flow and no synchronisation problems on the DC micro grid and hence no phase correction is required in the power flow [7, 8]. DC storage systems can be connected to the micro grid as a better approach to maintain the power flow during disturbances in the wind and solar energy generation resources. Also, energy generation resources can be connected efficiently to the micro grid through power electronic converters. DC-DC converters are required for the solar farm and AC-DC converters are required for the wind farm. Electrical power control techniques can be implemented to maintain constant voltage on the grid. DC loads such as car batteries can be connected to the micro grid at car charging stations. On the micro grid transmission network, it is very important to keep voltages close to nominal values else it can lead the system to instability [9-11]. Instability due to the addition of power from battery banks, wind/solar energy and fuel generators can create massive damage to the network, equipment and eventually the economy [12]. Stability measurements can examine whether the system is performing in the correct state or heading towards instability [13] and should be considered at every point of the grid in order to take the appropriate action.

This thesis proposes methods to improve the voltage quality on the micro grid by examining voltage spikes and transmission of transients to reduce the effect of external parameters that create instability due to wind flow/sunlight and internal elements such as capacitance, inductance, and frequency control of insulated gate bipolar transistor switches. A voltage and

power conversion closed-loop control system is implemented as part of the smart grid and investigated to assess whether the grid is capable of handling large scale power flow. The control system prevents voltage reduction by applying a controlled duty cycle to the power conversion system and applying low pass filter techniques to remove transients. Power flow is maintained and regulated on the grid by drawing power from the batteries during energy shortages and charging the batteries at off peak times. The system is investigated by performing simulations using MATLAB/Simulink to study environmental effects on electric power generation and to discover the effects of over loading and under loading in the micro grid and simulation results are compared with a mathematical analysis.

1.2 Aims and Objectives

The aim is to develop an isolated smart micro grid connecting renewable energy sources and storage devices/ electric cars by stabilizing and controlling power flow in the grid to obtain an efficient power transmission flow. The power is to be transmitted to electric car charging stations where hybrid and electric car batteries charge up.

The objectives are to

- (1) Perform a literature review to determine the state-of-the-art of smart micro grids and discover opportunities for contribution of new knowledge and innovative solutions.
- (2) Develop and validate mathematical models to investigate how a smart micro grid will be affected by power transmission to electric cars and by energy recovery from the cars when they are not in use.
- (3) Investigate the inclusion of battery storage and other forms of energy generation to deal with unexpected environmental conditions e.g. variations in wind/irradiance or technical issues.
- (4) Design a control system to develop a smart micro grid for renewable energy transmission with automatic stabilisation and management of power flow.

1.3 Literature Review

A power system comprises of generation units, a transmission network, transformers, and protection systems. A transmission network transmits the electrical energy from generation units to loads. Currently the transmitted energy is being generated from mixed sources like coal, oil, gas, nuclear and renewables. The main source is fossil fuel and the burning of fossil fuel is creating damage through greenhouse emission and adversely affecting the Earth's

climate. Therefore, in the future, energy companies will have to generate electrical energy from other sources such as nuclear and renewables [14]. The main source of power in the future is likely to be renewable energy because it does not produce carbon emissions and the reduction will be observed in the import of fossil fuels and coal e.g. a 47% decline was seen in the first quarter of 2016 to the UK compared to the first quarter of 2015 as shown in Fig.1-1. Solar and wind are the most prominent renewables. In 2020, 15% of the UK energy is expected to be generated from renewable energy resources [15].

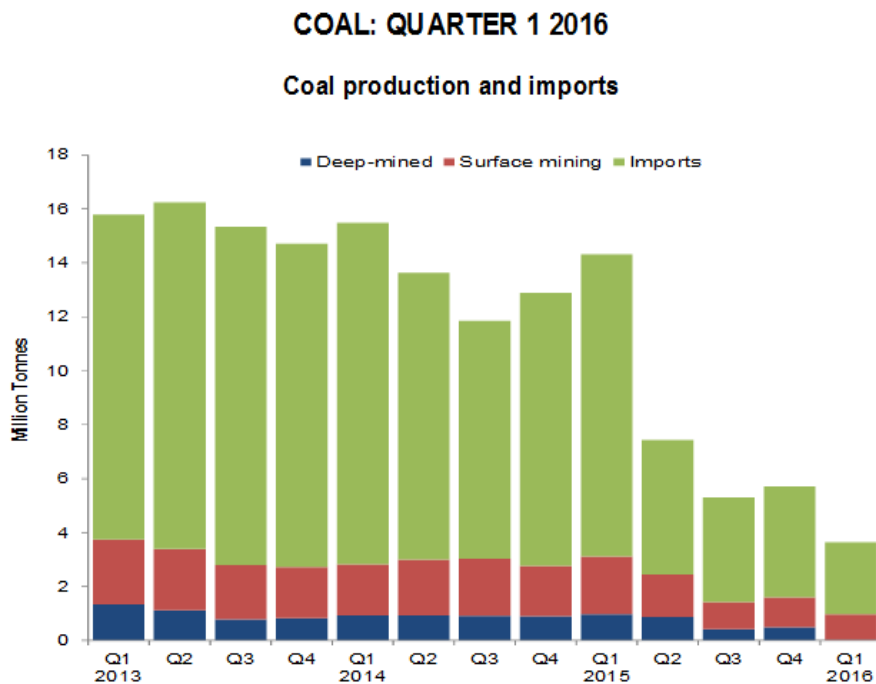


Fig.1-1: The reduction of coal import in the UK. Total demand of importation of coal was reduced by 47 percent in first quarter of 2016 compared to the first quarter of 2015 [16]

The number of plug in electric vehicles is increasing because they generate no carbon emissions and give better fuel economy. Charging up electric vehicles from the distribution network is not suitable as it increases the electrical demand on the network and creates power flow issues such as transients, harmonics and voltage reductions. The expected increase of electric vehicles in the UK by 2030 is shown in the Fig.1-2.

New Car Sales by Year Extreme Range Scenario

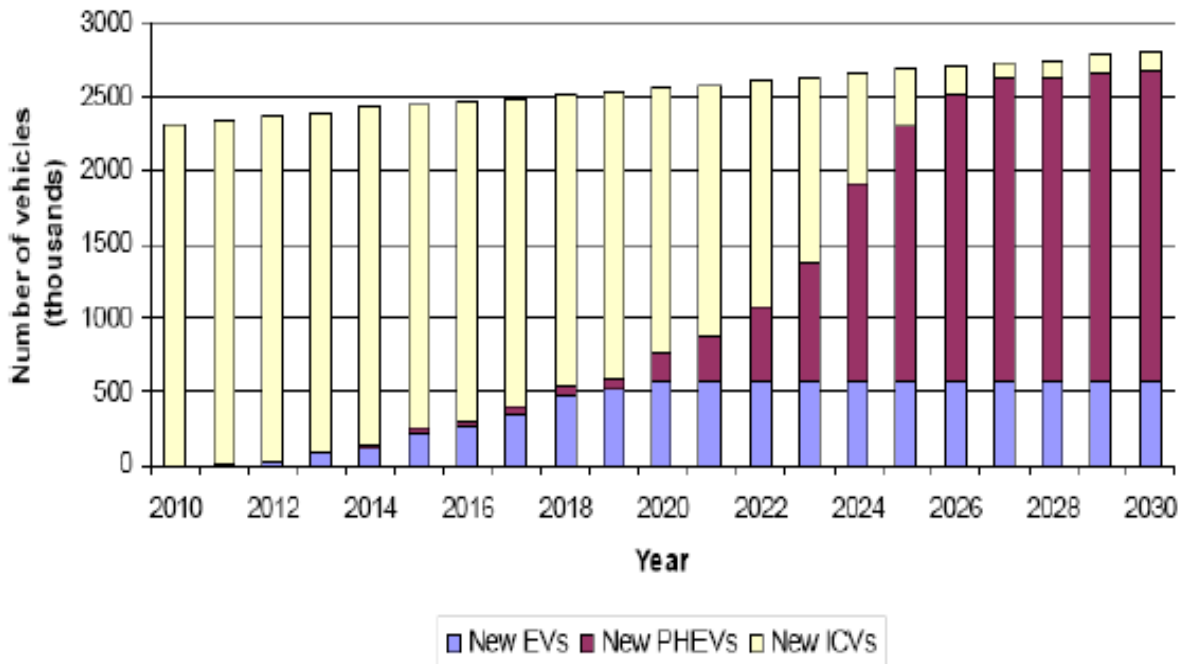


Fig.1-2: Plug-in electric vehicles, hybrid electric vehicles and probability of the increase in numbers of electric vehicles in the UK from 2010 to 2030 [17].

The DC micro grid is a new way of power transmission over short distances. This grid reduces the charging time for the plug-in-electric vehicle and improves the battery efficiency. Fig.1-3. shows a charging time comparison for the electric-vehicles batteries between the AC grid and DC grid. 8kWh battery takes 45 minutes to charge up from the AC grid while it is reduced to 10 minutes from the DC grid. It takes 160 minutes to charge up from the main grid. The purpose of designing such a system is to reduce the power flow issues at the existing transmission system. The power network should be able to deal with instability problems (due to changing climate conditions and load changes within the network) by maintaining stability at every point in the network.

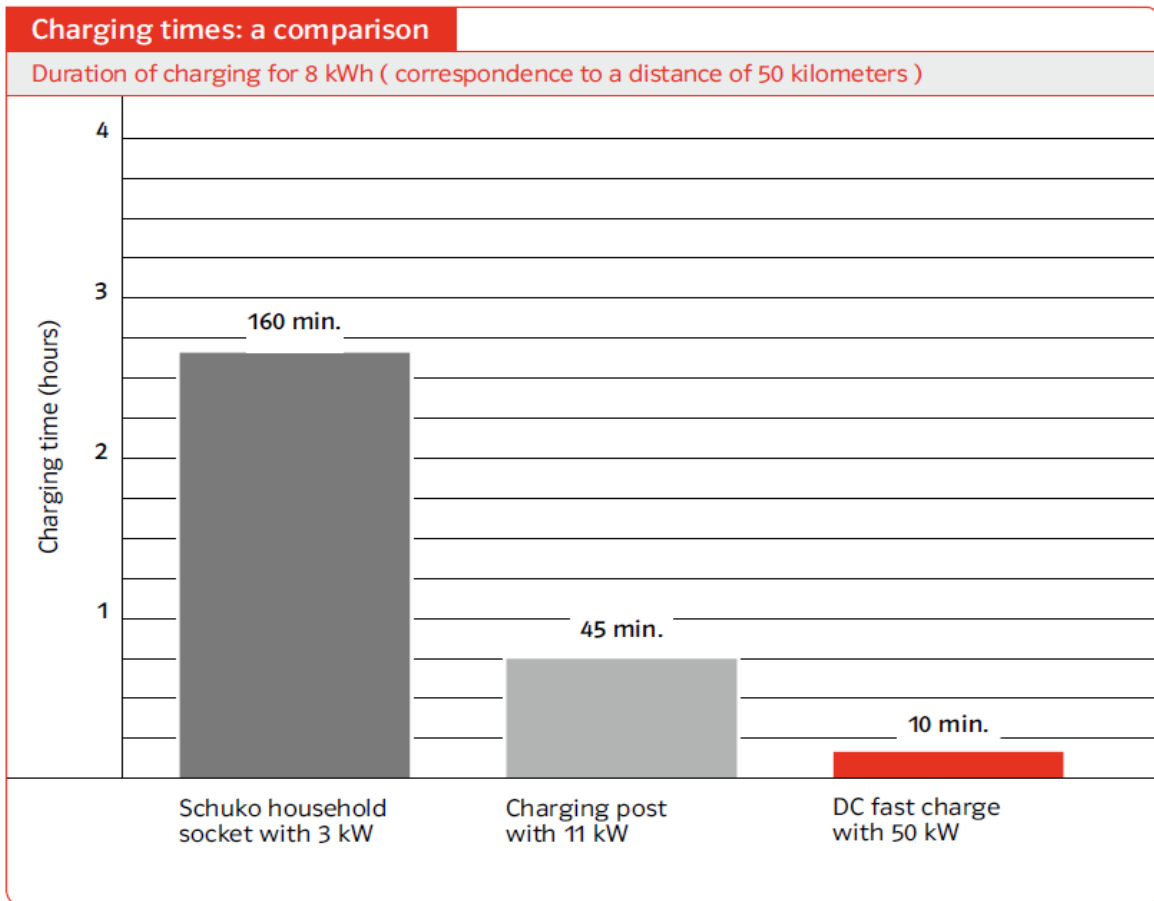


Fig.1-3: The vehicle charging from the AC grid and DC grid. It demonstrates the reduction of charging time from the DC grid compared to AC grid [18].

Instability can create massive damage to the network, equipment and eventually the economy. On the transmission network it is very important to keep the voltage closer to nominal values. If these parameters are not maintained, a power system will experience many blackouts, short circuit faults and equipment failure. Because of these problems, the system can become unstable. A transmission grid can also be subject to other various forms of disturbances such as lightning strikes, variations in generation, environmental conditions and so on. It is necessary to implement a smart protection system for the micro grid to increase its reliability and safety for power transmission. Micro grids can face low impedance faults, short circuit faults and ground faults and most of the faults can happen at any time at the power converter station due to unpredictable power generation from the renewable energy resources. It is necessary to investigate and correct the faults for a safe transmission else it can damage the system. When the power flow is interrupted from a fault then the system becomes unstable.

A fault in the DC converter station can affect the rotor angle of the wind generator and can damage the components at the converter station [19]. This depends on the duration of the fault and components used to protect the system. The fault in the DC grid can be between the lines or between the lines and the ground so it is beneficial to implement the communication system between the converters such as shown in Fig.1-4. The advantage of using the communication system between the converters is to identify the voltage drops and faults at different points of the system.

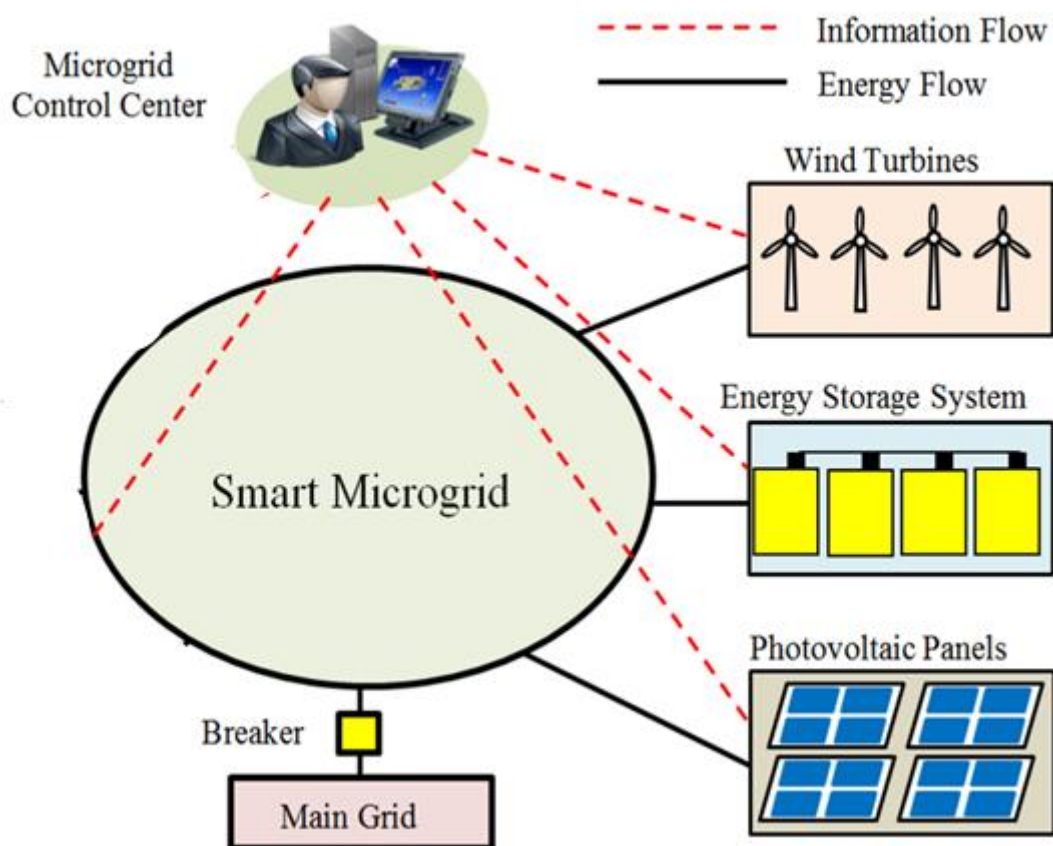


Fig.1-4: The renewable energy flow to the smart micro grid and way of electronic communication between them. It also demonstrates the injection of power on the network from several power generation resources such as wind turbine, photovoltaic panels and energy storage system [20]

The DC grid is fed from the renewable energy resources where power is always varying therefore a control system is required which transmits the signal at a very much faster rate. Specifically, if the load is inductive or capacitive then transients and spikes arise in the grid and a regulatory system is required to create balance in the grid. Achieving the desired voltage depends on the duration of current (A) flow where an inductor behaves superlatively at lower frequencies while a capacitor has better performance at higher frequencies. Voltage

and frequency are the two quantities that need to be controlled in AC power flow. Frequency can be controlled by controlling the rotation of a wind turbine and by increasing and decreasing the apparent power while voltage can be controlled by stabilising the reactive power. But in a DC grid, the frequency is equal to zero and reactive power does not exist because of zero phase shift between the voltage and current. It means that the voltage is the only quantity that needs to be stabilised on the DC grid [21]. The voltage on the DC grid can be maintained by supplying the required power to the loads. If the grid is over loaded than voltage will fall on the entire system and an energy boost will be required at this point. Thus to maintain the voltage on the DC grid, it is essential to keep energy balance on the grid at all times. A battery bank is another source for maintaining the power at the DC grid during the reduced power generation from the renewable energy units. However, batteries cannot regulate the voltage on the grid for a long period of time so there must be another energy resource that supplies power to the loads.

Electric vehicles are powered by batteries but currently it takes a long time to charge them up. The hybrid vehicle engine needs to be running to store power in the batteries, support vehicles when climbing hills and to maintain a given speed [22, 23]. To meet these requirements, demands on the new technology are investigated. Energy can be stored in vehicle batteries at the car charging station and also by means of regenerative braking when the vehicle stops. DC power flow is found to be most reliable and efficient for this task because it charges up batteries in a very short time [24]. DC power charging up also improves the efficiency of the power flow in electric cars by supplying the required power using converters to AC electric machines used in electric or hybrid cars [25].

1.4 Research Methodology

Construction of wind and solar farms is increasing every day. But in the meantime the transmission networks are getting overloaded and their efficiency is being reduced [26]. Due to variability of renewable energy, synchronization and instability issues are increasing in the grid [27]. It is also possible for the older transmission network not to be able to carry extra power. So there is a need for a grid, which should transmit the generated renewable energy perfectly up to 100%. For carrying out renewable energy transmission on a micro grid, it is essential to study environmental conditions and load variations. Because it is a fact that load and environmental conditions are changing all the time. Therefore, it is very complicated to

keep the constant stability for renewable energy transmission due to variations in load and the environment. The efficiency of the network is also reduced as a result of overloading and related types of variations. Hence there is the need for a separate type of network which should be able to transmit the power appropriately by accommodating constraints associated with these renewable resources. The power network should be able to deal with instability problems (due to changing climate conditions and load changes within the network) by maintaining stability at every point in the network. Instability can create massive damage to the network, equipment and eventually the economy.

The author is contributing and proposing a new model for transmitting renewable energy to improve renewable energy efficiency and to reduce power flow issues at the National grid. The model connects electric vehicles directly to the grid. The proposed model is also useful for transmitting renewable energy in rural areas and on islands. Specifically, a smart micro grid is designed with capability of handling large scale of power flow. Power flow control and stability are achieved automatically by means of closed loop control principles.

Investigations are performed by modelling and simulating energy sources such as wind turbines of energy generation capacity of 100kWh and solar panels of 100kWh. The electric vehicle charging station consists of 4 charging points with power consumption capacity of 103.50kWh. A storage system of capacity 200kW is included and is used when there is not enough power generated from the wind/solar energy. This storage system is connected to a diesel fuel generator that can supply 200kWh. The diesel generator charges up batteries only in emergency when there is deficiency of nominal power transmission on the grid. To control the frequency of insulated gate bipolar transistor (IGBT) switches, a power conversion system is simulated with AC/DC and DC/DC components. The schematic model of the system is shown in Fig.1-5. The electrical power control system is modelled in a MATLAB function coding environment. The simulation results from the proposed electrical control system are compared with other control systems such as the maximum power point tracking algorithm (MPPT) and space vector pulse width modulation. In order to achieve reliability, a smart protection and electrical control system is implemented at the grid station and at the smart grid. Transients and voltage spike waveforms are analysed and mitigated by using power electronics filters. Research is carried out on instability factors in the transmission grid which is required to transmit the wind/solar energy. It is discovered how environmental conditions, over loading, under loading and other conditions affect the power transmission in the smart micro grid. Various instability factors such as voltage instability, transient

instability are analysed. Power flow in the grid is maintained by using appropriate measures such as analytical techniques and modern power electronics control systems. Modern protection tools such as circuit breakers are placed to protect the grid.

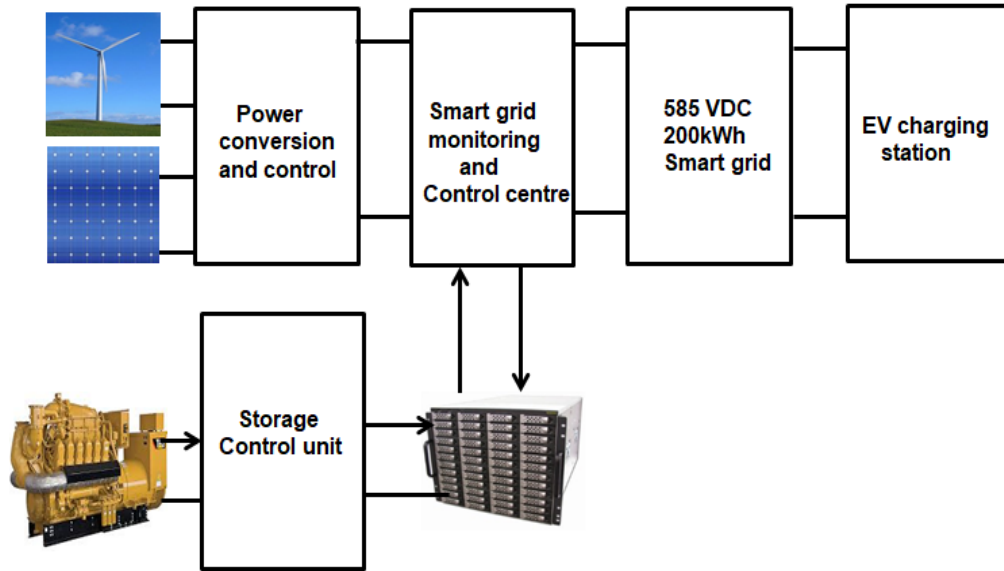


Fig.1-5: A schematic diagram of the integrated smart model consisting of Wind Generator (WG), Photovoltaic (PV) system, Energy Storage system, Electric Vehicle (EV) charging station, and other micro grid related components

The nominal generated power by each PV units is 330Wh with a voltage level of 12VDC which is boosted to 585VDC for efficient transmission on the micro grid by using converters. The total power generation capacity of the solar power plant is 100kWh where 304 PV units are installed to generate the electrical power for the electric-vehicle charging station. Variable irradiance from 250w/m^2 - 1000w/m^2 is used to observe the power flow from the solar panels. Scopes and other measurements tools are implemented to record the power flow from the solar system. In the wind energy system, a doubly fed induction generator is selected to generate electrical energy because it provides constant frequency and amplitude of the output voltage. It does not depend on the wind speed because its stator winding is directly connected to the grid. On the other hand, rotor windings transfer approximately 30% of the total power by using converters and operate at lower wind speed. The wind speed/temperature values are chosen as average values equivalent to the London weather forecast to compute the power efficiency. The speed values range from cut-in speed to cut-out speed and are generated by a real time function so that these values change with time. Tab.1-1. shows the energy

generation units that contain the wind/solar system to supply energy to the Electric-Vehicle charging station.

Tab.1-1: Energy resources and storage system/fuel generation system

Wind energy	100kWh
Solar energy	100kWh
Storage system	200kWh
Fuel generator	200kWh
EV max load	103.50kWh

The electric vehicle charging station consists of 4 charging points with total power consuming capacity of 103.50 kWh. The power consuming capacity of individual EV charging terminal is shown in Tab.1-2.

Tab 1-2: The operating features for the electric-vehicle charging station.

Electric-vehicle charging point capacity	Voltage at the grid side (DC)	Voltage at the load side	Maximum current flow in the grid
3.5kW	585V	12V	5.98Ah
7kW	585V	12V	12Ah
43kW	585V	16V	73.5Ah
50kW	585V	16V	85Ah
Fully operational	585V	Variable	320Ah

The power conversion system with AC/DC and DC/DC components used to stabilise the voltage and to control the frequency of insulated gate bipolar transistor (IGBT) switches is shown in Fig.1-6. It senses the voltage and current and applies the correct duty cycle to IGBT switches in order to regulate the voltage flow at the micro grid. Buck converters are implemented at the EV charging station to reduce the voltage. Boost converters are used to step up the voltage from the solar panels while buck-boost converters are used to regulate the voltage at the micro grid monitoring and control centre.

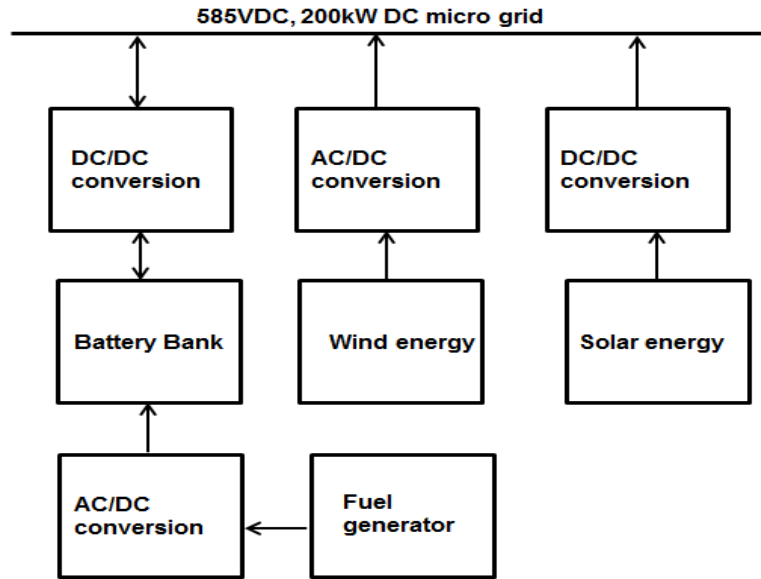


Fig.1-6: Block diagram of power conversion system connected to micro grid

In the AC/DC power conversion system, the structure of the control system used to regulate the voltage flow on the micro grid is shown in Fig.1-7. A MATLAB script is used to implement the feedback controller to calculate the correct duty cycle. The controller is equivalent to a microcontroller that would be used in practice to control the frequency of the converter IGBT switches by applying variable pulses to achieve the desired voltage. The controller receives two sensor signals from the converter output and compares them with reference signals to generate error signals and compute the correct output to reduce instability. The switching frequencies of high power IGBT switches are very low (20kHz) and they produce voltage spikes in the voltage. To solve this problem, a 50 kHz PWM control strategy is applied to reduce the harmonics and smooth the output waveforms. The output voltage of the power converters is decided by the PWM switching by applying eight ON and OFF states of the three phase PWM pulses [28]. The duty cycle applied to the power converter switches is between 0 and 1. The duty cycle controls the speed of the IGBT switches at the converter station. It is observed that by increasing the PWM pulse frequency, voltage spikes are reduced. Transients and voltage spike waveforms are analysed and reduced by using power electronic filters.

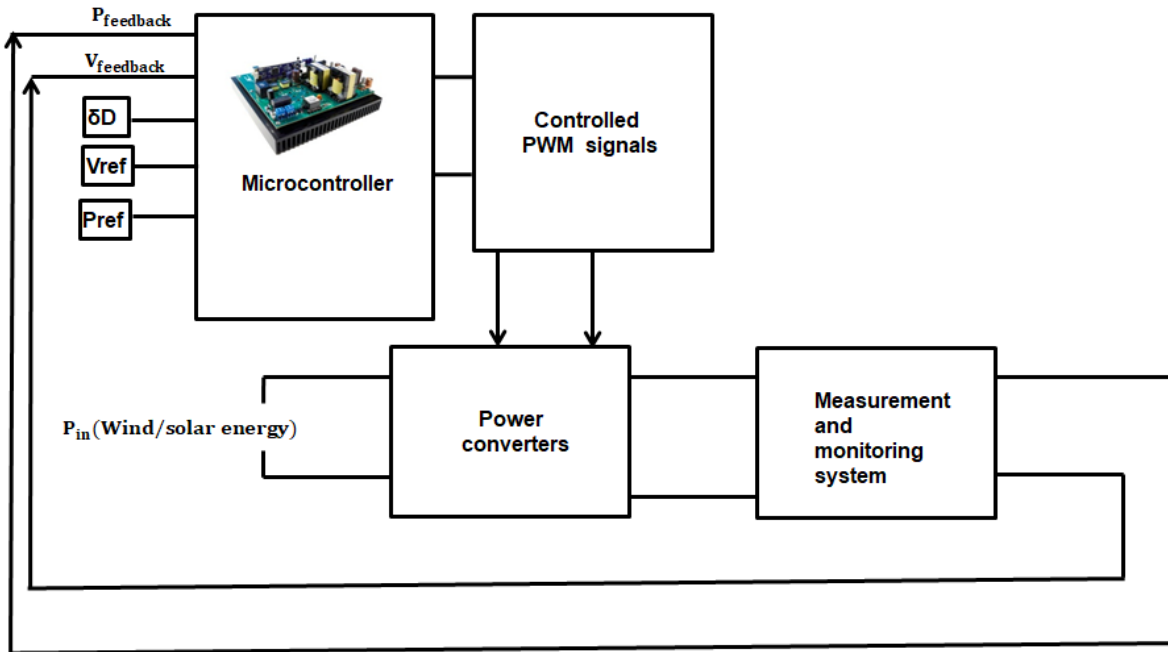


Fig.1-7: The block diagram of applied control system to achieve voltage regulation. P_{in} is the energy input from the wind and solar energy

The structure of the protection system used to protect the micro grid is shown in Fig.1-8. The protection system consists of all the necessary tools such as controller, sensors, relays and breakers or switches. Voltage and current flow signals on the grid are transmitted to a controller to perform required actions. The output of the controller is connected to a DC circuit breaker. The Controller isolates the grid and power components when voltage or current exceeds a high threshold level. The reference voltage represents the maximum voltage which a circuit breaker compares to the grid voltage.

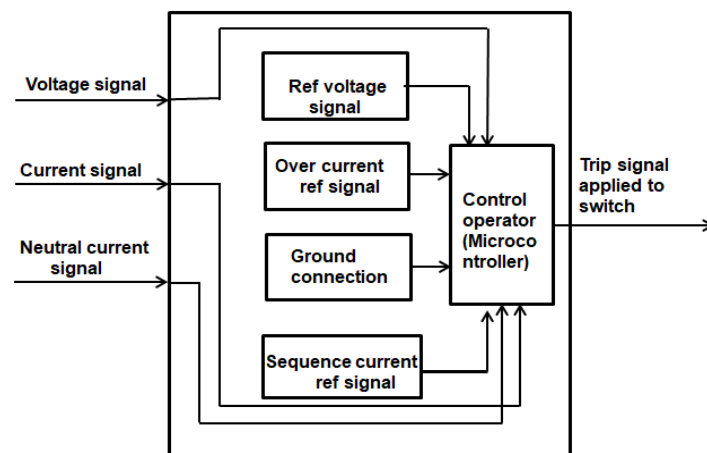


Fig.1-8: Block diagram shows a programmable power protection system implemented at the micro grid

Electric-vehicle engine needs to be running to store power in the batteries, support vehicles when climbing hills and to maintain a given speed [29, 30]. To meet these requirements, demands on the new technology are investigated. Energy can be stored in vehicle batteries at the car charging station and also by means of regenerative braking when the vehicle stops. DC power flow is found to be most reliable and efficient for this task because it charges up batteries in very short time as shown in Fig.1-9 [31]. DC power charging up also improves the efficiency of the power flow in electric cars by supplying the required power using converters to AC electric machines used in electric or hybrid cars [32].

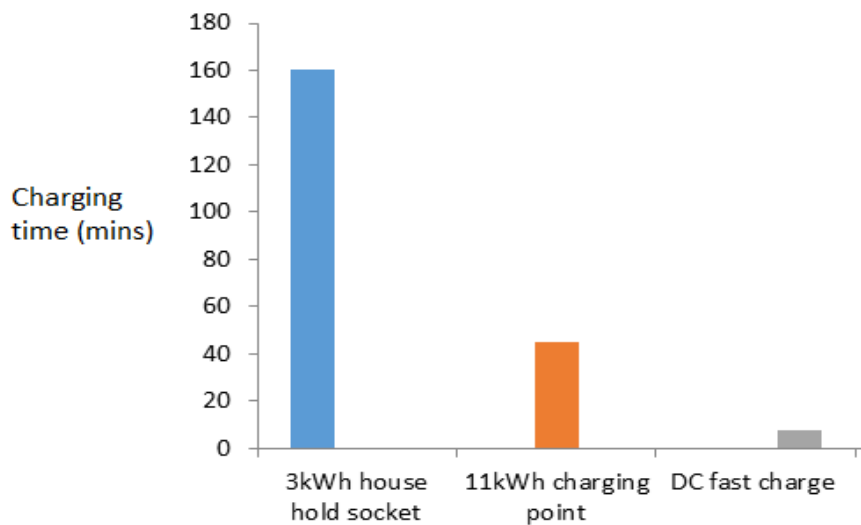


Fig.1-9: Charging time reduction between the AC grid (3kWh and 11kWh) and the DC grid.

Fig.1-10 shows the terminals of the EV charging station where 4 charging points with a total capacity of 103.50kw are operating during peak times. The total power consumption of Terminal 1 is 50kWh, Terminal 2 can consume maximum power of 43kWh, Terminal 3 has the capability to utilise maximum power of 7kWh, and Terminal 4 can utilise 3.5kWh to the electric vehicles.

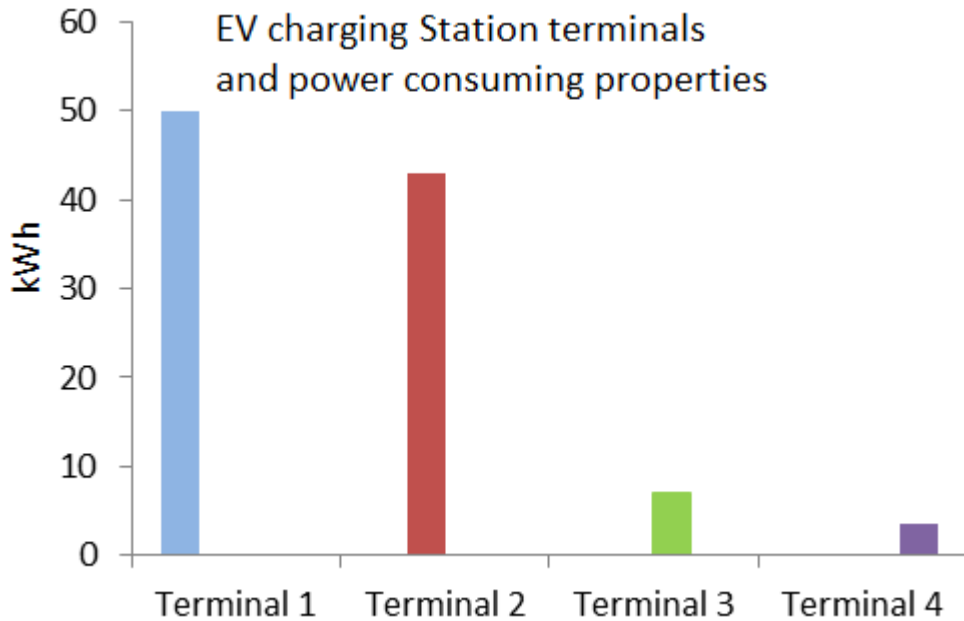


Fig.1-10: Charging station terminal features

1.5 Contribution to knowledge

A smart micro grid is proposed and investigated which is capable of handling large scale of power flow where control and stability is achieved automatically by means of closed loop control. The smart micro grid has the following advantageous features:

It consists of master control system connected to the sensors at the power converters stations and at the EV charging station. It receives the data from the converter stations/EV charging station to manage the power flow accordingly. The implementation of minute-ahead, hour-ahead and day-ahead strategy at the smart micro grid reduces the uncertainty in energy management and increases the efficiency of power transmission.

- This smart micro grid automatically fixes the power flow issues such as voltage reduction can be prevented by the controlled applied duty cycle at the power conversion system and the low pass filters remove transients. It manages the electric power on the grid by drawing power from the batteries during the peak times and charge up the batteries in the off peak times. The grid includes its own control and energy management capability. The proposed smart micro grid is beneficial to the UK national power industry because generated renewable energy is transmitted in this grid; instead of the distribution grid, which contributes to reduce the power flow issues such as transients, voltage reductions, harmonics and losses at the existing UK national transmission system. Initial findings indicate an improvement of the voltage

efficiency and reduction of electrical power losses in the micro grid by 99%. The proposed smart grid is also useful for transmitting renewable energy in rural areas and on the Islands. It is discovered how environmental conditions, over loading, under loading and other conditions affect the power transmission in the micro grid. Various instability factors such as transients and voltage spikes is analysed and then several control methods that are discussed in the bottom sections are proposed to find appropriate solutions.

- Programmable controlled circuit breaker is placed to protect the smart grid that is capable of switch in/out the power flow automatically. A smart sensing system is used at several points of the grid to measure the power in seconds. Power is delivered to charging stations to charge hybrid and electric car batteries and power is recovered from the batteries when needed. Investigations are performed on how the micro grid is affected when large numbers of super capacitors car batteries are charged at the same time.
- A smart electric vehicle charging terminal is implemented at the vehicle charging station. Several steps of voltage such 12VDC, 24VDC, 36VDC and 48VDC can be attained at this terminal. A smart measurement and protection system is included inside the terminal to increase the reliability in power flow to the electric vehicles.
- An electrical control system is applied at the smart grid to stabilise and control the power flow. Then the applied control system is compared with the other systems such as maximum power point tracking algorithm and space vector pulse width modulation. Several techniques from maximum power point tracking algorithm is implemented to analyse the power flow on the smart grid such as perturb and observe method, incremental conductance with integrator and fixed duty cycle method. A smart storage system is implemented to maintain the power flow on the smart grid during the energy shortages. Storage system is connected to the smart grid by means of converters and control system.
- Electric power generators have been investigated to find suitable generators for wind turbines.
- Investigations have been performed to study the factors (such as rotor angle instability, frequency instability) that affect a standalone wind energy system for the EV charging station
- Temperature effects on the PV module have been studied.

1.6 Journal and Conference publications

Journal papers

1. Asif Khan, Saim Memon, Tariq Sattar “Analysing integrated renewable energy and smart-grid system for improving voltage quality and harmonic distortion losses at electric-vehicle charging station”, IEEE Access Journal, Vol. 6, Issue:1, pp. 26404-26415

Conference publications

- Asif Khan, Saim Memon, Tariq Sattar (2017). Integration and management of solar energy for electric vehicle charging station. In: Solar World Congress 2017 - Innovation for the 100% renewable energy transformation, Abu Dhabi, UAE. doi:10.18086/swc.2017.16.03 Available at <http://proceedings.ises.org> (Published)

1.7 Thesis outline

Chapter 2 Voltage and frequency instabilities of renewable energy sources

This chapter describes the implemented renewable energy resources (Wind and solar) used in simulations of the proposed smart grid. These resources are used to generate and supply electrical energy to charge the electric vehicle at the EV charging station. Power parameters in renewable energy transmission are always varying so there must be a control system which reduces the disturbances and maintains stability in the system. In this chapter, instability issues related to renewable energy transmission are described with analysis and solution. The major parameters which are focused on are voltage instability and frequency instability and what factors affect them. By using the appropriate power flow techniques such as PWM waves, the instability issues are reduced.

Chapter 3 Implementation of the smart microgrid architecture

This section explores the implementation of the smart micro grid architecture. It outlines the proposed smart micro grid model and analyses the simulation results. The results are explained in terms of power losses which assists us to develop solutions to achieve the optimal voltage for transmission and reduce the transient spikes on the transmission network.

Chapter 4 Energy conversion and applied control techniques

This chapter describes the applied control techniques used to regulate the voltage on the micro grid. It describes the types of DC-DC converters such as Buck converter, Buck-Boost

converter and Boost converter. It shows the performance of of two control algorithms such as the maximum power point tracking algorithm and space the vector pulse width modulation algorithm that are used to control the frequency of the insulated gate bipolar transistors.

Chapter 5 Connection of Electric Vehicle Charging Station and Battery Storage to Smart Grid

This chapter explains the electric-vehicle charging station and energy management in the system. It describes the critical features of the smart micro grid required to charge up the electric-vehicles during the energy shortages from the wind and solar energy resources.

Chapter 6 Conclusion and recommendations for future Work

This chapter describe the conclusion and future work. It define the work that was completed during the research period and the areas where further research needs be carried out.

Chapter 2 Voltage and frequency instabilities of renewable energy sources

Every wind turbine produces energy at a different wind speed. It depends on the size and design of the wind turbine. Most wind turbines start functioning at a wind speed of 3ms^{-1} to 5ms^{-1} and generate a rated power at around wind speed of 12m/s to 15m/s [33]. It is a fact that wind speed is not constant and it changes all the time. Therefore, in the simulations, numerous wind speed values were used to drive the wind turbines. At low wind speeds the torque is not sufficient to drive the blades. As the wind speed increases, blades start rotating and generate power. The speed when turbine begins to rotate is known as the cut in speed and is 3m/s to 5m/s . When the wind speed is above the cut-in speed then power is generated. At the rated wind speed, a generator produces nominal power. When the wind speed is higher than the rated speed, the generator output power is still limited to nominal power. The nominal power is therefore the generators full generating capacity. . A braking system is implemented to limit the over speeding of the turbine. Over speeding normally occurs at around 25m/s . The available power as a function of wind speed [34] is given by equation 2-1:

$$P = \frac{1}{2} \rho d U^3 \quad (2-1)$$

Here U is the wind speed, ρ is density of the rotor and d is the rotor diameter in meters.

While the amount of power extracted from the wind depends on the wind speed, it is not possible to consume all the wind; there is a limit that depends on the design of turbine blades [35]. The maximum wind that can be extracted by the turbine to generate power is 59%. This is Belts limit [36]. Since power increases by the cube of wind flow, for example, if the wind speed is doubled then power increases 8 times. This means that a small change in wind speed has a big impact on energy variation [37]. In the following research, several values were chosen for wind speed to observe the power output from the generator. The values range from cut-in speed to cut-out speed. A periodic repeating real time function is used to implement the changing wind speed as shown in Fig.2-1 and Fig.2-2. It repeats itself in every 0.1 second. The wind speed generator is an input to the wind turbine. The parameters for the simulation block are shown below:

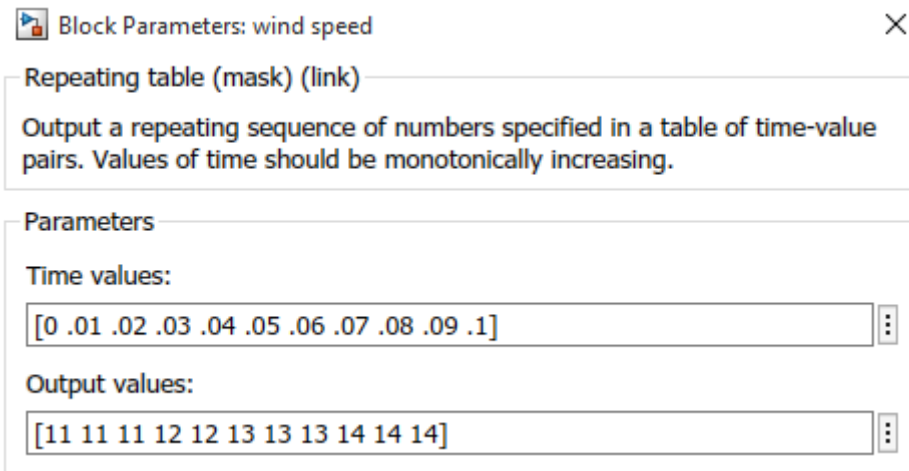


Fig.2-1: Wind generator with time in second and wind speed m/s

The variation of wind flow will have a severe impact on the amount of power and hence voltage variation.

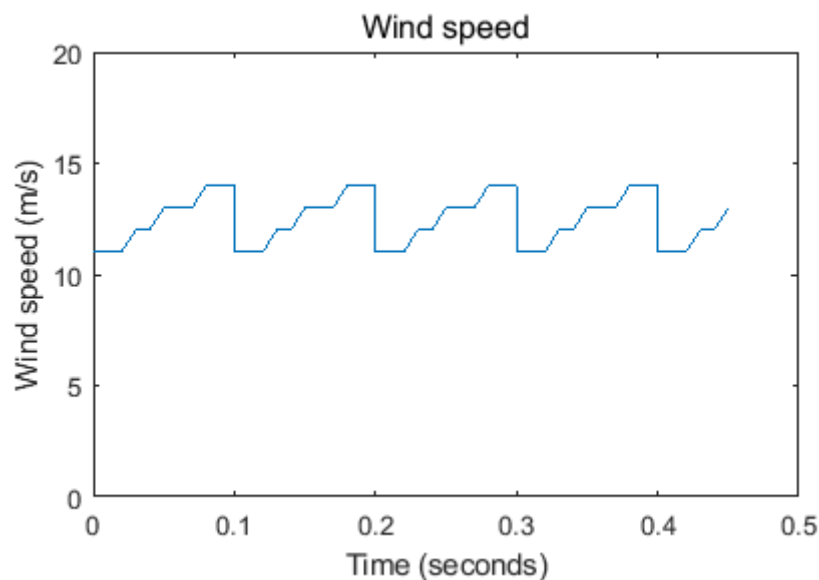


Fig.2-2: Simulation of applied wind speed to generate electrical energy.

2.1 Testing and evaluation of energy generation at changing Pitch Angle

Investigations were performed on the features of wind turbine blades. Wind turbine blades must be designed to efficiently drive the shaft of the generator. Pitch angle is the angle at which blades contact with the wind. It is normally kept between (0-15)°. Angle of attack is the angle where force hits the blades to start its rotation. Higher angle of blades stalls the wind turbine and decrease the air pressure on the blades [38, 39]. The main parameters considered for blade design are control of the pitch angle, tip speed ratio and rated wind speed. The relationship between pitch angle of the blades and output power was investigated.

It was observed that as wind speed increases the turbine efficiency increases. Variations in pitch angle increase or decrease the range of power generation [40]. Pitch angle control is also necessary to reduce the speed of the rotor in the higher windy areas. In the lower windy areas, pitch control can increase the efficiency of the wind turbine by capturing more wind. By adjusting the pitch angle, a balance between the electrical power and turbine power can be maintained. Fig.2-3. shows the block parameters to produce pitch angle variations for simulation purposes.

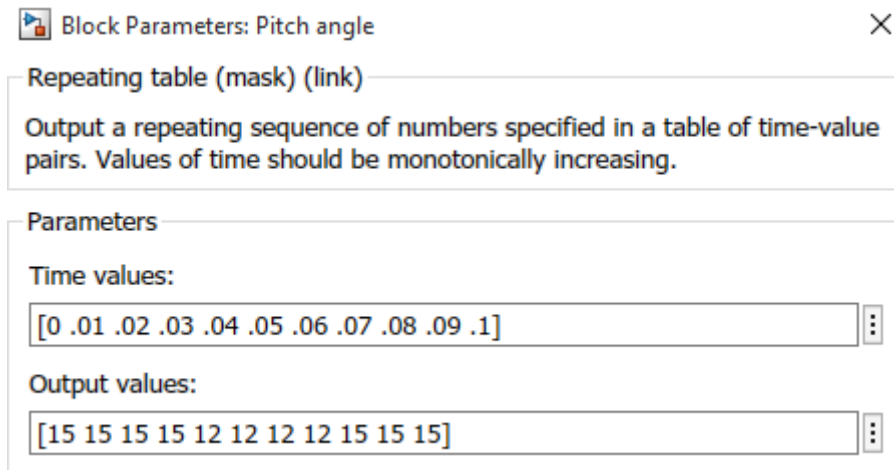


Fig.2-3: Examining of the wind turbine energy generation features by the variation in blade pitch angle. Output values are in degrees and time in second.

Fig.2-4. shows the variations in pitch angle. A repeating function was used to vary the pitch angle. It was observed that variations in pitch angle have greater impact on the amount of power generation. By not adjusting pitch angle appropriately huge amount of power can be wasted. Wind speed and pitch angle have a direct relationship. Correcting the pitch angle in the lower wind areas can increase efficiency of the turbine. Pitch angle adjustment is also very important during the higher windy conditions.

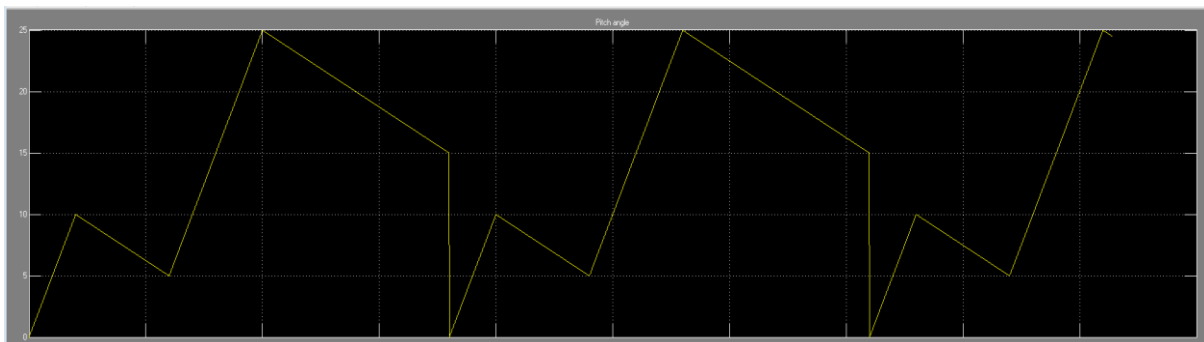
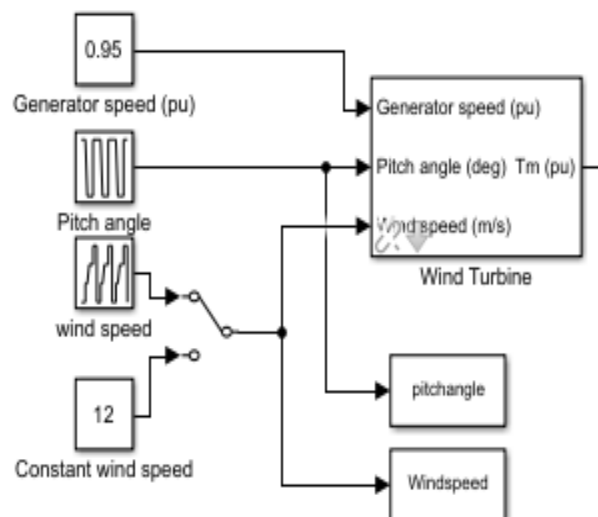


Fig.2-4: Simulation of variable blade pitch angle

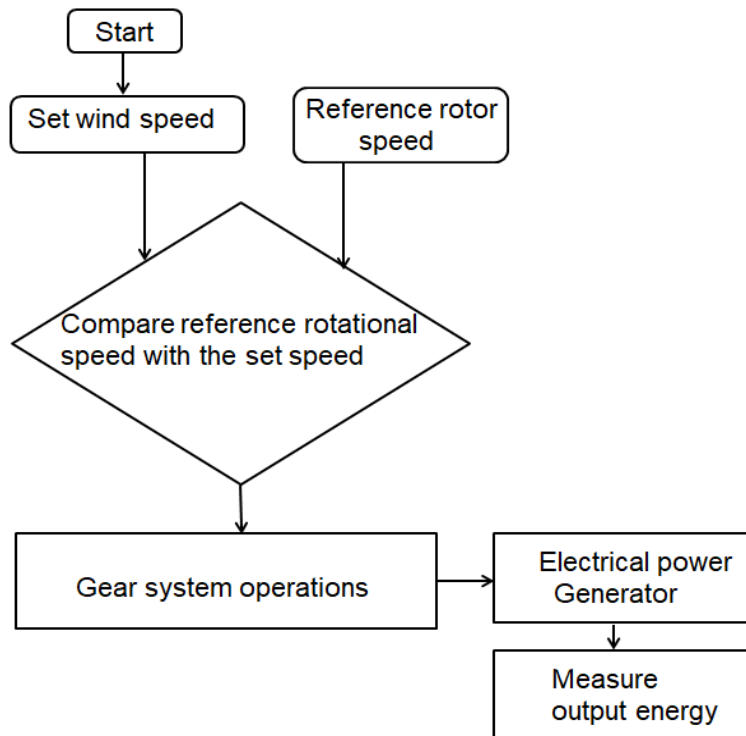
2.2 Simulation and analysis of doubly fed induction generator

Doubly Fed Induction Generator (DFIG) is used to generate the wind energy as it provides higher efficiency because its stator winding is directly connected to the grid while rotor windings are connected to converters which transfer approximately 30% of the total power generated [41]. The maximum power generating capacity of the DFIG is 100kW during the nominal wind speed of 12 m/s. By implementing the DFIG, spikes and transients in the grid are minimised due to less power transfers from the converter. For variable wind speed areas DFIG is the most suitable choice. DFIG provides constant frequency and amplitude of the output voltage and does not depend on the wind speed. To achieve the same results from the other generators, there is a need to use higher power electronics converters. But for DFIG only a fraction of power needs to be converted using power electronics converters because the stator is directly connected to the grid [42]. Power generated from the rotor varies so it needs to be stabilised using power electronics components. It is first converted into DC and finally connected to the grid.

Fig (2-5-2-6) shows the Simulink model of a doubly fed induction generator. The rotor of the DFIG is connected to the converters while stator is directly connected with the grid. This type of generator requires reactive power for excitation. It can receive the reactive power from the grid or by installing capacitors. Alternatively, a synchronous excitation generator can be used to provide excitations. Using the stator, it sends power directly to the grid, and from the rotor side only a small amount of power can be processed. The main advantage of DFIG over other generators is that it operates efficiently in varying wind areas. Even if a wind speed is very low e.g. 4ms, it still generates constant frequency and amplitude as shown in Fig.2-7.



(a) Wind turbine Simulink model



(b) Energy generation algorithm for the wind turbine

Fig.2-5: Wind turbine generator Simulink model and an algorithm to compare the set wind speed with reference rotor speed

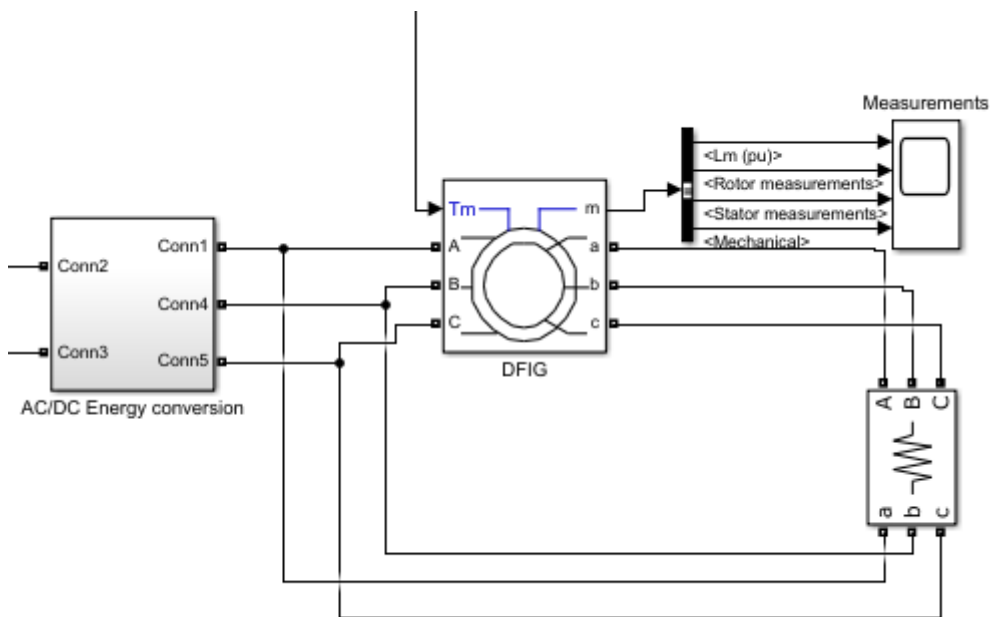


Fig.2-6: DFIG used to generate electrical energy and connected to grid via converters

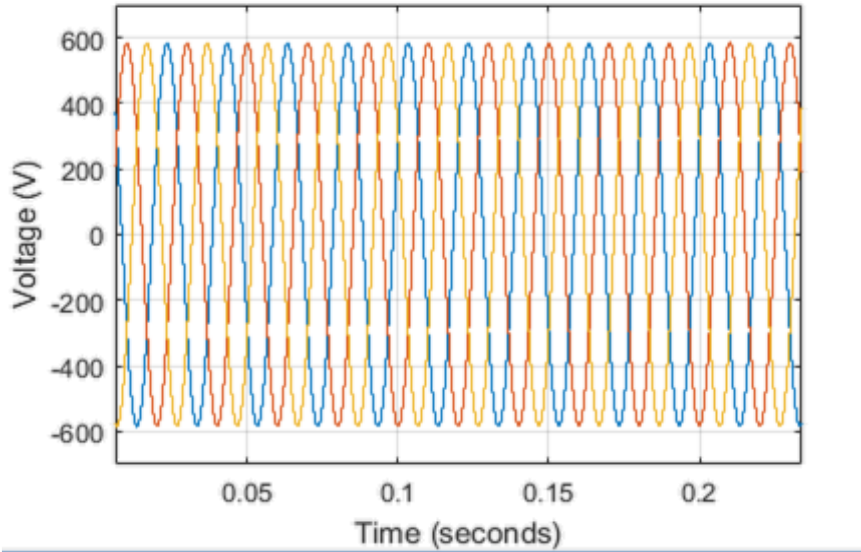


Fig.2-7 : Constant and regulated voltage is received from DFIG. The three sinusoidal plots are the three phase voltage.

2.3 System testing by applying permanent magnet synchronous generator

Permanent Magnet Synchronous generator (PMSG) based wind turbines are also investigated for generating electrical energy as they are popular in the power industry due to variable speed and constant output frequency, they are lower in weight, volume and have higher efficiency and reliability. PMSG is a variable speed power generator which functions at various ranges of wind speed. It consists of a rotor, high speed and low speed shaft gearbox and generator. Because PMSG is excited by permanent magnets, there is no reactive power exchange between the machine side of the converter and between the generators [43]. Two types of control are implemented for PMSG; one is to keep the machine at nominal power at strong wind speeds and other is to maintain the maximum tip speed ratio when there is very low wind. This is achieved by adjusting the pitch angles of the blades. . In low wind areas, pitch angle is actuated to a optimum value of 2 degree while in higher wind it limits the extracted wind by selecting the most appropriate pitch angle. Due to requirements of high rotor revolution; a gearbox is also used in the generator which requires constant maintenance. To increase the reliability of the wind turbine, the gearbox needs to be removed. The PMSG can also function without using a gearbox but its efficiency is reduced due to not achieving the desired speed rev/min [44]. By increasing the number of poles in the PMSG and using low pole pitch, the number of revolutions is reduced from 200r/min to 20r/min. However, increasing the number of poles will make generator construction more complex. Electromagnetic construction of a wind turbine is more complex than other wind turbine

generators such as DFIG, fixed speed or variable speed induction generators. Converters are an important part of the PMSG because it converts the energy to AC power with fixed frequency and voltage. The sizing of nominal power conversion of power converters should be larger than the nominal power of the generator [45, 46]. Due to the use of converters, reactive power generation, transients and harmonics are also observed in the system. To reduce the number of harmonics, a low pass filter is required. The generated voltage from the wind turbine needs to be maintained constant before connecting it to the grid. Therefore, voltage source converters VSC based converters with Insulated gate bipolar transistors IGBT are used to regulate the output voltage.

Fig.2-8 shows the modelling of the permanent magnet based wind turbine. A gear system is used to vary the speed of rotation. By adjusting the gear ratio, the turbine speed can be fixed. The generator has the capacity to generate power up to 1MW. The nominal generated voltage is 415VAC. Scopes are used to graphically analyse the results of the turbine's operation.

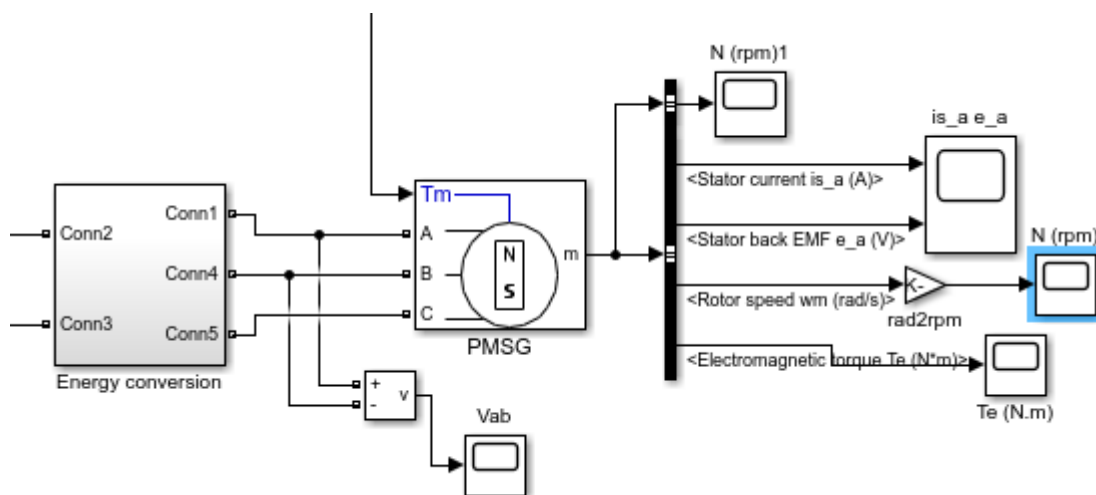


Fig.2-8: PMSG based wind Turbine

Variable Wind speed

Output of the PMSG is shown in the Fig 2.9. It can be seen that when the wind speed is low then voltage generation is reduced to a lower level. The nominal voltage is 415Vrms but it has reduced to 260Vrms due to a lower wind speed. There is need to rectify this voltage at the output and then stabilize it for transmission purposes. It is not possible to transmit the voltage without conversion. The phase angle is also changed by the varying wind speed as shown in Fig.2-10.

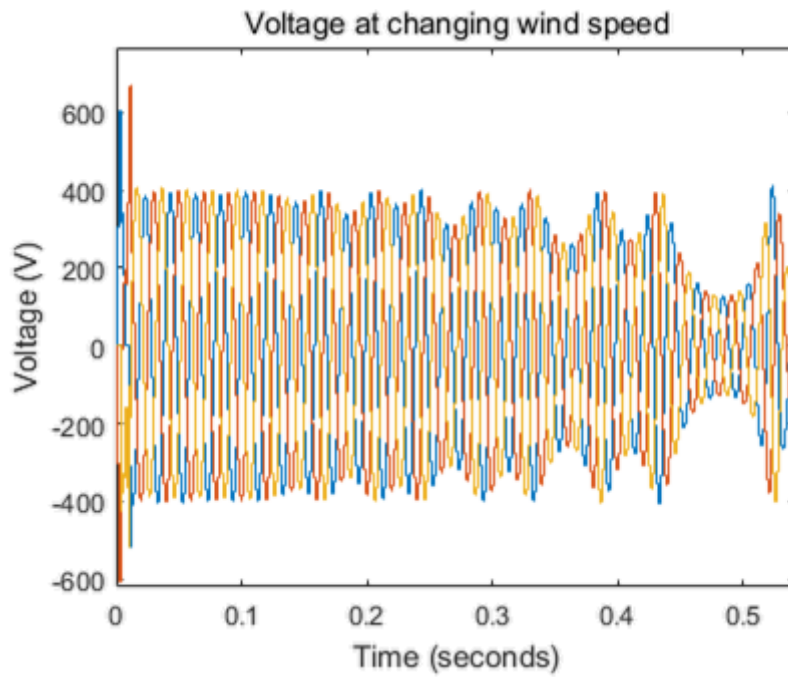


Fig. 2-9: Three phase output voltage at the varying wind speed. Severe variations in voltage are observed

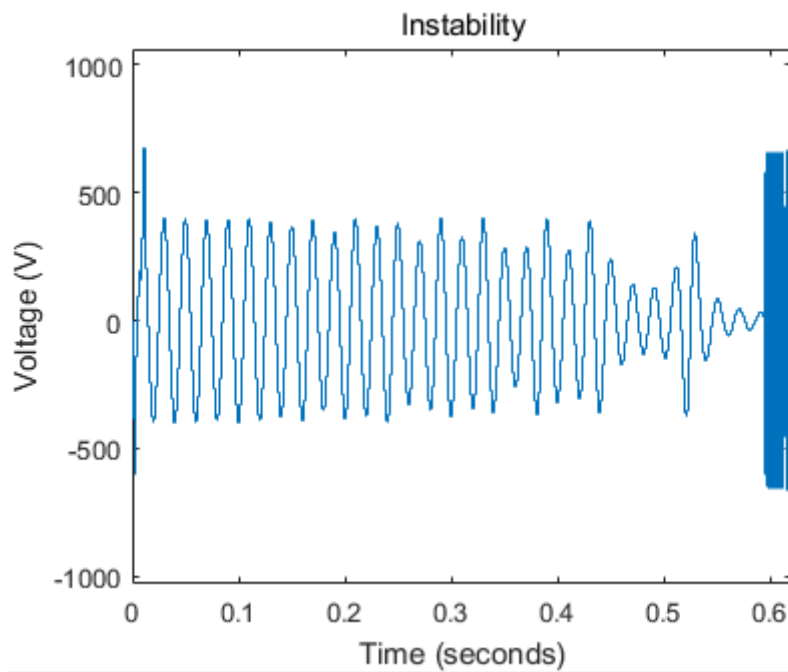


Fig.2-10: Voltage variations at varying wind speed

Fixed wind speed

Power flow on the micro grid was investigated using a fixed wind speed where a 12m/s is chosen as the nominal wind speed and a constant output is noticed from the PMSG Generator. A switch was placed between the variable wind speed and fixed wind speed to select one or the other. It was found that generator output is more smooth and constant when

the fixed values are used for wind speed. Fig.2-11 shows the three phase output voltage from the PMSG.

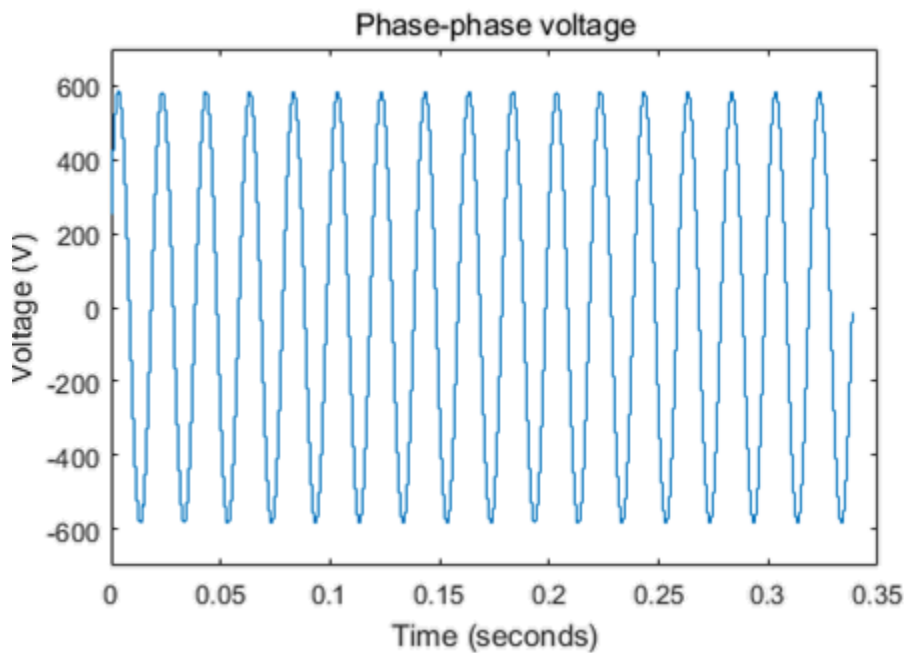


Fig.2-11: Voltage output from three phase power PMSG

2.4 Factors creating instability issues in wind energy generation units

A system is called a stable system if it retains its original state after facing disturbances. The main reasons for instability issues in wind energy transmission are environmental conditions, synchronisation, over loading, and massive variations in power generation. Typically, the basic factor of instability is lack of synchronisation between wind turbines. Synchronisation between wind turbines is very complex due to wind speed variations [47]. Some wind turbines generate the power at full capacity while some do not. Renewable energy units face stress conditions during overloading and easily lose stability and the failure of a single turbine can create massive power issues such as inrush current [48]. A control and protection system is required due to constantly changing environmental conditions and loads. It is also necessary to manage the reactive power in the system. The system should be able to produce and absorb reactive power when required.

Instability factors in a wind farm can be categorised into the following cases:

Frequency instability

Voltage instability

Rotor angle instability

Due to changes in weather conditions, temperature and load changes, it is very hard for the renewable energy system to remain stable [49]. Maintaining stability in the face of voltage oscillations and electromechanical oscillations between loads and renewable energy units is very important. It is a challenge to maintain constant voltage in renewable energy transmission due to the changing of various factors. It is observed that oscillation in voltage and damping factors can be produced by machine inertia and external impedance. Voltage fluctuations also create current variations in the network as shown in Fig.2-12 [50]. Voltage surge is related to inductive elements and current surge is related to capacitive elements. When a generator is switched on the transmission line does not switch on simultaneously due to the presence of inductive and capacitive components in the line. The delay depends on the frequency and conductive material. Less capacitance and inductance minimises the energy transmission delay. Voltage stability is also called load stability because after disturbances happen in network voltage, the loads will not have energized appropriately [51]. The main reason for fluctuations in voltage is when a generation unit was not able to supply the required reactive power. The other factor which creates instability is lack of synchronisation between the turbines. When one wind turbine is faulty or there is loss of synchronism then it's the other units will not be able to transmit the required power to the loads. This will overload the network and lead to system failure. A power surge is produced by sudden change in the loads. Some other elements which can cause disturbances are flashover, lightning strikes, switching elements and short circuit faults. . Fig.2-13 shows the instability in voltage between the wind turbines due to not synchronised between them. When PMSG and DFIG are connected then due to variable wind speed synchronisation cannot be achieved. Fig.2-14 shows power generation for a synchronous generator.

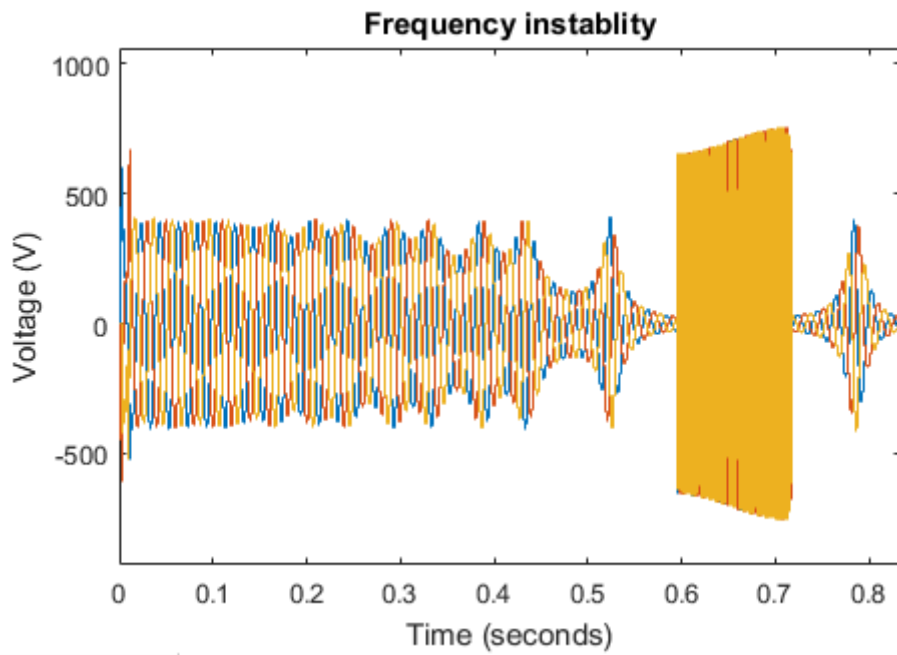


Fig.2-12: Frequency instability creates severe voltage variations in the system

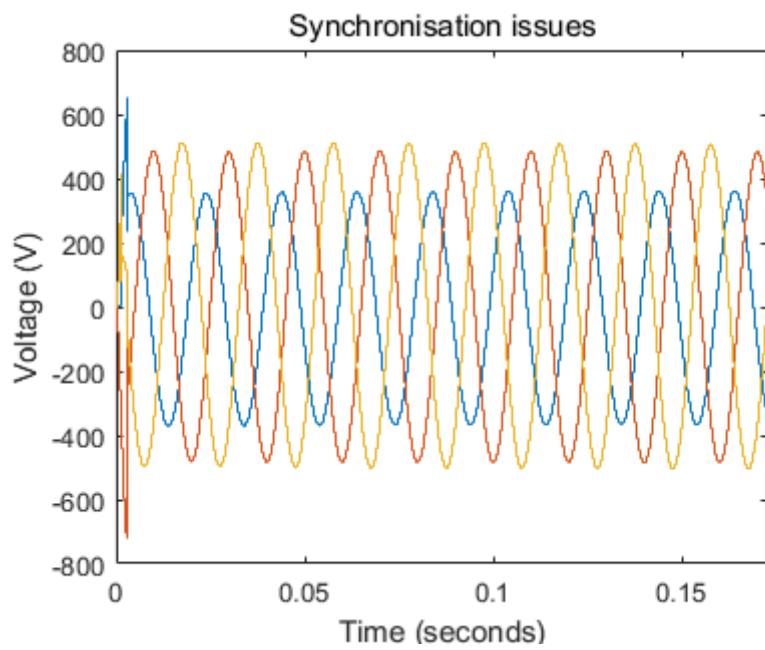


Fig.2-13: Synchronisation issues between wind turbines

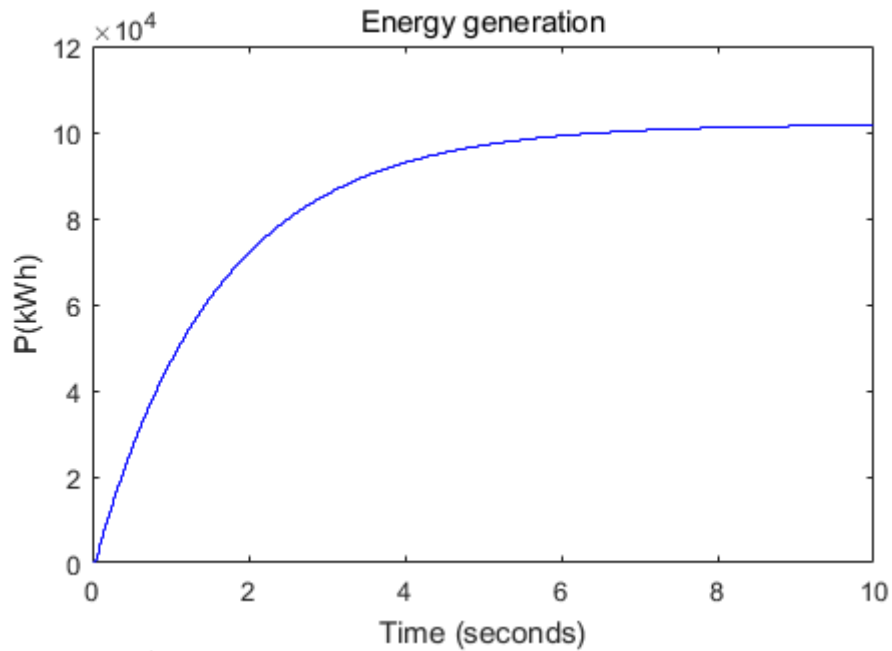


Fig.2-14: Energy generation produced by the synchronous generator at varying wind speed.

. Maintenance of frequency close to nominal values of 50Hz is very important in power transmission. Instability in frequency occurs when the wind speed is very low or very high [52]. Frequency variations are created by synchronisation or issues at the generation units. A big power surge is observed by just small variations in frequency. It also produces mechanical vibrations at the generator and overheats transformers [53]. Changes in frequency also produce undesirable changes in the speed of machines in industry. Frequency changes are noticed by unpredictable rotation of armature in the generator. The rotation of the wind generator armature is driven by air flow around the wind turbine blades and changes in wind speed create frequency variations [54]. Instability also results from harmonics particularly multiples of third harmonics. Harmonics are created by converters, computers, and motors. Instability can damage transmission conductors and transformers. Loss of synchronism also causes rotor angle instability. Due to loss of synchronism, the rotor angle will increase and then can go into overshoot. Fig.2-15 shows the instability in power generation. It can be seen that due to massive variation of power flow, the generator voltage overshoots and oscillates.

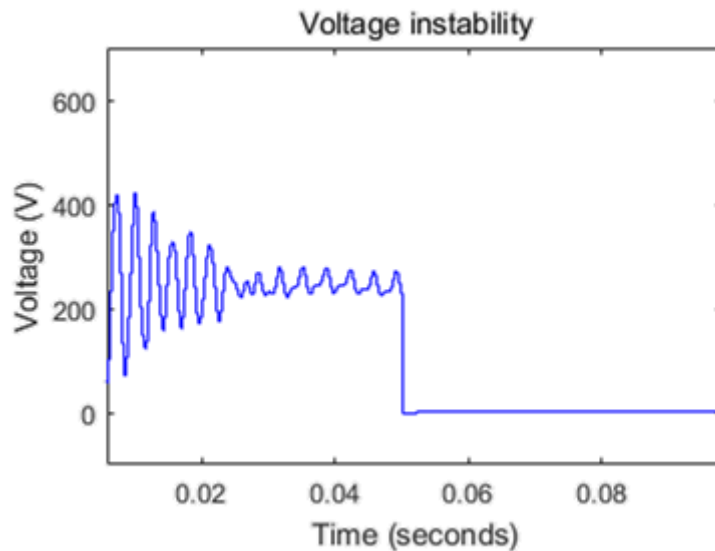


Fig.2-15: System Overshoot due to synchronisation and frequency instability

Rotor angle instability is another factor in wind turbines. It happens during an imbalance between electromagnetic torque and mechanical torque at wind generators operating at variable wind speed. It is a phase angle related instability problem. The equilibrium between electromagnetic torque and mechanical torque needs to be maintained [55]. When a balance between available power and demand power is lost, then this problem can happen. It is further termed as transient stability and small signal stability. Small signal stability means the system remains in synchronism after a few disturbances in the system. Transient stability means that the system remains in synchronism after major disturbances. Rotor angle instability also occurs due to various other factors such as a fault in the network, short circuits, switching disturbances, massive variations in loads and generators and so on. Fig.2-16 shows the instability in rotor angle. If the rotor angle increases after a disturbance, then the system will overshoot. But if the rotor angle starts decreasing then system stability can be achieved.

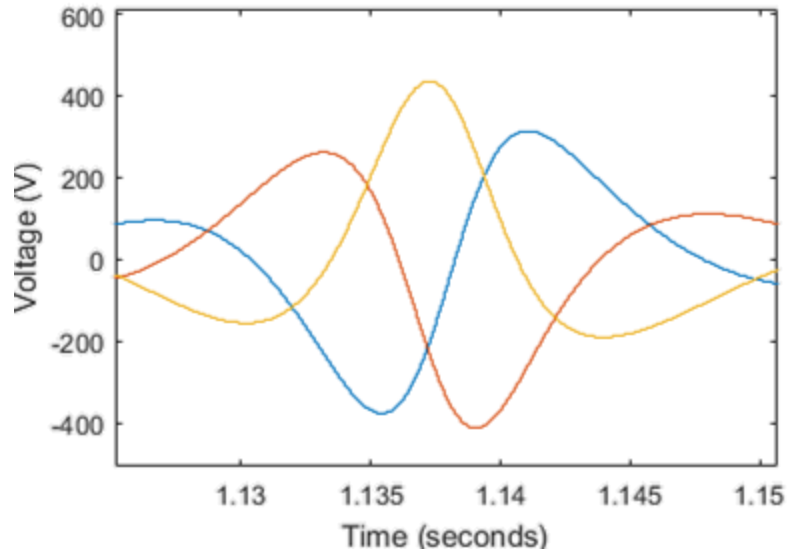


Fig.2-16: Rotor angle instability in the wind turbines

2.5 Modern techniques to minimise instability issues

Using sensing data from the applied sensors, decisions and actions can be taken to correct an unstable system. By measuring the transient response of the wind generator it is subjected to disturbances, a stability analysis can be performed. The first stabilisation method used is a time domain method where changes in generator angle are measured with respect to time. The resulting graph is known as a swing curve and the calculations are done using swing equations. Stability or instability is analysed by drawing the angle curve. It is found that if the angle is increasing continuously and does not decrease, then the system becomes unstable. But if the angle starts decreasing then the system will regain its initial state [56,57].

The other implemented stabilising method used is the equal criterion method that provides a graphical analysis of the generator stability or instability [58]. Fig.2-17 shows the graphical analysis of a system due to initialization of the charging up of the inductive/capacitive components in the power converter stations. Voltage disruption is due to variability of the power angle when changes in power generation occur due to changes in the loads [59]. When the power drawn is bigger than the input power, the power angle is observed to increase. If the input power is larger than that drawn by the load then the system remains stable, but if the output power is continuously increasing then the system becomes unstable.

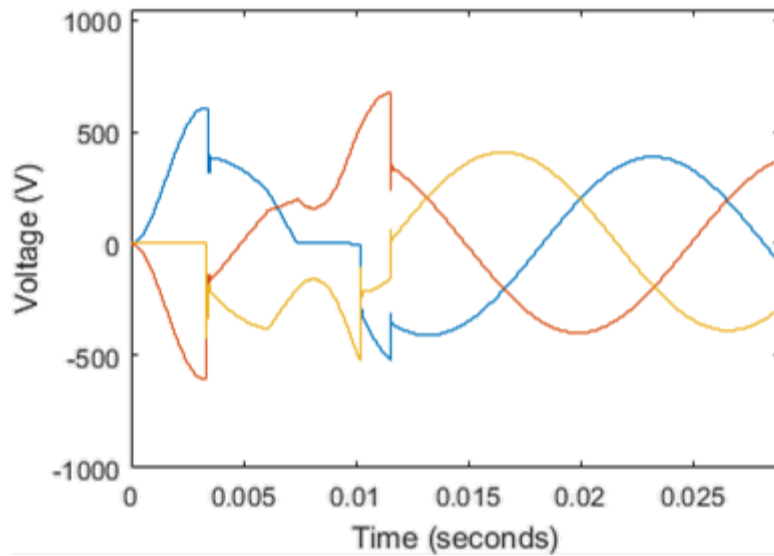


Fig. 2-17: Instability issues at the start up process of a wind energy generation system due to load variations

The other stabilisation method is the direct method which analyses the stability of the power system [60]. In this system results are compared before and after disturbances in the generators and stability results are measured. This common method does not depend on time and it provides a measure of the degree of stability accurately and quickly.

Voltage stability is analysed by sensing the supplied voltage to the load. Voltage stability is actually called load stability. It can be caused by some component failure or loss of synchronism. When a power variation happens in a load sector it signals voltage instability [61]. When the system is overloaded, then a frequency drop is observed in the system. The generator rotation speed tends to be lowered. To maintain a constant voltage frequency on the grid, there is a need to insert more input power from the turbines. Primary frequency is measured by turbine-governor control systems, while secondary frequency is measured by a load frequency control system. Rotor angle stability is observed by reading the output of the generators. The instability in rotor angle generates transients in the system. When a voltage collapse is observed in the transmission network, then the rotor angle is noticed to be unstable.

2.6 Solar Farm

This section presents the Simulink model of a solar power generation system that supplies 100kWh energy to the charging station. Solar power is achieved by using photovoltaic devices to convert sunlight energy into electrical energy. Large amount of energy is obtained by using photovoltaic arrays. Fig.2-18 shows the model of a solar farm. The voltage generated by each panel is 12VDC and the maximum generating capacity of one panel is 330W. An irradiance block is used to provide solar power to the panels. Input from the irradiance is variable. 12VDC is not feasible for transmission and it was boosted to 585VDC by a boost converter. Output voltage is adjusted by changing the duty cycle ratio of the boost converter. An oscilloscope is used to measure the output voltage. Capacitors are used to remove the ripples and balance the voltage flow. A diode is used to stop current flowing in the reverse direction. The amount of power generated depends on the efficiency and size of a panel. The power generated is directly fed to the grid by using converters. This clean power is used to charge the electric vehicles at the consumer end without producing carbon emissions. A PV converts the sun's energy directly into electrical energy and does not require any rotational machines [62] and hence, it does not produce any noise or any harmful emissions to the environment. A PV also requires less maintenance and has a longer life. PV arrays are made up of more than one solar cell which can be connected in a series or parallel configuration. Solar cells are connected together to boost the output voltage because the voltage generated by each cell is very low of around 0.5V. Series connected solar cells provide more voltage while parallel configurations balance current requirements [63] The energy generation pattern for simulation purposes is shown in Fig.2-19.

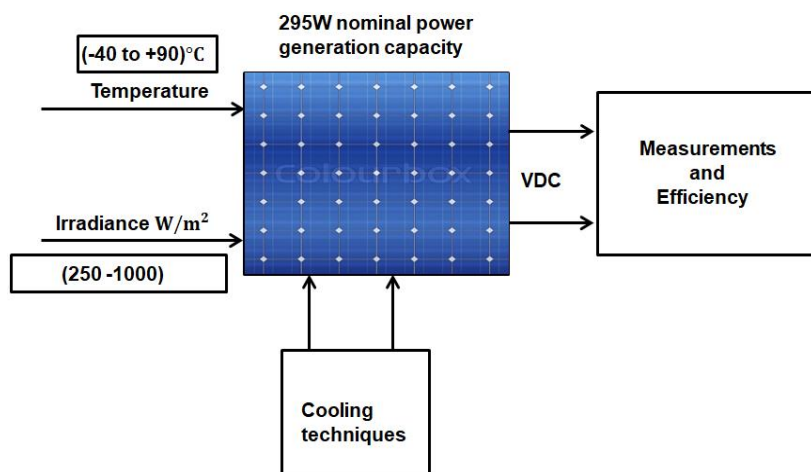


Fig.2-18: Simulation of the solar system that is used to generate electrical energy

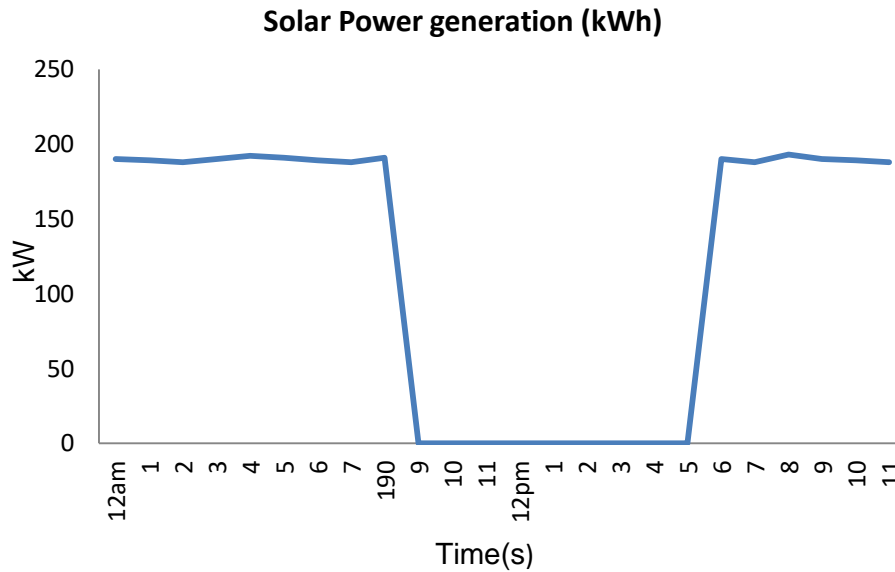


Fig.2-19: Shows the power generation by the solar system. From 9pm-5am no power is generated therefore a storage system and fuel generator will meet the energy demand at this time

The simulation model of a solar energy system developed here is validated with a case study in section 2.7 by using data collected from solar energy systems in Pakistan. The focus is on the influence of temperature on photovoltaic systems.

2.7 Case Study: Solar energy system in Pakistan

The influence of temperatures on the energy efficiency performance of PV-integrated buildings in Pakistan

Domestic dwellings in Pakistan have predominantly implemented low-carbon strategies by harvesting solar energy using photo-voltaic (PV) modules as a long-term vision of a low-carbon economy. Until recently, PV domestic users are facing the problem of prolonged disruption to solar energy due to overheating of the PV modules. PV-module efficiencies decline and are damaged due to exposure to surface temperatures in different parts of the country. Our investigations are performed on the surface temperature effects on the performance of PV integrated buildings during the summer and winter seasons. The results show that the Northern region of Pakistan is suitable for the installation of PV-systems due to optimal operating temperatures. During summer months, cooling strategies have to be implemented to overcome the heating effects to reduce degradation effects on installed PV-systems. The analysis performed shows that cooling techniques improve the quality of power generation and power converter losses but increase operating costs to households. Therefore, there is a need to optimally regulate voltages during peak fluctuating temperatures.

2.7.1 Overview of energy generation system in Pakistan

Substantial efforts to tackle the energy crises and carbon emissions with the rollout of PV modules integrated into buildings in Pakistan have already reduced the energy consumption of fossil fuels. It is well-known that electrical energy demands in Pakistan are increasing and are further creating the energy crisis within country. There is a huge gap between the energy generation and consumption [64] with a deficiency of 4000MWh of electrical energy in Pakistan and there are still many areas where there are no supplies of electrical energy [65] causing many hours of load-shedding and damaging economic growth. Due to this reason, most urban areas are suffering from 10-12 hours of power load-shedding. In rural areas, load-shedding occurs for between 16 and 18 hours a day [66]. The energy generation from current resources is not enough to overcome the energy demand. The utilisation of large amounts of fossil fuel produces carbon emissions that are contributing to climate-change [67, 68]. To reduce the effect, renewable energy resources are one of the solutions [69, 70]. Among renewable energy PV integrated buildings are important because buildings are responsible for over 60% of total energy consumption. The installation of photo-voltaic (PV) modules in the domestic housing of Pakistan is a relatively new and is growing faster due to a large demand for energy and its greater benefits in reducing carbon emissions [71]. In recent years, Pakistan is shifting its energy generation policy to renewable energy resources as it is installing massive power plants based on solar systems [72]. The government of Pakistan introduced new laws to increase the import of PV modules. As a result, there has been an increase of domestic residents across Pakistan who has installed solar systems to minimize the effect of load shedding [73, 74]. This assists in the reduction of loading on the network, improving the economy and improving the environment. Several projects have been completed such as the Quaid-e-Azam solar park installed in East Pakistan with a capacity of 300MW [75]. Another 150MW solar system has been installed at Faisalabad (Eastern Pakistan). o Many other projects are under construction in the west and other areas of Pakistan [76].

A recent study [77] from 69 metrological stations over the recent 30 years period shows that more than 70% the area of Pakistan receives an average yearly solar radiation of 5.5 kWh/m²/day as shown in Fig.2-20. Data collected by the Pakistan metrological department for the five major cities of Pakistan shows that the west of Pakistan (Quetta) located in Baluchistan receives 21.6 MJ/m²/day. The annual average in the other cities of Pakistan such as Lahore receives 19.25 MJ/m²/day, Karachi has 18.7 MJ/m²/day, Multan has 18.36 MJ/m²/day and Peshawar receives 17.0 MJ/m²/day. The investigations were carried out by

using temperature ranges from minimum to maximum in those areas and by considering the sunshine duration. This data was compared with the National Renewable Energy Laboratory (NREL) of USA which shows a better average capacity of 5.5kWh/m²/day to 7.5kWh/m²/day [78-80]. Some cities in the province of Baluchistan and Sindh such as Larkana, Quetta receives 5.5 kWh/m²/day. The other studies [81,82] show that areas of Pakistan that are situated from North latitude 24°C to 37°C and East longitude 65°C to 75°C latitude [83] receive the best solar radiation in the world. Therefore, there is the potential to extract high amount of solar energy.

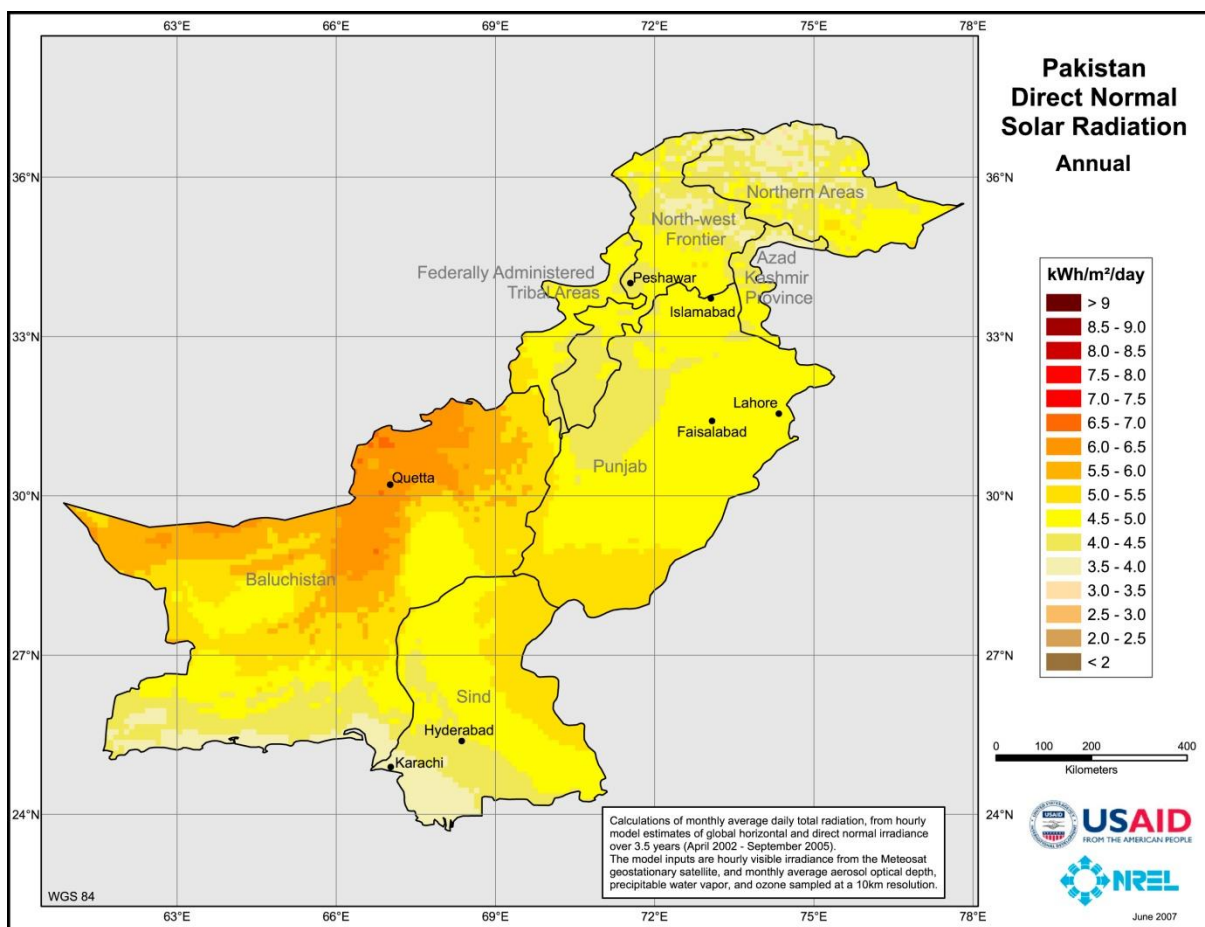


Fig.2-20. Pakistan annual direct solar radiations (Abdullah et al. 2017)

Energy generation from PV systems depends on environmental conditions due to the variations in surface temperatures across different parts of Pakistan [84]. During the summer months, consistent higher temperatures reduce the power generation capacity of the solar system, ultimately damaging the performance of PV modules. In the winter, temperatures fall to a low level and the PV modules again underperform at [85]. To address the overheating and

low temperature issue, a temperature regulation system is required with high reliability and fast real-time features. This will improve the reliability of the power flow from solar energy [86]. Therefore, heating and cooling strategies have to be implemented to overcome losses due to the temperature effects in several parts of Pakistan to maintain power generation from the solar system across the year, irrespective of the changes in weather conditions. The following sections investigate the effects of temperature and duration of solar radiation on a simulated model of a PV system and compare the results with data from real PV systems in different regions of Pakistan.

2.7.2 Model of a monocrystalline Photovoltaic (PV) system

The sunlight incident on photovoltaic cells can be absorbed or reflected or pass through the cells. The absorbed light by the cells generates electrical power, also known as solar power [87, 88]. Solar cells achieve better efficiency in a cold environment compared to a hot climate. So it is very important to examine the climate changes in several areas before considering the installation of a solar system. The investigations show that the best temperature for solar panels to produce energy is between 0°C and 25°C. For every degree rise in temperature above 25°C, the efficiency of the solar panels reduces by 0.25% for amorphous cells and 0.4-0.5% for crystalline cells [89]. During summer the temperature in most areas of Pakistan reaches 45°C which reduces the efficiency of the panels by 15% so that 295Wh rated solar system generates up to 195Wh.

A PV monocrystalline system is designed and modelled with the nominal power generation capacity of 295W and nominal power point output voltage of 31.5 VDC for the residential sector in several areas of Pakistan. A schematic diagram of the model is shown in Fig.2.21. The system is validated by analysing the simulation results in MATLAB and Simulink and comparing with the output power measured at different temperatures across several areas of Pakistan such as the North-East, North-West, South-East and West side of Pakistan. The efficiency of the power generation from the solar system is measured for winter and summer months.

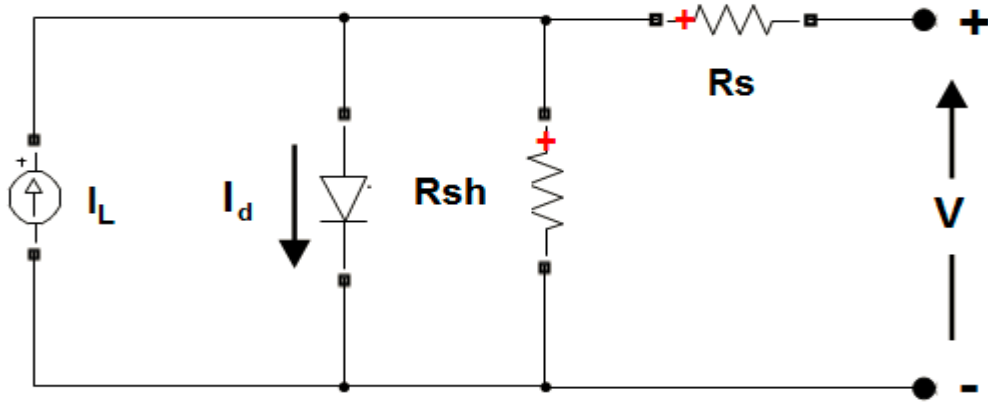


Fig.2-21: illustrates the schematic model of the solar system. The measurements are used to examine the output at different temperatures.

The temperature and irradiance directly affect the power generation from the solar system. The relation of the solar photovoltaic current to the temperature is described as [90].

$$I_{ph} = (I_{scn} + K_1 \Delta T) \frac{S}{S_n} \quad (2-2)$$

Where I_{scn} is the current generation at the suitable conditions i.e 25°C and 1000W/m². ΔT is the difference between the actual temperature and nominal temperature. I_{ph} is the photo voltaic current. S is the actual irradiation on the solar panels and S_n is the nominal irradiance.

The temperature effects on the diode saturation current I_o can be described as [91]

$$I_o = I_{on} \left(\frac{T}{T_n} \right)^3 e^{\left[\frac{qE_{Go}}{N_s k} \left(\frac{1}{T_n} - \frac{1}{T} \right) \right]} \quad (2-3)$$

Where I_o the saturation current, E_{Go} is the bandgap semiconductor energy, N_s is the total number of solar cells which are linked with series as [92].

$$I_{on} = \frac{I_{scn} + K_1 \Delta T}{e^{((V_{ocn} + K_v \Delta T) / V_T)}} \quad (2-4)$$

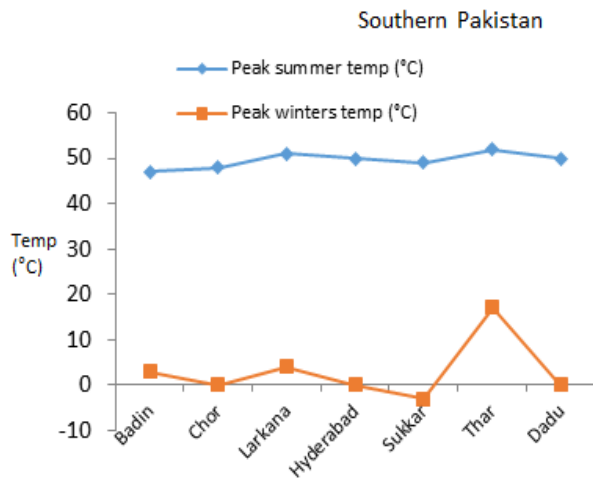
I_{on} is improved by including the K_1 and K_v temperature coefficients of the PV module. This modification is used to determine the voltage at the several ranges of temperatures. The I_o saturation current is dependent on the temperature.

Tab.2-1: The nominal parameters of the implemented PV system

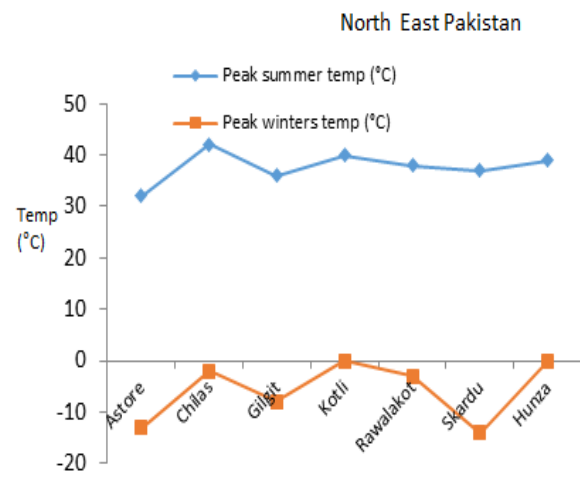
Parameters	Values
Nominal Peak Power Output	295 W
Maximum power point voltage	31.5 V
Maximum output current (A)	5.71 A
Open circuit voltage	40.0 V
Short circuit current	10.10 A
Maximum power point current	9.45 A
Module efficiency	17.59%

2.7.3 Temperatures across Pakistan

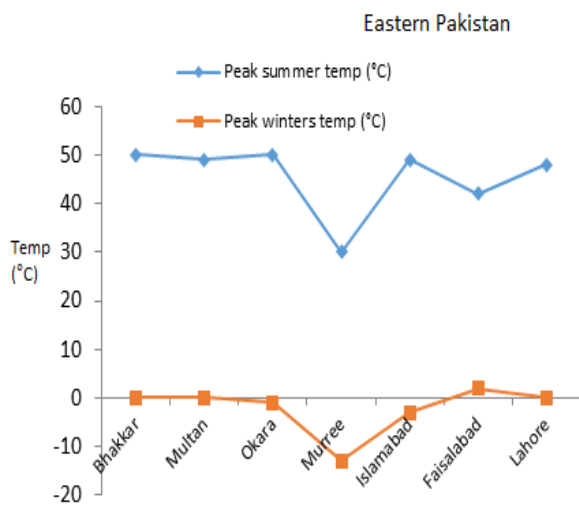
Temperature is one of the major elements which conclude the climate of any area. Any change in temperature results in climate change of the region. The change in climate affects the power generation from the solar system. Most of the areas in Pakistan experience high temperatures being above 45 °C in the summer season. During winter months the temperature goes down to -15°C in some areas. Such extremes of consistent temperatures for many months reduce power generation from the solar system. Fig.2-22 (a) shows the temperature across several areas of Sindh (Southern Pakistan) where Thar and Larkana have the highest temperature during the summers. These areas are also in the high temperature range during the winter season. Fig.2-22 (b) illustrates the surface temperature in Gilgit Baltistan and Azad Kashmir (North East Pakistan) where the winter temperature goes to -15°C and in the summer the temperature remains between (30-40) °C. Temperature values in the Punjab (East Pakistan) are shown in Fig.2.22 (c) where the summer temperature remains (40-50) °C. The temperature in the area of Khyberpakhtoonkhaw (North West Pakistan) is shown in Fig.2-22 (d). In this region, temperature is different across several areas. Fig.2-22 (e) demonstrates the temperature in the province of Baluchistan (West Pakistan). During the winters some areas see a very low temperature of - 15°C.



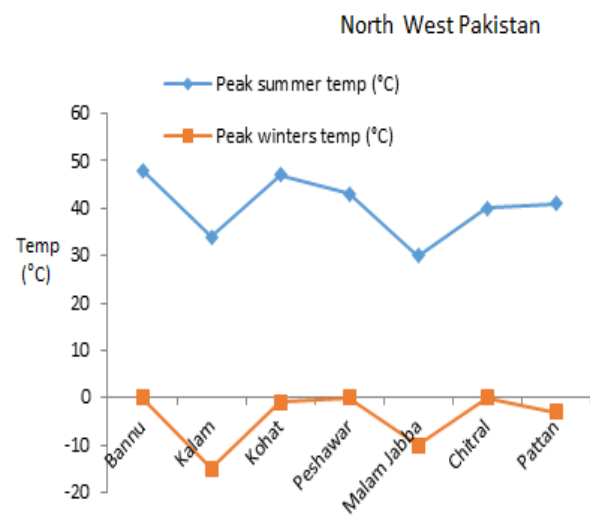
(a)



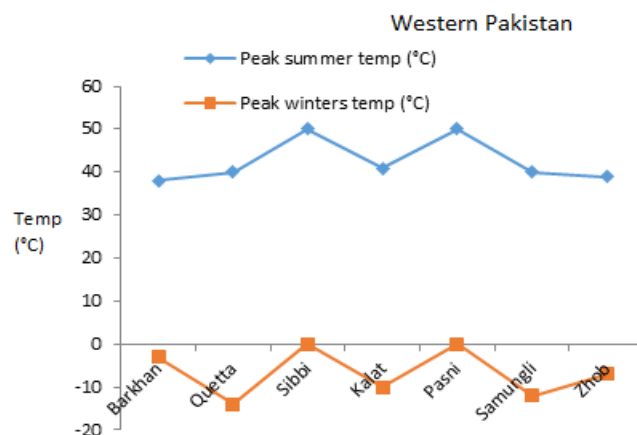
(b)



(c)



(d)



(e)

Fig.2-22: (a) Shows the temperature in Southern region of Pakistan (b) Temperature analysis in North East of Pakistan (c) Temperature found in Eastern areas of Pakistan (d) Temperature analysis in North West Pakistan (e) Temperature forecast in Western region of Pakistan.

The average temperature in several areas of Pakistan is shown in Tab.2-2 in terms of summer and winters. As the performance of the solar panels is linked with temperature, hence the average temperature in different areas of Pakistan needs to be known for design and installation purposes.

Tab.2-2: Average temperature in most of the areas of Pakistan [93]

Parameters	North average ambient temperature	South average ambient temperature	East average ambient temperature	West average ambient temperature
Summer	45	55	50	49
Winter	-15	-3	-15	-13

2.7.4 Simulation results from the model and discussion

A solar system simulated in MATLAB Simulink is tested at temperatures between -40°C - 55°C at irradiance of $1000\text{W}/\text{m}^2$. These parameters are similar to the real time climate condition in Pakistan during several seasons. The measurements are obtained for voltage, current and the maximum power against temperature. The results are analysed to improve the power output, voltage and short circuit current at different temperatures. Fig2-23 shows that the rise in temperature reduces the voltage power and current. The output voltage can be fixed (maintained at desired voltage) by using power electronic converters such as DC/DC or DC/AC, but the output power can only be balanced by addressing the heating effects on the solar system.

Tab.2-3: The measured output power/voltage and current (A) results at several temperatures from the simulated system

#	Temperature °C	Open circuit Voltage (V)	Maximum power point voltage	Maximum power point current (A)	Max power (W)
1	-40	37.6	30.5	8.69	265
2	-35	38.0	30.6	8.69	265
3	-30	38.2	30.7	8.72	267
4	-25	38.4	30.8	8.75	269
5	-20	38.6	30.8	8.8	271
6	-15	38.7	30.8	8.87	273
7	-10	38.8	31	8.87	274
8	-5	38.9	31.1	8.87	275
9	0	39.4	31.2	8.86	276
10	5	39.0	31.3	8.9	278
11	10	39.0	31.3	8.92	279
12	15	39.3	31.4	8.95	281
13	20	39.4	31.4	9	282
14	25	39.9	31.5	9.45	295
15	30	38.9	30.8	9.05	278
16	35	38.2	30.4	9	273
17	40	37.5	30	9.2	276
18	45	36.9	29.6	9.1	269
19	50	36.2	29.2	8.95	261
20	55	35.5	28.7	8.81	252
21	60	34.8	28.25	8.67	244
22	65	34.2	27.8	8.53	237
23	70	33.5	27.2	8.37	227
24	75	32.8	26.7	8.22	219
25	80	32.1	26.2	8.07	211
26	85	31.4	25.6	7.91	202
27	90	30.7	25.2	7.75	195

The recorded data have been plotted to determine the correlation between power (W), current (I) and voltage (V) with temperature ranging from -40°C to 90°C . Fig 2-23 (a) illustrates the voltage reduction by the increase in surface temperature. It shows the output voltage from the PV system in the range of $1000\text{W}/\text{m}^2$. The desired voltage is 31.5 VDC and the achieved voltage is reduced to 25.2VDC when increasing the temperature but at the $0\text{-}25^{\circ}\text{C}$ voltage is very close to the nominal voltage. As the temperatures are dynamic, it is necessary to install the PV system in lower-temperature areas or by using cooling techniques which then increases the energy cost. However, it will increase the output efficiency of the

power generation when operating the PV system under nominal weather conditions. Fig. 2-23(b) shows an influence of increasing the surface temperature on the output power of the modelled PV system. The output energy generated is reduced due to the increase of surface temperature effects on the PV modules. Fig2-23 (c) shows the temperature effect on the output current from the PV system, illustrating the output current for several temperature ranges.

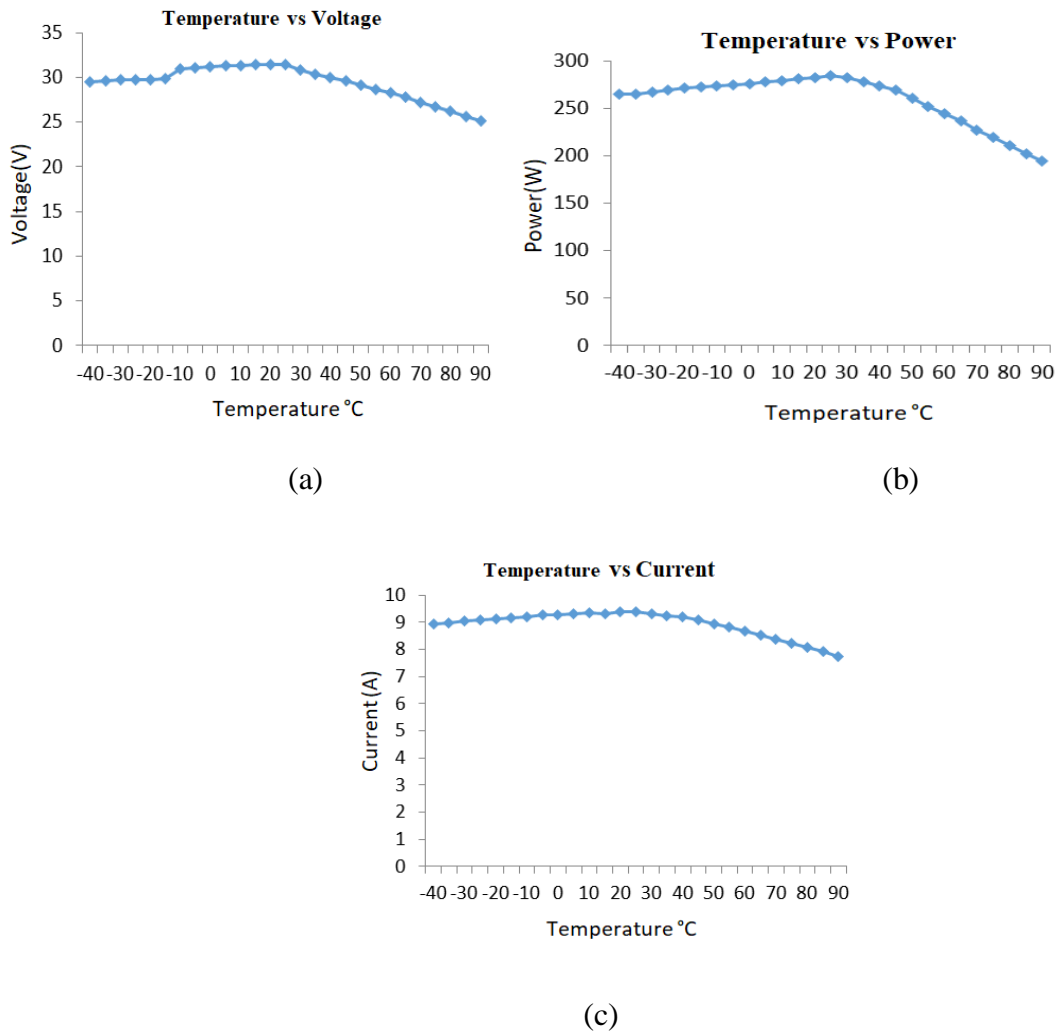


Fig.2-23: (a) Illustrates temperature effects on the voltage (b) Temperature vs solar system electrical power (c) Output current variations at different temperature.

The simulation is carried out to validate the temperature effects on the PV structure where the voltage (V), current (A) and Power (W) are measured to analyse the temperature effects on the system. A fixed irradiance of $1000\text{W}/\text{m}^2$ is applied constantly as shown in Fig.2-24. A 100W load is applied at the load side to measure the efficiency of the system.

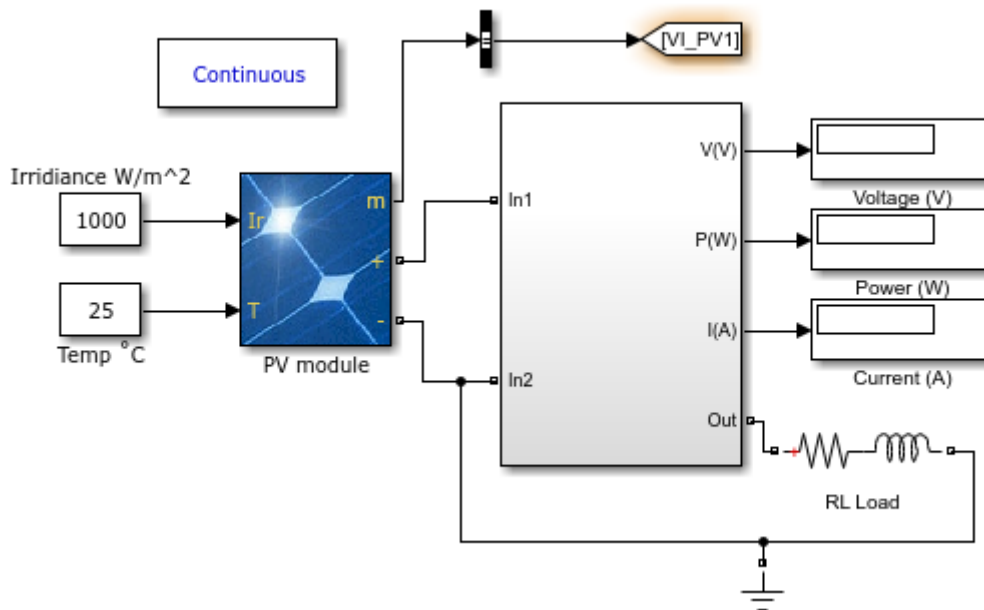


Fig.2-24: Shows the model of the simulated solar system tested at 25°C, this system is also tested at different temperatures. 100Wh resistive/inductive loads are used to measure the efficiency of the system.

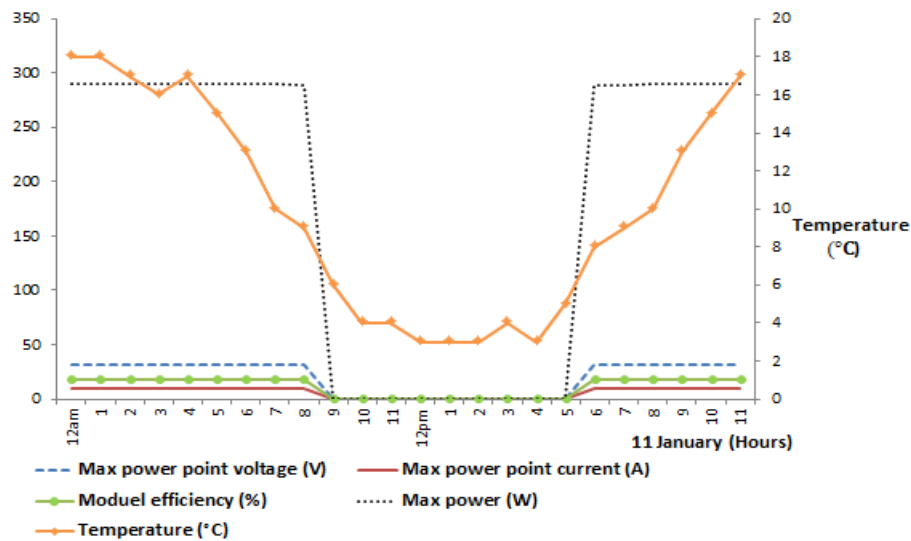
2.7.4.1 PV integrated buildings in Eastern Pakistan

Investigations were performed to discover the conversion of solar radiation into electrical energy and ways to achieve the desired output power at different temperature, PV orientation and irradiation level. In order to investigate the power flow from the PV system, current-voltage linkage is analysed. Solar arrays can be designed in parallel and series to achieve the required output power. The current-voltage and efficiency are investigated in Eastern Pakistan to examine the temperature power flow in integrated buildings. In this study, one day (24 hours) the effect of temperature is carried out in different seasons such as summer and winter. The performance of a PV array changes according to the weather changes. Day light hours in summer have more impact on the PV structure due to severe changes in temperature, air speed and humidity. Therefore, different weather conditions were focused on to measure the energy generation efficiency from the solar system. This knowledge can be used to manage energy of integrated buildings across Pakistan, reduce the installation cost of the solar system. Investigations were carried out in Eastern Pakistan to examine power generation efficiency from a PV structure. The output power, short circuit current and voltage

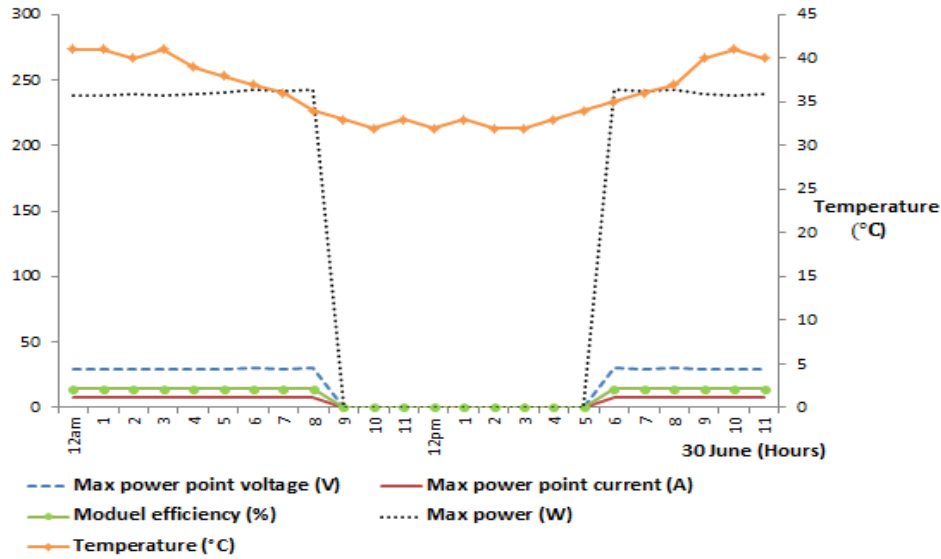
were recorded against temperature. It is observed that during the cold season, the efficiency of power generation remains very close to the nominal values. Fig2-25 (a) shows the electrical parameters of the solar panels at several temperatures during 11th January. The results are concluded in the eastern Pakistan where the capital of eastern Pakistan ‘Lahore’ is taken for investigations. The recorded voltage (V), power (W) and Current (A) are plotted to investigate the variations in these parameters. As expected, the power output, voltage and current decrease with the increase in temperature. Output current I_{sc} undergoes marginal changes. The efficiency in power generation during June is lower than January.

Tab. 2-4: Demonstrates the average reduction in power generation during the winter and summer season in Eastern Pakistan.

Days	Average Power loss (W)
11 January	28
30 June	56



(a)



(b)

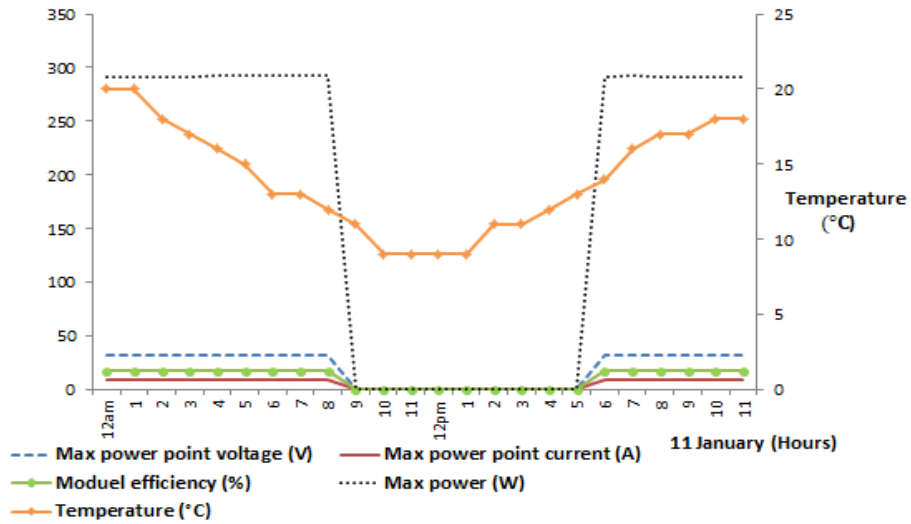
Fig.2-25: (a) Shows temperature effects on the PV structure in peak winter day in Eastern Pakistan. (b) Peak summer day analysis in eastern Pakistan.

2.7.4.2 PV integrated buildings in West Pakistan

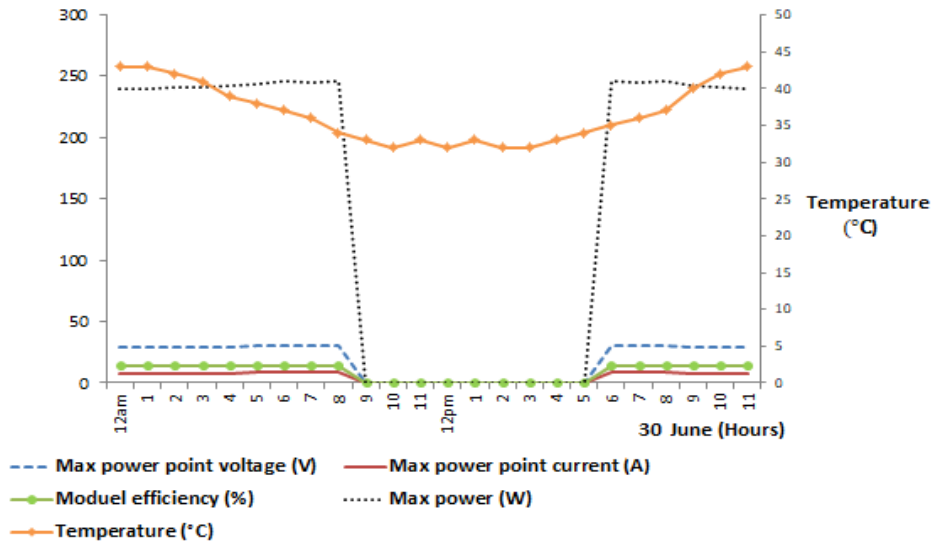
In order to test the performance of the PV structure, 1000 W/m^2 and real time one day (24) temperatures are applied for the different seasons in Western Pakistan where the capital city ‘Quetta ’ is chosen for investing the power flow from the PV module. The results are shown as current/voltage and efficiency against temperature. The PV array has open circuit voltage of 31.5VDC, short circuit current is 8.1A and the maximum load circuit voltage is 29.5VDC. Here the load circuit voltage and current is considered to examine the voltage/power drops at different temperatures. The solar panels performed better on the coldest day with an efficiency of 93.46% and the voltage flow remains closer to the nominal value during the winter day (11 Jan) as shown in Fig 2-26 (a) PV module operating hours between 9pm-5am do not generate power due to little irradiance. During the hot season, the efficiency is reduced to 86.45% and the voltage level drops considerably during the hottest day. Fig 2-26 (b) illustrates power generation in Quetta, West Pakistan on 30 June. The voltage flow is very close to the nominal value and the power efficiency is improved.

Tab.2-5 S Average reduction in power during the hottest and coldest day in western Pakistan.

Days	Average power losses (W)
11 January	24
30 June	52



(a)



(b)

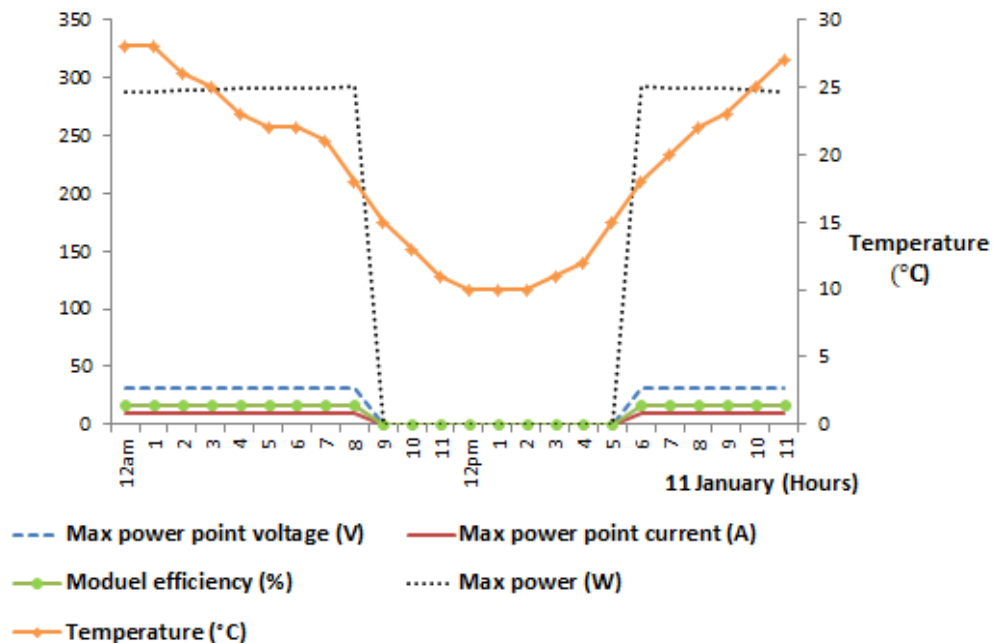
Fig.2-26: (a) Temperature effect on the solar power in Quetta on the hottest day, West Pakistan. The voltage/efficiency is reduced during both seasons. (b) Peak winter day power generation

2.7.4.3 PV integrated buildings in Southern Pakistan

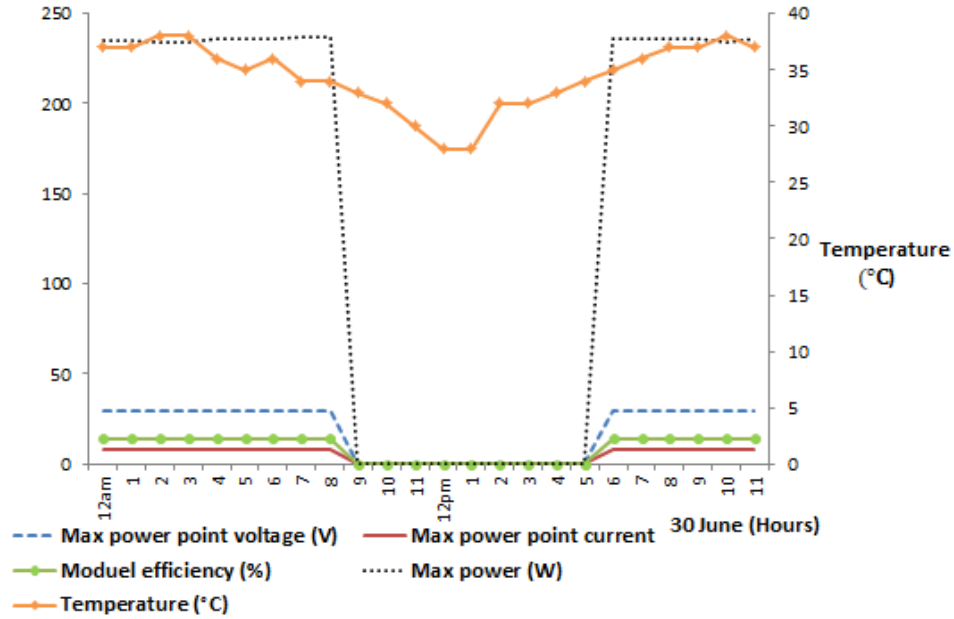
An off-grid PV system is examined with a nominal power generation capacity of 100Wh at different temperatures and irradiance level of 1000 W/m² with a rated load short circuit voltage of 29.5VDC. During the investigations, the data has been collected for 24 hours, to investigate the weather effects on the PV system to compare the efficiency of the system during winter and summer seasons. The maximum temperature observed in the southern region (Thar) during the winter season is 29°C and the temperature remains between (30-40) °C during the summer days. The results showed that this area is the worst for installation of solar panels in both summer and winter seasons and the PV array performance is severely reduced because the temperature remains high during both seasons due to being closer to the Indian Ocean. The voltage is dropped to 26.3 VDC where the nominal voltage is 31.5VDC. The efficiency is 87.7% on the summer's hottest day and 91.9% during the winter season at the operating hours from 5am-9pm. Fig.2-27 shows the power flow analysis on the Thar, Southern region of Pakistan.

Tab.2-6 The output power reduction from the solar system

Days	Average Power losses (W)
11 January	32
30 June	57



(a)



(b)

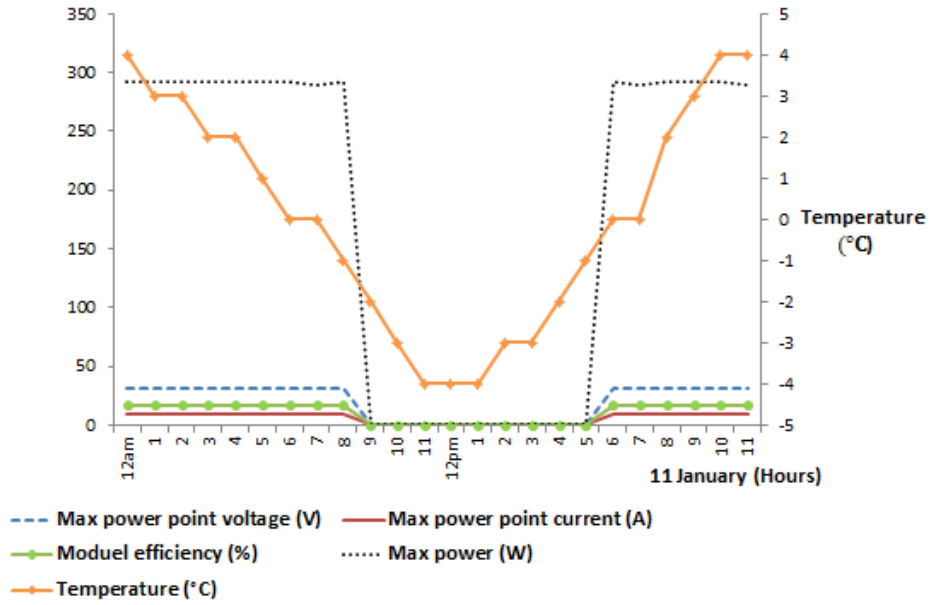
Fig.2-27: (a) The efficiency of power/voltage generation at the peak winter day temperature - PV structure in the southern region of Pakistan. (b) Peak hottest day: power drops at the PV module are increased

2.7.4.4 PV integrated buildings in North Pakistan

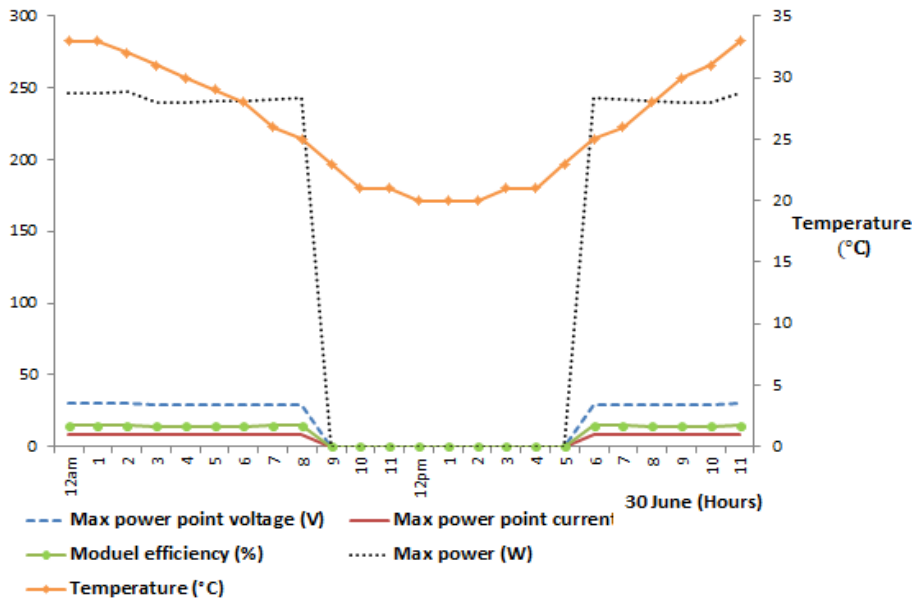
PV module works efficiently at a certain temperature and the best temperature for the PV module is 25°C. There is a need to design new ways to improve the efficiency of the PV system during non-optimal temperatures e.g. by including cooling techniques. In this section, investigations are performed to examine the solar power generation at North Pakistan Gilgit area. This is the hilly area where the temperature remains between (-5 to -33)°C throughout the year. This area is more suitable to install the solar panels because of efficient temperature. Fig.2-28 illustrates the temperature effects on the power generation at Gilgit, North Pakistan. The PV power generating efficiency and voltage are improved as being closer to the nominal values. This is the best areas that show the improved results for the PV module throughout the year.

Tab.2-7 Demonstrates the decline in power generation in northern Pakistan

Days	Average energy losses (W)
11 January	17
30 June	48



(a)

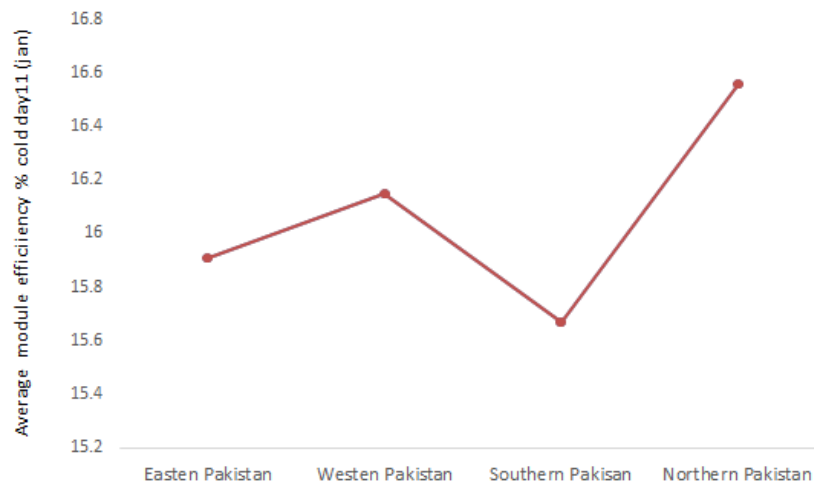


(b)

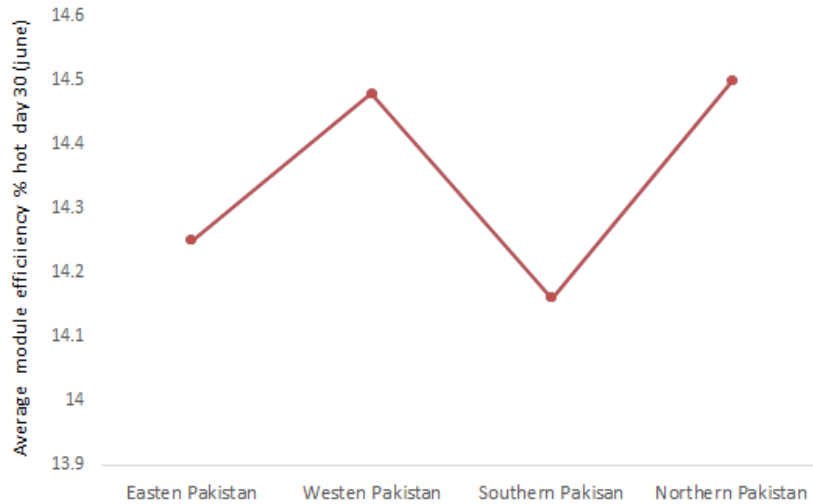
Fig.2-28: (a) Power generation from the solar system in Gilgit, North Pakistan in the winter season. During this time, the PV module is generating power/voltage efficiently and better than the rest of Pakistan. (b) Power analysis on the hottest day of 30 June

2.7.5 Comparative analysis of PV integrated buildings in different regions of Pakistan

It can be seen that the northern areas have the lowest power reduction in all weather conditions. In other parts, during the summer losses increase with a temperature rise and are areas that are not perfect for installation of solar systems. The effect can be minimised by the implementation of cooling techniques that reduce the temperature effects on hot days. Fig.2-29 (a) shows the results taken during the coldest day of the year where temperature remains between -5° to 35° in several areas. During this day, all of the areas are showing better performance for power generation from the solar system. Fig.2-30 shows the efficiency analysis of the PV module across Pakistan.



(a)



(b)

Fig.2-29: (a) Module efficiency analysis for the peak winter day. (b) Efficiency analysis during the summer day

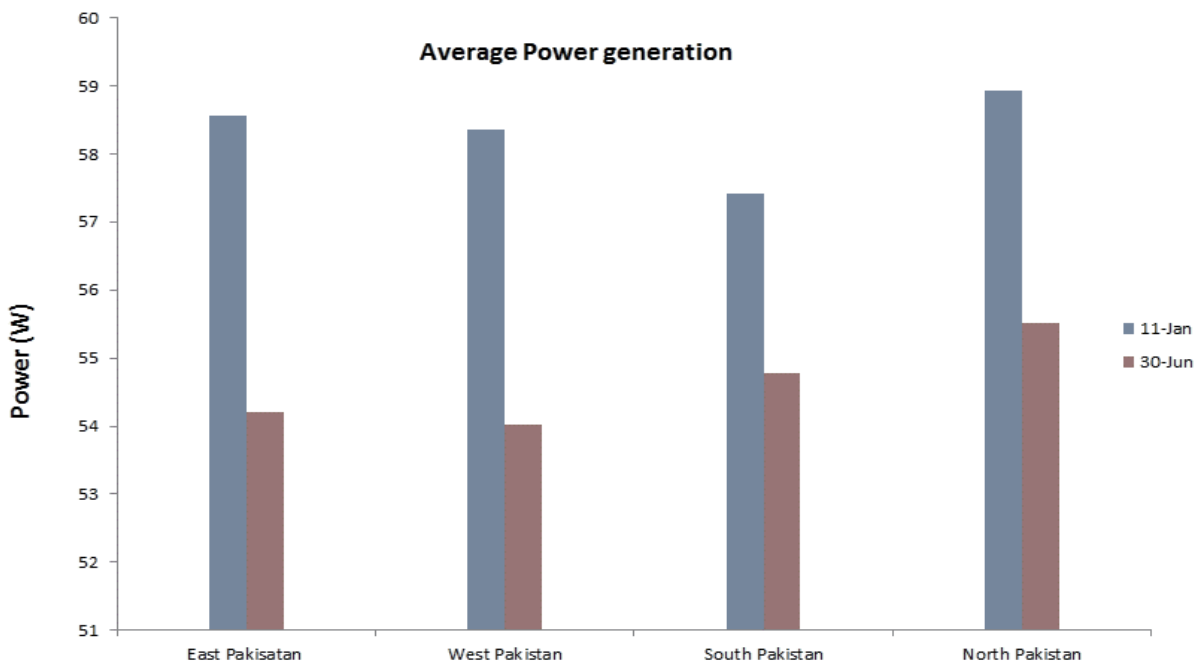


Fig.2-30: Average solar power generation on two days, irradiance of 1000 W/m^2 between 5am-9pm and 0 W/m^2 for from 9am-5pm. Nominal power generation capacity of the solar panel is 100. It is reduced to (53-56) % due to temperature and irradiance effects

Summary

In this chapter, a renewable energy (solar and wind) based electric-vehicle charging station is investigated. Investigations are carried out to determine whether the renewable energy generation system is capable of supplying the required energy during the peak/off-peak times.

Research is carried out on instability factors in the transmission grid which is required to transmit 100 % of generated renewable energy. Power parameters in renewable energy transmission are always varying so there must be a control system which reduces the disturbances and maintains stability in the system. Instability issues related to renewable energy transmission are described with analysis and solution. The major parameters which are focused on are voltage instability and frequency instability and what factors affect them. It is proposed that by using the appropriate power flow techniques such as PWM waves, the instability issues can be reduced. There must be a protection system as well which isolates the line during faults and connects it again as the fault cleared. If instability remains for a long time it will damage the grid systems. Solutions to these problems are proposed and investigations conducted to determine how environmental conditions, over loading, under loading and other conditions affect the power transmission in a micro Grid. Various instability factors are analysed and then methods proposed to find appropriate solutions.

Most of the urban areas in Pakistan stay hot and humid in the entire year. Since all the locations in Pakistan have different temperatures, a study needs to be performed before installing the PV system. In this chapter, a simulation study has been performed to examine thermal effects on the solar system. As part of the investigations; the day (24 hours) analysis was made for the four provinces of Pakistan where the worst cold and hot day's temperatures are taken for investigations. The study has identified the efficiency decrement in power generation by the rise in temperature. It is found that during the summer season in the southern and eastern regions of Pakistan, voltage drops by 25.2 VDC and the power efficiency reduces by more than 15% during e PV operating hours. It is seen that the areas in the North region of Pakistan such as Gilgit achieved the best results where the voltage/power generation efficiency of the PV module is closer to the nominal values than the other regions throughout the year and is a better place for the installation of solar panels. This area is found to be efficient for solar power generation because of a suitable temperature range between 0-30 degrees throughout the year. During the summer, in the rest of Pakistan, the temperature goes very high which reduces power generation from the solar panel. But during the winters, solar power is more efficient throughout Pakistan. The future work is to investigate other cities of Pakistan which are close to the Indian Ocean and mountainous areas.

Chapter 3 Architecture of a proposed smart microgrid

A smart scalable and modular DC structure is proposed that allows unidirectional energy flow from the wind/solar and bidirectional networking of the storage system and which efficiently transmits the energy to the EV charging station. This type of grid is becoming possible by the development of higher processing units such as FPGA's and other micro processing units. This grid has advanced features and is different from the conventional grid because it transmits power directly from the wind and solar energy sources as well as from conventional sources such as hydro, nuclear or fossil fuels. The inherent benefit of the proposed grid architecture is the sharing of power resources that increases the system efficiency. Furthermore, it reduces the losses on the micro grid by matching the consumption and the load in a close proximity. Hence, the micro grid has improved transmission efficiency and increased the power quality. The implemented smart grid has the features of sensing the network overloading and managing power to prevent the power outage. It works autonomously during the conditions that require responding rapidly to achieve the aims of power generation companies and the consumers. The grid has the features to sense the energy shares from different resources and is capable of functioning from the conventional energy generation system as well as renewable energy resources. The smart features are included in the micro grid system due to uncertainty in load variations and equipment failure. The sensors are applied at different points of the system that are connected to the micro grid centralised control unit. The centralised control unit is connected to sensors to record the data and take appropriate action. The purpose of designing the smart grid is to deliver the electrical energy in an efficient way from generation point to the electric-vehicle charging station. The energy flow is unidirectional from the wind and solar energy and the smart grid. The energy flow is bidirectional between the storage system and the micro grid system. Advanced control implementation and energy management techniques contribute to improved efficiency of the overall system. These technologies include smart sensors, centralised control units, protection and voltage regulation systems. The smart grid is capable of meeting the consumer demand with the integrated infrastructure. The smart micro grid reduces the load on the conventional transmission network and transforms control to the consumer from the centralised electric industry. It makes this happen by implementing modern technologies that enable the users to create a share in the electric grid and enable the users to achieve the full potential and control in power consumption. Many of these ideas are

already operational such as smart meter implementation that enables users to monitor the usage of electric power.

3.1 DC Power implementation with Analysis

The technology advancement in power conversion, transmission and generation has increased the demand for DC power flow. However, there are still many challenges in the DC type power applications such as protection, control, spikes and oscillations in the power flow. One of the other factors is that there is no standardization for the low voltage DC micro grid. The implementation of the DC micro grid for residential sectors requires the installation of a power conversion system in each house that connects the loads to the micro grid [94]. These converters should have a protection system to isolate the power connection during short circuits. The installation of these converters is generally expensive to deal with the higher power usage at the load sectors. Relatively little implementation of the DC system in industry and residential sector are hindering the spread of the DC type power transmission.

However, DC technology is being implemented into high voltage transmission systems where it has achieved higher efficiency. The domination of the AC type power flow is reducing by the advancement in power electronics components that allow attaining the required voltage level by using fast microcontrollers and microprocessors. The usage of high voltage direct current for power transmission is one example. High Voltage DC (HVDC) has lower losses and transmits power to longer distances than high voltage AC systems [95]. The higher switching frequency of the DC/DC power conversion system also results in advancement of DC type technology. Electrical power transmission is changing to DC systems to cope with the increasingly distributed energy sources. The DC type loads such as electric vehicles, telecommunication systems, ships and data centres requires the DC type power flow for efficient functioning. The usage of DC power in these types of loads improves the reliability and reduces the cost of the components. This requires the investigation of the efficiency, protection, reliability and power quality of the system which will increase design choices about the power generation and consumption.

3.2 Smart grid modelling and validation

A micro grid is simulated that is connected to the energy resources and car charging terminals. The basic parameter of this grid is resistance where inductance and capacitance are not considered due to DC type of power flow. The conductor of this grid is considered to be

manufactured of different materials such as aluminium with lower weight and higher reliability that can tackle higher current flow. Voltage on the micro grid is 585VDC which is equivalent to three phase AC voltage transmission in the UK. It is converted to user required voltage by implementing the Buck converter at the Electric Vehicle (EV) charging terminal. The voltage is converted to other levels by automatically applied duty cycle and the control system maintains the voltage flow on the micro grid and protects it from internal and external disturbances. It includes a sensor system to measure the power flow to protect the micro grid. Fig.3-1 represents the power flow on the micro grid used to charge up car batteries where the nominal power flow is 200KW. Power flow is investigated by using two different types of loads which are EV batteries and the ultra-capacitors by using the manual switch. This switch enables us to select the voltage during the simulation run. The amount of power flow depends on the numbers of cars and type of batteries.

3.3.1 Smart grid system description

The proposed smart micro grid structure consists of a control and monitoring centre, a smart protection system, stability and control system, a measurement system, and the storage communication system to regulate the power flow on the micro grid. The DC grid is fed from wind and solar energy generation units where power is always fluctuating due to variable wind flow/sunlight and if the load is inductive or capacitive then transients and spikes arise in the grid. A regulatory system is required to create balance in the grid because achieving the desired voltage depends on the current (A) flow where an inductor behaves superlatively at lower frequencies while a capacitor has better performance at higher frequencies. In a DC grid there is no phase shift between the voltage and current. It means that the voltage is the only quantity that needs to be stabilised. Fig.3-1. illustrates the structure of the low voltage DC micro grid with the necessary components. A DC centralised unit plays an important role for balancing the power flow at the micro grid. Buck-boost converters are designed at DC link to control the voltage level. Circuit breakers are used to protect the DC grid. Bidirectional converters transfer power between the batteries and the grid. A bidirectional converter is placed between the DC micro grid and the battery bank. This converter will charge up and discharge the batteries and monitor the power flow at the grid and battery bank. If a fault occurs at the micro grid or energy demand increases, this converter will transmit the power from the storage system to the grid. This will enable the micro grid to

continuously operate at the isolated mode and will improve the system stability. The power flow in the micro grid is a unidirectional.

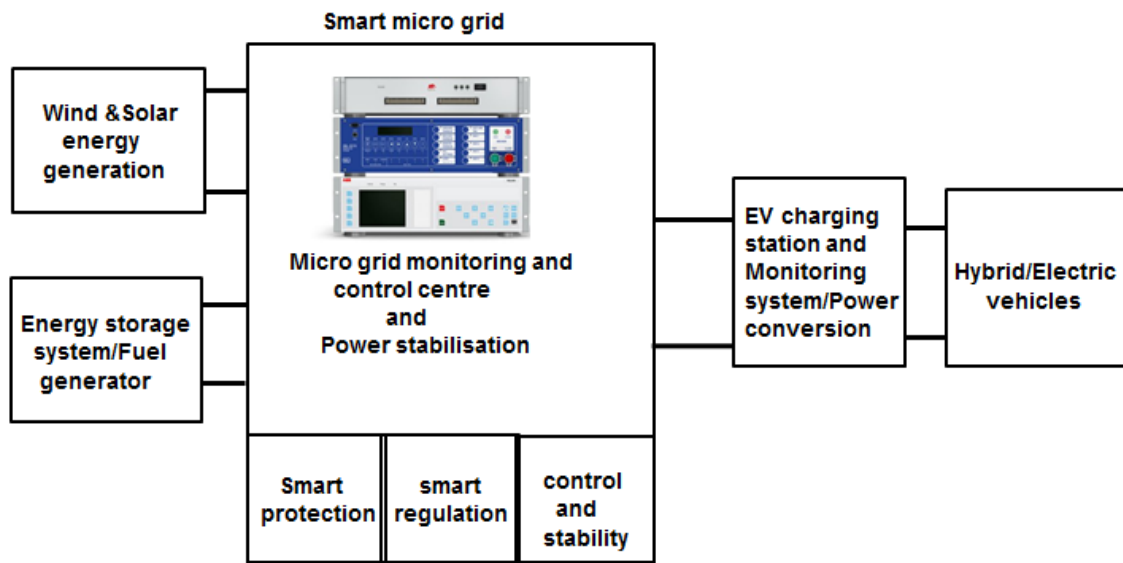


Fig.3-1: Block diagram of the integrated smart grid consisting of wind/solar photovoltaic (PV) system, storage system and Electric Vehicle (EV) charging station.

3.3.2 List of power conversion stations connected to the grid terminals

1. AC/DC power conversion station for the wind turbines
2. DC/DC power conversion station for the solar units
3. Central micro grid control and monitoring centre for the power regulations
4. DC/DC bidirectional conversion systems for the storage system
5. AC/DC conversion systems for the fuel generator

In order to examine the stability of power flow on the micro grid let us assume constant resistance, constant power and constant voltage at the terminal of the micro grid to create the mathematical formulation. Constant voltage is considered at every terminal because it is stabilised by the converter stations which are linked to the grid. The other converters are taken as constant power regulators that connect the renewable energy resources, storage system, and fuel based generation system with the grid. Constant resistance is taken due to fixed size conductors used for power transmission.

The power in the DC micro grid is divided into three subsets of $\{V, R, P\}$. Multiple constant voltage terminals are represented by $V = N \times N$ with a linked resistance. The single constant voltage terminal is not analysed because of five converter stations that are connected to the

grid at several points. The main terminal to maintain constant voltage on the grid is the micro grid control and monitoring centre and is linked with the others terminals. The nodes are classified in terms of control being used to regulate the voltage and power flow from the terminals. The admittance matrix for the terminal voltage and current on the grid $G \in \mathbb{R}^{N \times N}$ is shown as [96].

$$\begin{pmatrix} \mathbf{I}_V \\ \mathbf{I}_R \\ \mathbf{I}_P \end{pmatrix} = \begin{pmatrix} \mathbf{G}_{VV} & \mathbf{G}_{VR} & \mathbf{G}_{VP} \\ \mathbf{G}_{RV} & \mathbf{G}_{RR} & \mathbf{G}_{RP} \\ \mathbf{G}_{PV} & \mathbf{G}_{PR} & \mathbf{G}_{PP} \end{pmatrix} \cdot \begin{pmatrix} \mathbf{V}_V \\ \mathbf{V}_P \\ \mathbf{V}_R \end{pmatrix} \quad (3-1)$$

$$\text{Here is } \mathbf{I}_R = -\mathbf{D}_{RR} \cdot \mathbf{V}_R \quad (3-2)$$

For the single step node such as smart grid control and monitoring centre this matrix can be singular. Where \mathbf{D}_{RR} a diagonal matrix is for admittance is comprises of constant power links and \mathbf{B} is the susceptance.

$$\mathbf{V}_R = -(\mathbf{D}_{RR} + \mathbf{G}_{RR})^{-1} (\mathbf{G}_{RV} \cdot \mathbf{V}_V + \mathbf{G}_{RP} \cdot \mathbf{V}_P) \quad (3-3)$$

$$\mathbf{I}_P = \mathbf{J}_P + \mathbf{B}_{PP} \cdot \mathbf{V}_P \quad (3-4)$$

The power flow is evaluated by using the constant medium voltage of 585VDC. Power terminals are linked by the following equations where \mathbf{V}_P the voltage on the micro grid is and \mathbf{I}_P is the current flow.

$$\mathbf{P}_P = \text{diag}(\mathbf{V}_P) \cdot \mathbf{I}_P \quad (3-5)$$

The main terminal to regulate the power flow on the grid is the storage system connection with the micro grid. This terminal detects the voltage drops and power requirement on the grid to activate the storage system for supplying electric energy. \mathbf{P}_P can be simplified to

$$\mathbf{P}_P = \text{diag}(\mathbf{V}_P) \cdot (\mathbf{J}_P + \mathbf{B}_{PP} \cdot \mathbf{V}_P) \quad (3-6)$$

With

$$\mathbf{J}_P = \mathbf{G}_{PV} - \mathbf{G}_{PR} \cdot (\mathbf{D}_{RR} + \mathbf{G}_{RR})^{-1} \cdot \mathbf{G}_{RV} \cdot \mathbf{V}_V \quad (3-7)$$

$$\mathbf{B}_{PP} = \mathbf{G}_{PP} - \mathbf{G}_{PR} \cdot (\mathbf{D}_{RR} + \mathbf{G}_{RR})^{-1} \cdot \mathbf{G}_{RP} \quad (3-8)$$

Therefor the level of voltage on the DC micro grid can be set by solving the equation as.

$$\mathbf{V}_P = \mathbf{B}_{PP}^{-1} \cdot (\text{diag}(\mathbf{V}_P^{-1}) \cdot \mathbf{P}_P - \mathbf{J}_P) \quad (3-9)$$

P_1 = Node for Wind and solar power generation

P_2 = Node for Storage system

P_3 = Node for fuel generator

P_{load} = Electric vehicle load and losses on the line

$$P_T = P_{gen} - P_{utilised} \quad (3-10)$$

All these assumptions are completely verified by the analysis and the simulations results. P_1-P_T is unpredictable and are balanced by the P_2 and the regulation is achieved by the micro grid monitoring centre. The assumptions of P_1-P_T , can be solved by using successive approximation shown as [97].

$$\alpha = \frac{\|B_{PP}^{-1}\| \cdot \|P_{PP}\|}{V_{min}^2} \quad (3-11)$$

The voltage on the DC grid is maintained by supplying the required power to the loads and by applying the correct duty cycle at the converter switches as shown in Fig.3-2. Battery bank is another source for maintaining the power at the DC grid during the power shortages on the micro grid. However, batteries cannot regulate the voltage on the grid for a long period of time so a fuel generator is added to charge up the storage system.

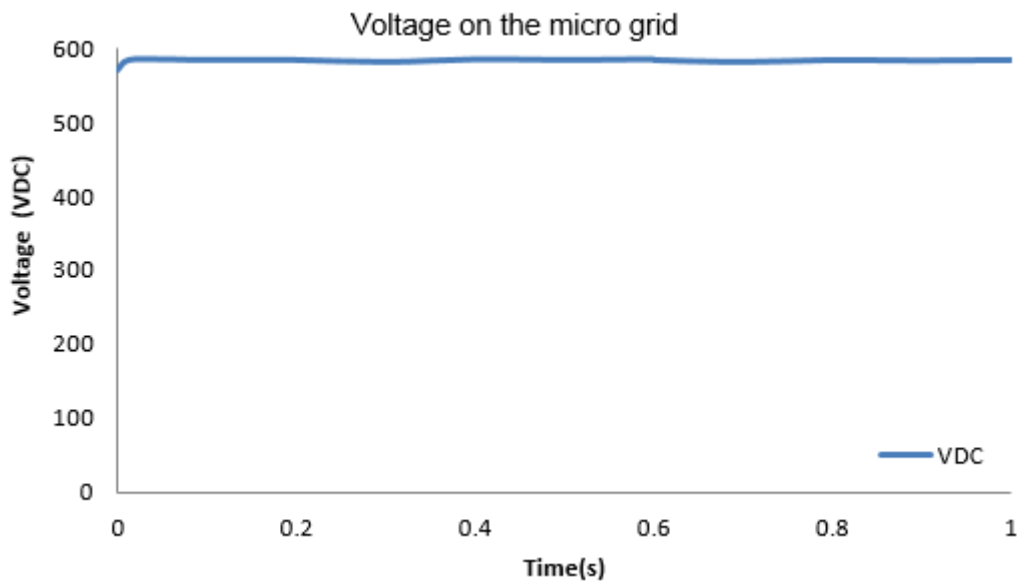


Fig.3-2: Voltage regulation on the micro grid.

3.3 Risk handling features of the smart grid

The power generation and energy consumption at the EV station are random hence there is always a chance that the load and the energy generation are not matching. The concept of risk handling to balance the power on the network must be taken into account. The aim of the proposed model is to reduce the risk that is calculated by implementing a centralised control

unit at the micro grid station. The major aim of the centralised unit is to balance the energy supply $s(t)$ and load side $d(t)$ at the fundamental point t , hence $s(t) = d(t)$. The energy consumption at the load side is stochastic with a probability distribution of power $P\{s(t) = d(t)\} = 1$. The energy generation has the features of reducing the supply by a certain amount ε . The failure to meet the energy demand is described by $P\{s(t) < d(t)\}$ or $P\{d(t) < s(t) - \varepsilon\}$. The probability of failure $P\{d(t) > s(t)\}$ and $P\{d(t) < s(t) - \varepsilon\}$. There is a need to reduce the risk to a minimum level.

$$P\{d(t) > s(t)\} < \alpha \text{ and } P\{d(t) < s(t) - \beta\} \quad (3-12)$$

Where α and β are the small digits 0.1% and 0.01% that are specified by the user.

The terminology of “generation following load” is a fact that the generation is always controllable and the load is not controllable because it is always changing. To further evaluate the load and energy generation system, the terms are separated to generation $REG(t)$ and load $EVL(t)$ into.

$$REG(t) = REG_d(t) + REG_s(t) \quad (3-13)$$

$$EVL(t) = EVL_d(t) + EVL_s(t) \quad (3-14)$$

Where $REG(t)$ includes wind and solar energy while $EVL(t)$ represents the load side that includes electric-vehicles. The energy balance between the load and the generation side can be arranged to

$$REG(t) - EVL(t) = EVL_s(t) - REG_s(t) \quad (3-15)$$

The left side of the equation can be described as a deterministic component generation/load, the total energy supply $s(t)$ and the net demand $d(t)$. The energy net supply is partly controllable and deterministic and the demand on the load side is stochastic.

3.4 Modelling of Smart grid decision procedures

The smart grid equipped with sensors and a centralised control unit are used to reduce the uncertainty in the system. The error between the load side and the generation side reduces following an exponential decay. For example, the error in the wind forecast can be inscribed as day ahead would be larger by 30% but the error a minute ahead would be zero. Simply, the probability of the net demand at the EV charging station can be used by the centralised control unit and the result would be steeper and sharper. Hence the multistage decision process can be adopted to reduce the uncertainty. The stages can be divided into the net

energy demand at the EV station e.g. a day ahead demand, an hour ahead demand and a minute ahead demand at the load side.

The net energy demand $d(t)$ is stochastic and updated at each stage day ahead, an hour ahead and a minute ahead by the information provided at the micro grid $P\{d(Y)\}$ at stages. The function J must be explained to reduce the overall expected uncertainty. The J is a function of dispatch decision of total energy supply $s(K_1, \dots, K_i)$ where $i = 1, 2, \dots, m$ analysed at all stages.

The RLD shown as π is derived to:

Choosing regulated net energy generation.

$$(K_1, \dots, K_i) \quad i = 1, 2, \dots, m \quad \text{e} \quad s(K_1, K_2), s(K_1, K_2, K_3) \quad (3-16)$$

To optimise the dispatch function J .

Referring to risk reducing parameters e.g.

$$P_m\{d(t) > s(t)Y_m\} < \alpha, P_m\{d(t) > s(t) - \epsilon/Y_m\} < \beta \quad (3-17)$$

3.5 DC centralised unit implementation on the smart grid

The modelling of the DC micro grid centralized unit is achieved to regulate the energy received from the wind/solar converter systems. If the input voltage recorded is lower than the nominal values, then it functions to boost the voltage and during the fluctuation it stabilises the voltage closer to nominal values. A DC link is established at the micro grid station where a low pass filter is applied to remove the transients and harmonics. It also supports to control the current and maintain the DC voltage level. According to changing loads at the charging stations, quality and stability should be achieved for a stable system.

Sum of power generation at the DC link can be described as

$$P_{DC \text{ link}} = P_{WT} + P_{PV} \quad (3-18)$$

$P_{DC \text{ link}}$ is the DC link where the power is added up, P_{WT} the wind turbine power and P_{PV} is the power received from the solar panels.

The overall supply to the grid can be described as

$$P_{DC \text{ grid}} = P_{WT} + P_{PV} + P_{\text{battery bank}} \quad (3-19)$$

$$P_{\text{system}} = P_{WT} + P_{PV} + P_{\text{battery bank}} - P_{\text{losses}} - P_{\text{load}} \quad (3-20)$$

During the peak times at the EV charging station larger oscillations are observed at the DC link. These are impacting the DC micro grid and creating variable voltage in the grid. Capacitors are used to reduce the oscillations at the DC link but it is affecting the converter properties. By decreasing the capacitance massive fluctuations at voltage were observed. Low capacitance can cause the breakdown in the semiconductor switches. When the value of DC link capacitor is reduced, distortions in the current happen. During the operational timings, voltage regulation at the DC-link is achieved by controlling the energy storage at the DC-link capacitor.

The model of the DC-link can be described as [98]

$$\frac{C V_{DC}}{dt} = i_{dc} - i_L \quad (3-21)$$

Where i_{dc} is the DC link current and i_L is the load current drawn by the loads.

Back-to-back converters are used to control the power flow at the micro grid. It is observed that the fluctuations in the DC power can be minimised if inverter side dc power and rectifier side dc power are equalised by using the PWM technique. By using PWM techniques current distortions are minimised. The voltage is also distorted due to existence of transients in the system. The best solution is to connect larger capacitors built with aluminium electrolyte to behave as an energy storage element. In some areas, electrolytic capacitors are not considered feasible due to reliability, weight and size. Also features of electrolytic capacitors weaken gradually with time. Choosing the right capacitor is very important because it reduces the ripples and extends lifetime of the converter. Reliability of VSC converters is also enhanced by using film capacitors instead of electrolytic. Buck-boost converters also play an important role in balancing the voltage flow at the DC link. If the voltage output of the rectifier is not balanced, then using the PWM buck-boost converter will stabilise it.

3.6 Smart grid protection system simulation and analysis

When the power flow is interrupted from a fault then the system can become unstable [99]. A fault in the DC converter station can affect the rotor angle of the wind generator and damage the components at the converter station. This depends on the duration of fault and components used to protect the system. The fault in the DC grid happens between the lines or

between the lines and the ground. When voltages at the micro grid are reduced then over current flow can happen which introduces transients in the system [100]. Due to reduction in voltage level, current flow can increase and cause more losses. The increase in current can also damage the conductor material and the equipment such as power conversion system. Controlling the current in DC grid is more complicated than AC grid. By switching on a DC current, electrical arcing can damage the switch. So there is special attention required to protect the components for DC power flow.

The implemented protection system has the capability to function correctly during a short circuit and other types of faults. The protection system consists of all the necessary tools such as controller, sensors, measurements, relays and breaker or switches. A programmable smart protection system is designed to protect the micro grid. Voltage and power flow are sensed at the grid and then signals transmitted to the controller for performing a required action. The input of the controller is connected to the voltage and current measurement sensors and the output is connected to the DC circuit breaker. The controller isolates the grid and power components when voltage or current exceeds a high threshold level. The output of the breaker is logical 1 or 0 where 1 means closed circuit and 0 means open circuit. The circuit remains closed during normal conditions and only goes to the open position when inappropriate power flow happens in the system. It is required for the circuit breaker to remain open during the first few seconds as higher power flow due to charging up of inductance and other components in the system. The protection system has to operate correctly or else the micro grid and other power components can be damaged. Fig.3-3 shows the structure of the protection system used to protect the micro grid. A MATLAB block operates as a major controller which compares the real time transmitted voltage with the reference voltage and then operates accordingly. The circuit breaker receives signals from the controller to protect the system. The breaker has the capacity to withstand a maximum variation of 5% of the nominal power. If the current exceeds the breaker nominal values, the logic zero signals will be sent to the circuit breaker to open it and stop transmitting power through it. But when the system returns to the nominal values, the breaker will go to close state to allow the power to flow through it.

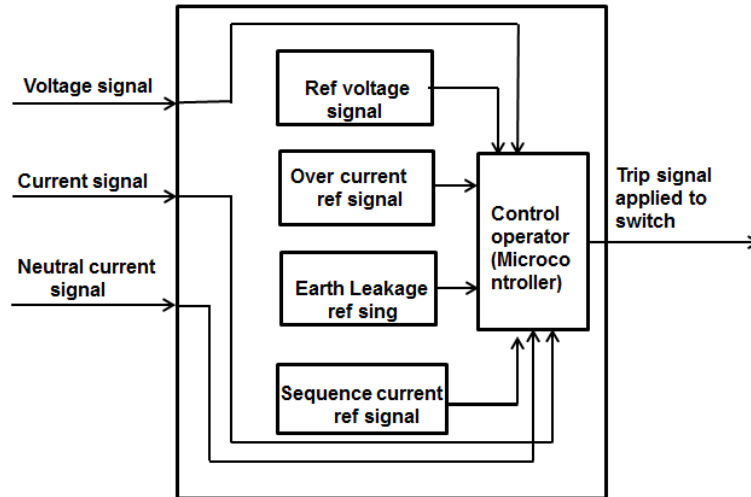


Fig.3-3: The internal structure of the protection used to protect the micro grid

3.7 Simulation results and transient responses on the smart grid

The Micro grid receives power from the renewable energy resources and is associated with several uncertainties. To reduce the uncertainties in energy generation, power flow on the grid is analysed and stabilised. Transients in the micro grid are observed as it consists of resistance and inductance (in converters) Transients arise in the micro grid due to variations in energy supply and charging up of car super capacitor batteries. Transients also occur due to usage of power electronics components used for conversion of power. Larger transients tend to change the microgrid power flow and make it less effective for power transmission. The transients are minimised by using low pass filters. It can be seen in Fig.3-4 that in the first 0.2 seconds the voltage and current overshoot and then settle to the nominal values.. This is due to charging and discharging of passive elements in the line. The transient can be more severe if the centralised control is not used to stabilise the generated power from renewable energy resources. Initially the observed power flow is observed to be higher due to charging up of converter components such as inductance and capacitance. Fig.3.4 shows the transients in voltage flow on the DC grid. Initially a spike is observed for few seconds and then the required voltage is achieved. A spike was observed at the start of a simulation due to charging up of inductance and power flow from unpredictable renewable energy resources and the existence of electronics components. Due to start up process of wind and solar system and charging up capacities and inductance elements a voltage spike was detected and then reached a constant level after 0.013s. VSC converters are used to convert the power from wind turbine and solar farm. Then at the DC link a buck-boost converter controls the

power flow at the grid. A bidirectional converter is placed between the DC micro grid and the battery bank. This converter charges up and discharges the batteries from the micro grid and monitor the power flow at the grid and battery bank. If a fault occurs at the micro grid or energy demand increases, this converter transmits power from the storage system to the grid. This will enable the micro grid to continuously operate in a isolated mode and will improve the system stability. The power flow at the micro grid is unidirectional.

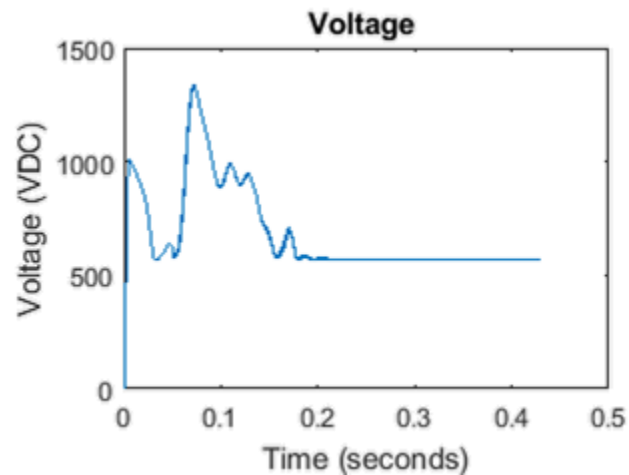


Fig.3-4: Voltage transients due switching ON/OFF of the wind turbine and solar units by changes wind and sun light

To remove the transients and harmonics from the micro grid transmission system low pass filters are implemented which regulate the voltage and maintain the current level by reducing voltage spikes. Fig.3-5 shows the minimised spikes and transients in current (A) on the micro grid created due to usage of a super capacitor as a load. A bidirectional converter with control is placed between the DC micro grid and the battery bank which charges up and discharges the batteries by monitoring the power flow at the grid. Different inductors provide different load response [101]. A large inductance creates lower peak currents and reduces losses and improves the efficiency. Also, the switching frequency of the IGBT switches affects the current flow on the micro grid. Higher switching frequency creates lower ripples in current and vice versa [102].

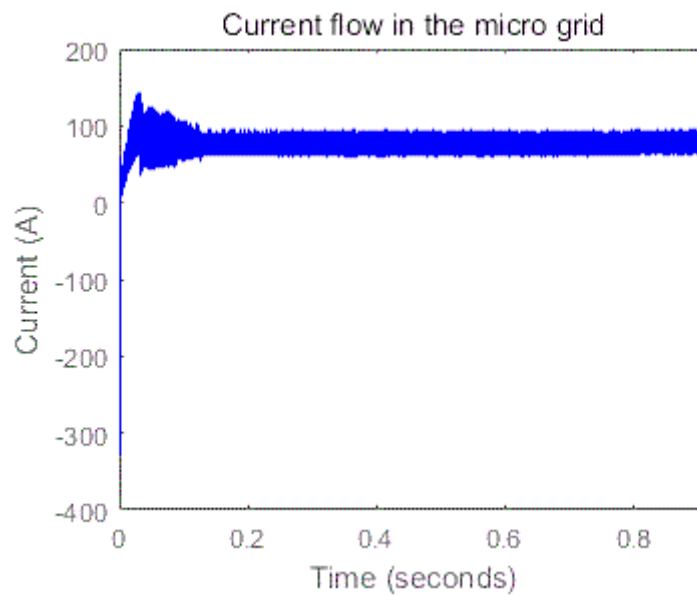


Fig.3-5: Observations of current flow in the micro grid

The losses on this grid are very low due to its short length and no reactive power. It includes a smart measurement system, a smart protection and storage system. Voltage and current sensors measure the values and send signals to process the correct duty cycle. This grid increases the efficiency of power flow and reduces the number of converters. The Battery bank connected to the micro grid enables the continuation of power flow during inappropriate environmental conditions. This type of concept is feasible for the charging stations where fewer terminal links exist.

Summary

A DC micro grid is simulated that connects renewable energy sources directly to the plug-in electric-vehicle charging station to analyse power flow at lower voltage levels. Smart sensors and a programmable protection system are added to increase the reliability of the grid. Smaller fluctuations are observed due to switching periods of the converter. These fluctuations are minimised by increasing the switching frequency of the converters. It is found that the independent micro grid is beneficial for lower power flow applications which are typical for charging stations. The micro grid improves the efficiency of higher power flow due to lesser losses and voltage drops on the line. Output results are monitored by using a sensing system comprising of voltage sensors and current sensors. In this setup, it is possible for the user to select the required voltage level. This set up is feasible for both higher and lower power flow and improves the overall efficiency of the system. Characteristics of the DC micro grid are described by analysing the power flow during peak demands, off peak and normal circumstances. It is observed that when the wind farm was generating the power at full capacity there was less power loss. The generated voltage is close to nominal values which enhances the stability of the system. But when the wind speed is lower, then the output generated power from the wind turbine is reduced. The frequency is also varying with changing wind speed. Due to variations in frequency, massive transients in the line occur and can cause failure of the system. But by using the converter at the DC link, the voltage and the frequency are corrected.

Chapter 4 Energy conversion and applied control techniques

A control system is designed for the DC-DC converters to achieve a desired output by measuring the voltage and current and applying the correct duty cycle to regulate the voltage flow at the micro grid. The control system uses IGBT switches to control the voltage and current flow. The converter components are capacitors, inductors, diodes, and off-on switches. As capacitor is a passive device which resists the change in voltage and an inductor resists the change in current. It means that the voltage across the capacitor does not change instantly and the current in the inductor cannot change rapidly.

An inductor behaves best at lower frequencies while a capacitor has better performance at higher frequencies. If the load is inductive or capacitive than a very complex control is required. Achieving the desired voltage depends on the duration and level of flow of current which is achieved with an automatic controller. The controller is usually a microcontroller which controls the frequency of the switches by using PWM waveforms which have the capability to switch ON and OFF the IGBT device and current direction. Pulse duration is controlled by the ON time of the PWM. If the PWM is generated from a sinusoidal signal, then output will be sinusoidal as well. By applying the signals appropriately, the desired output voltage can be achieved.

4.1 MOSFET/IGBT

MOSFET is a device that control the voltage and not current. It has features of a drain diode and handles freewheeling current. MOSFETs are useful in higher frequency circuits, longer duty cycles, lower voltages and load variations. A MOSFET have lower losses at higher frequency but it can only operate in lower power regions [104]. It is not feasible at higher power due to large temperature rises. A IGBT is also a voltage controlled device which has the capability to switch its output and has conduction parameters of bipolar transistors. It has the features of tackling higher currents. IGBT's are mostly used with PWM switches, as a diode and in lower frequency applications. The reason for using the IGBT in converters is that it has break down voltage level above 1000V, which means it is suitable for higher voltage applications [105]. While the MOSFET breakdown voltage is a maximum 250V or lower. An IGBT has also capability to control and remain stable for higher power flow of up to several kilo watts. It has been found that a IGBT can operate more precisely than a

MOSFET in higher power applications. The switching frequencies of high power IGBT switches are very low and they produce lower order harmonics and distorted output waveforms. To solve this problem, a PWM control strategy is applied to reduce the harmonics content and smooth the output waveforms. Output voltage of the converters is decided by the PWM switching. Three phase PWM pulses have 8 ON and OFF states and are applied to switches to control the ON and OFF states.

The duty cycle is applied to the input and is between 0 and 1. The switching frequency controls the speed of the device. It is observed that by increasing the PWM pulse frequency, harmonic components are reduced.

Fig.4-1. shows the IGBT switch. It is a three terminal conducting device. Where g represents the gate, C is the collector and E is the emitter. Current flows from the collector to emitter and is controlled by the gate signals.

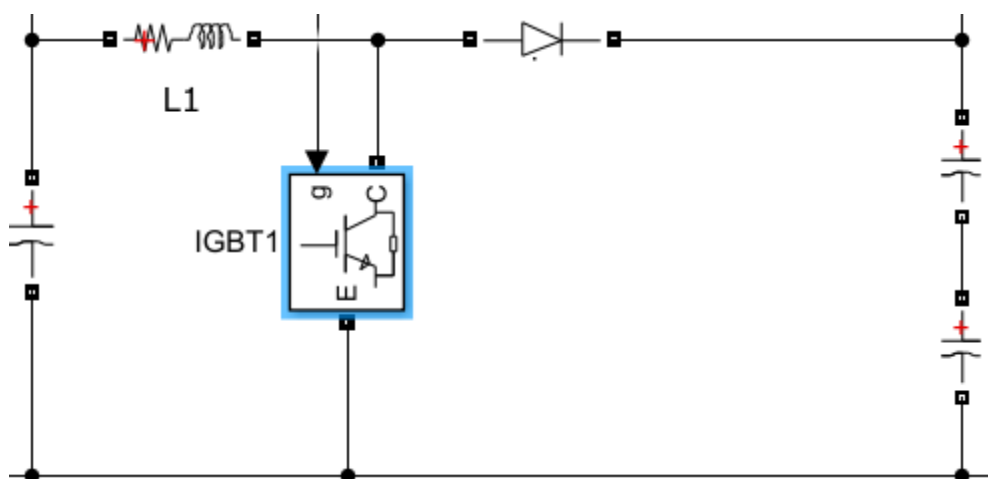


Fig.4-1: Insulated gate bipolar transistor (IGBT) used to convert electrical energy

4.2 Power conversion system

There are three types of DC-DC converters are Buck, Buck-Boost and Boost. Buck converters are used at electric-vehicle charging stations to reduce the voltage to suitable levels for charging. Boost converters are used to increase the voltage of the solar panels. While buck-boost converters are used at the DC link to regulate the voltage flow. If the voltage is above the nominal level it operates as a buck converter and in the case of lower voltage, it functions as a boost converter.

4.2.1 Modelling and simulation of Boost Energy Convertors

Boost converters are used to convert the DC-DC voltage level. Boost converters play an important role in modern power conversion. Voltage output of solar cells and wind units is not enough to function properly, so there is a requirement to increase the voltage. To design the boost converter, the basic parts used are IGBT switches, diodes, capacitors and inductors. Pulses are applied to control the frequency of the switches. An inductor also plays an important role as it resists variations in current. A Boost converter functions in two different ways depending upon frequency of switching period and energy storage capability of the components. The two operating ways are the continuous conduction mode and the discontinuous conduction mode. The equation for achieving the desired voltage at the output is given as [106].

$$V_0 = \frac{V_i}{1-D} \quad (4.1)$$

Where V_0 the output voltage is V_i is the input voltage and D is the switching duty cycle

In boost converter mode, when the switch stays ON the circuit is divided into two states; the inductor voltage is increasing meanwhile the capacitor maintains the output voltage utilising the stored energy. In this state current through the inductor never reaches to zero, and it discharges partially. The main parameter of the boost converter is the inductor which resists the instantaneous variations in current. It stores energy in the form of magnetic field and releases energy at close of the switch. The inductor current increases whilst the switch in the ON position. The capacitor is large to maintain a high time constant (RC) of the circuit. During the switch ON position, the diode behaves as an open circuit due to a higher voltage on the N side compared to the P side. When the switch goes to OFF position, the load receives energy both from the stored energy and from the source. The diode is short circuited in this state and it steps up the output voltage level. In this stage, the inductor becomes fully discharged and current reaches to zero until the next switching cycle comes ON. By controlling the switching sequence, the desired output voltage can be achieved. During normal conditions, current flow in the inductor does not vary suddenly. Therefore, current level should remain equal at the end of switch ON time and at the end of switch OFF time. Current level should also be the same at the start of switch OFF time and at the end of the switch ON time.

The relation between input and output voltage with duty cycle is given as

$$\frac{V_0}{V_{IN}} = \frac{1}{1-D} \quad (4.2)$$

$$D = 1 - \frac{V_{IN}}{V_0} \quad (4.3)$$

From the equation above it can be seen that the desired output voltage can be achieved by adjusting the duty cycle. By increasing the duty cycle, output voltage is boosted up and power flow is enhanced in the same proportion. At unity duty cycle $\frac{V_0}{V_{IN}}$ goes to zero due to parasitic elements in the lumped component capacitor, inductor and resistor. The duty cycle can be controlled by using a micro controller, FPGA or other PWM technique.

Fig.4-2 shows the circuit for a boost converter. 24V is received from the solar panels. Inductance is used to achieve the require voltage by varying the current ratio. Pulse width modulation (PWM) techniques are used to control the frequency of the IGBT switches. Applying the correct duty ratio is very important because it is directly related to the voltage level. Capacitors remove the ripples.

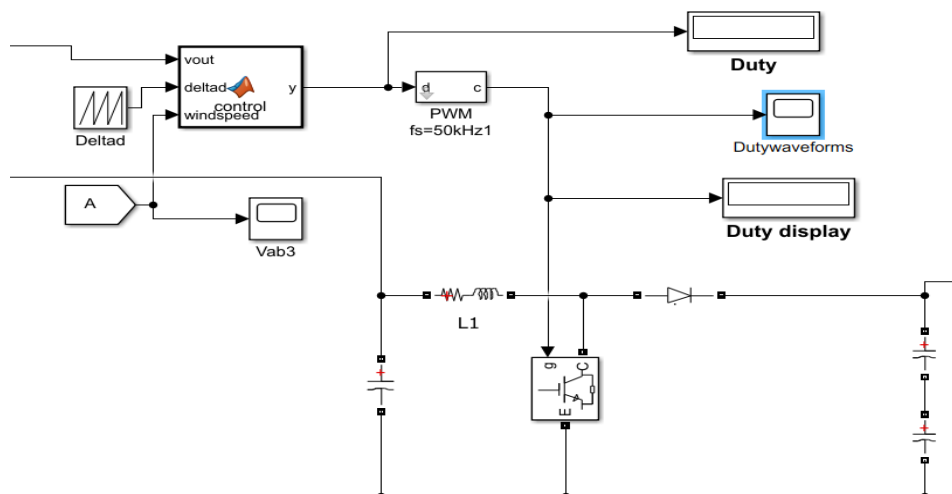


Fig.4-2: Boost Converter used to convert the DC/DC power

4.2.2 Implementation of buck energy converter

A Buck converter is applied at the EV charging terminal and at the wind turbine units to achieve the required voltage as shown in Fig.4-3. When switch is ON, power flows in the circuit and results in an output voltage across the resistor. Energy is stored in the inductor and capacitors charge up gradually to maintain the voltage flow to the load. The diode is reverse biased and there is positive voltage across it. When switch is turned OFF then energy is released by the inductor and the capacitor is discharged via the resistor. During this time, voltage across the inductor is now in reverse mode but enough energy is available to maintain current flow in the circuit until the switch is open [107]. The Diode now forward biased and current flows through it. As stored power in the inductor tends to decrease due to the load, voltage tends to be at a lower level as well. The capacitor is the source of current during this time until the switch goes to ON position. By controlling the switching of the converter, desired lower output voltage is maintained.

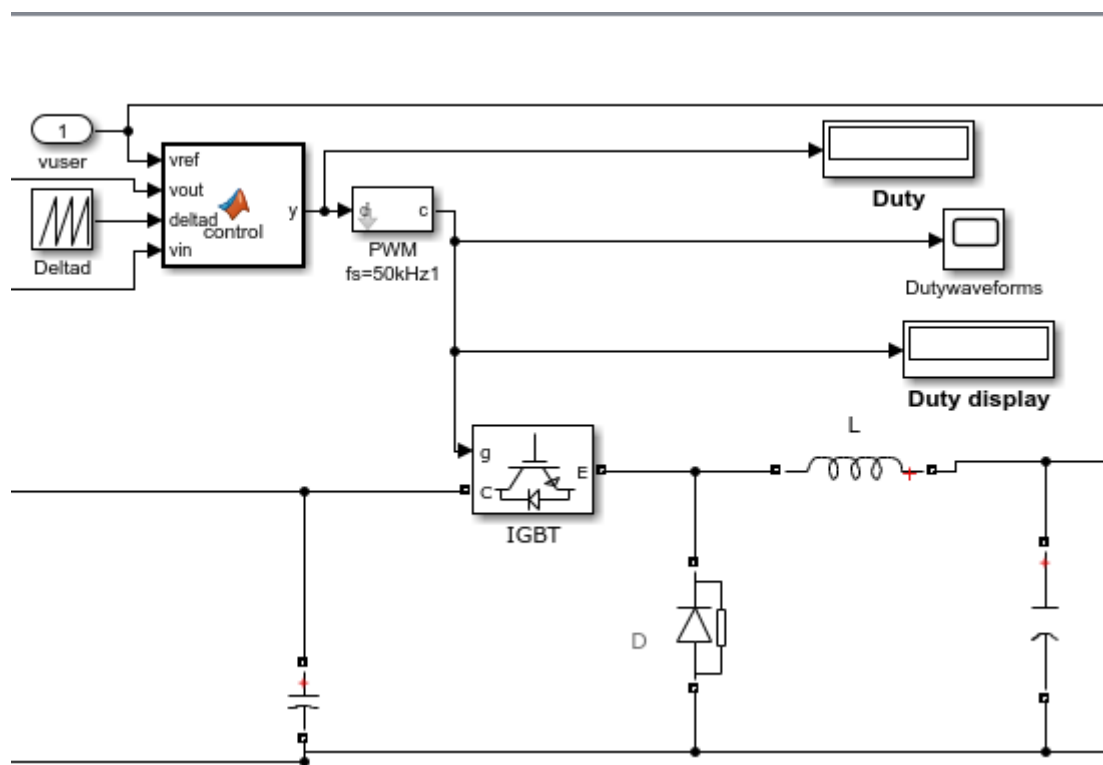


Fig.4-3: Simulation of Buck converter at the electric-vehicle charging station

4.2.3 Modelling and simulation results of buck-boost energy conversion system

In the buck-boost energy conversion unit, charging and discharging of the inductor is represented by 1 and 0. By controlling the switching sequence, higher/lower output voltage can be achieved. Output voltage polarity is opposite to the source voltage as the inductor cannot change the current direction. In this type of converter two IGBT switches are used. Both are connected to the PWM control unit. The control unit has to decide whether to step up or step down the voltage. IGBT switch1 is connected to the source while IGBT switch2 is connected parallel to the inductor and diode as shown in Fig.4-4. In the buck converter mode switch2 remains off all the time, whilst switch1 is turned ON and OFF by the control unit. The control unit applies the pulses at the gate of the switch. When the switch1 is ON then current flows in the inductor and generates a magnetic field, charging the capacitor and supplying power to the load. The diode is inactive due to positive voltage at the cathode. When the switch1 goes off then the main current source is the inductor. It supplies current by collapsing its magnetic field; back e.m.f. is developed due to this collapsing and reverses the voltage polarity. Now the diode is active and current flows through the second diode to the load. When the amount of current reduces in the inductor then the capacitor also supplies current to the load [108]. This helps to achieve the buck operation in the buck-boost converter. In the boost mode, switch1 remains OFF all the time and PWM signals is applied to switch2. During the switching ON period current will flow through the inductor and switch2 and diode2 cannot conduct due to higher voltage potential at the cathode and the load is supplied power by the capacitor and the source.

The size of the capacitor determines the ratio of output ripples and transients. When switch2 is turned off, the capacitor is partially discharged and the inductor is charged. Back e.m.f is generated by the inductor and its range depends on the rate of variation of current and size of the inductive coil [109]. Therefore, e.m.f. can be a different voltage. At this point voltage polarity across the inductor is reversed, which adds to the input voltage and gives an output voltage which is bigger than the input voltage. Diode2 is now in conducting mode and current flows through it to the load and recharges up capacitor simultaneously. Controlling the switching of the buck-boost converter is very important. Switch 1 and switch 2 are both controlled by the same control unit. They must be synchronised and controlled in an appropriate way.

The inductance and the output capacitance in the DC-DC power converters form a second order low pass filter. This filter is used to reduce the ripples in the energy supply generated by PWM pulses as shown in Fig.4.4. Any changes to inductance or capacitance affect the voltage and output current from the converter system. The output capacitors of a low pass filter are an important part of the feedback converter system because it is the key component to reduce the transient response in the power supply. The load current has a direct impact on the input voltage deviations. If the transient increases in the output current then the transients in the input voltage to the converters are increased as well. Higher input capacitance is required to minimise the transients in the voltage because lower input voltage will allow higher current to flow and increase the transients. The output capacitors of the converter must be charged and discharged to allow the flow of energy and reduce the voltage. The voltage drop is proportional to the output current where a higher output current causes the voltage drop in the system. The transients are reduced by increasing the capacitor values and by increasing the switching frequency of the converters. When a transient occurs in the system, the controller receives the changes in the output voltage and compensates it by changing the duty cycle. The change in output current is limited by the inductance of the output filters even if the duty cycle rises to 100%.

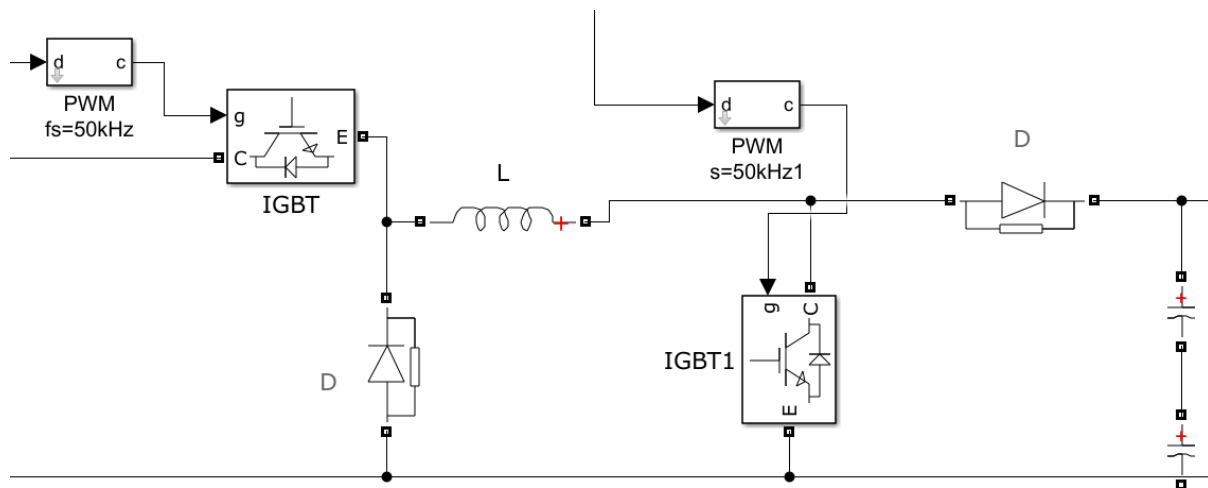


Fig.4-4: Simulation of Buck-Boost converter at the microgrid station

4.2.4 AC-DC VSC based energy conversion system

The output power waveform from the generator is AC type. Then it is converted into DC waveform by using IGBT diodes. Six diodes are used to implement this conversion. These

diodes are divided into three rows. Each row has two series connected diodes. The upper diodes are connected to the positive source while the lower diodes are connected to the negative source. So it means that during the positive waveform upper diodes are operational while during the negative waveform lower diodes are operational and convert three phase AC power into DC power. The generated input voltage is 585VAC (peak) and then converted into 585 VDC. The simulation model for the rectification is shown in Fig.4-5. The power generated from the wind is converted into DC power. The controlled rectifiers are used for conversion of power. Six IGBT diodes are used to make this conversion.

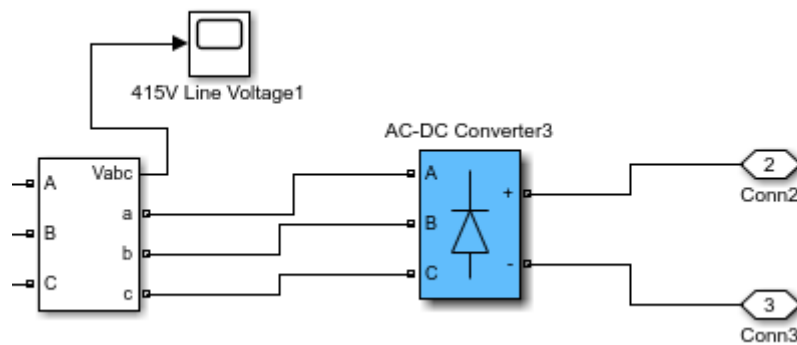


Fig.4-5: Three phase voltage to DC voltage rectification

4.3 Modelling and validation of voltage regulation and control

The voltage on the DC micro grid is maintained by implementing the correct duty cycle at the AC/DC IGBT converter switches and by supplying the required power to the loads. The closed loop feedback system, shown in Fig.4-6 is used to generate the precise duty cycle. The controller receives a signal from the output of the converter by closed feedback links and generates the variable duty cycle by comparing the output feedback voltage with the reference voltage. It updates the duty cycle by detecting the voltage difference between the output voltage and the reference voltage. The regulated voltage is then transmitted on the smart grid to the electric-vehicle charging station.

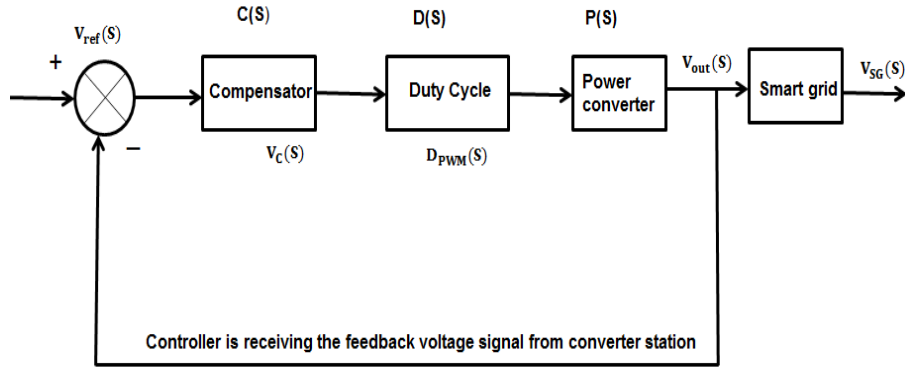


Fig.4-6: Closed loop feedback control system for the converter sections for voltage regulation.

By using transfer functions an expression is derived to generate the duty cycle and to perform converter analysis. For the state space representation inductor current and capacitor voltage are considered. The inputs are duty cycle, the input current i_{DC} and the converter output voltage. D is the duty cycle applied to the converters, v_c represents the capacitor voltage and i_l is the inductor current and controller is represented by $R_{contoller}$. $\frac{di_l}{dt}$ is the change in current and $\frac{dv_{c_i}}{dt}$ is the change in voltage in the converters.

$$\mathbf{D(S)} = \frac{\mathbf{D_{PWM(S)}}}{\mathbf{V_c(S)}} \quad (4.4)$$

$$\mathbf{PS(S)} = \frac{\mathbf{V_0(S)}}{\mathbf{D_{PWM(S)}}} \quad (4.5)$$

The expression below illustrates the transfer function for the duty cycle generation

$$\mathbf{D(S)} = \frac{\tilde{\mathbf{D}}_{\mathbf{PWM(S)}}}{\tilde{\mathbf{V}}_{\mathbf{C(S)}}} \quad (4.6)$$

The following equations describe the voltage that is driving the PWM controller.

$$\mathbf{v_c} = \mathbf{V_c} + \tilde{\mathbf{v}}_{\mathbf{c}} \quad (4.7)$$

$$\text{If } \tilde{\mathbf{v}}_{\mathbf{c}} = \mathbf{a} \cdot \sin(\omega\mathbf{t} - \varphi) \quad (4.8)$$

The duty cycle generation from the controller is given by

$$\mathbf{D_{pwm}} = \frac{\mathbf{V_c}}{\mathbf{V_{max}}} + \frac{\mathbf{a}}{\mathbf{V_{max}}} \sin(\omega\mathbf{t} - \varphi) \quad (4.9)$$

where

$$\mathbf{D}_{pwm} = \mathbf{d}_{PWM} + \widetilde{\mathbf{d}}_{pwm} \quad (4.10)$$

By combining the two equations the transfer function for the PWM controller can be obtained.

$$\mathbf{D} = \frac{\mathbf{D}_{pwm} \frac{V_C}{V_{max}} + \frac{a}{V_{max}} \sin(\omega t - \varphi)}{\widetilde{V}_C \frac{a \cdot \sin(\omega t - \varphi)}{V_{max}}} \quad (4.11)$$

$$\mathbf{D} = \frac{1}{\frac{V_{max}}{1}} \quad (4.12)$$

$$\mathbf{D} = \frac{1}{V_{max}} \quad (4.13)$$

The two differential equations are:

$$\frac{di_L}{dt} = \frac{vc_i}{L} - \frac{v_b(1-D)}{L} \quad (4.14)$$

$$\frac{dvc_i}{dt} = \frac{i_{DC}}{C_i} - \frac{vc_i}{C_i * R_{cnt}} - \frac{i_L}{C_i} \quad (4.15)$$

In matrix form:

$$\begin{bmatrix} \frac{di_L}{dt} \\ \frac{dvc_i}{dt} \end{bmatrix} = \begin{bmatrix} \mathbf{0} & \frac{1}{L} \\ -\frac{1}{C_i} & -\frac{1}{C_i * R_{cnt}} \end{bmatrix} \begin{bmatrix} i_L \\ vc_i \end{bmatrix} + \begin{bmatrix} v_b & \mathbf{0} & \frac{-1+D}{L} \\ \mathbf{0} & \frac{1}{C_i} & \mathbf{0} \end{bmatrix} \begin{bmatrix} i_{DC} \\ v_b \end{bmatrix} \quad (4.16)$$

$$\dot{\mathbf{x}} = \mathbf{A}_1 \cdot \mathbf{x} + \mathbf{B}_1 \cdot \mathbf{V}_d \quad (4.17)$$

$$\text{Therefore } \mathbf{x} = \begin{bmatrix} i_L \\ vc_i \end{bmatrix}, \mathbf{A}_1 = \begin{bmatrix} \mathbf{0} & \frac{1}{L} \\ -\frac{1}{C_i} & -\frac{1}{C_i * R_{cnt}} \end{bmatrix}, \mathbf{B}_1 = \begin{bmatrix} v_b & \mathbf{0} & \frac{-1+D}{L} \\ \mathbf{0} & \frac{1}{C_i} & \mathbf{0} \end{bmatrix}, \mathbf{V}_d = \begin{bmatrix} \mathbf{d} \\ i_{dc} \\ v_b \end{bmatrix} \quad (4.18)$$

The equations, as detailed below, are used to measure the magnitude of ripples for the capacitor voltage and inductor current where T_s is the switching frequency applied to converter switches and D is the duty cycle.

$$\Delta i_L = \frac{vc_i}{2L} \mathbf{D} T_s \quad (4.19)$$

$$\Delta vc_i = \frac{\mathbf{D} T_s}{2C_i} \left(I_{DC} - \frac{vc_i}{R_{cnt}} - i_L \right) \quad (4.20)$$

From the state space equations, the transfer function $G_d(s)$ between input voltage to the converters and the duty cycle is given by

$$\mathbf{G}_d(s) = -\frac{R_{cnt}L v_b}{LC_i R_{cnt} s^2 + Ls + R_{cnt}} \quad (4.21)$$

The observability matrix of the system shows that the system is observable.

$$\mathbf{O}b = \begin{bmatrix} \mathbf{0} & \mathbf{1} \\ -\frac{1}{C_i} & \frac{1}{C_i R_{cnt}} \end{bmatrix} \quad (4.22)$$

From the controllability matrix below, the system is always controllable if the determinant of this matrix is non-zero, similarly the observability.

$$\mathbf{C}o = \begin{bmatrix} V_b & \mathbf{0} \\ \mathbf{0} & -\frac{v_b}{C_i} \end{bmatrix} \quad (4.23)$$

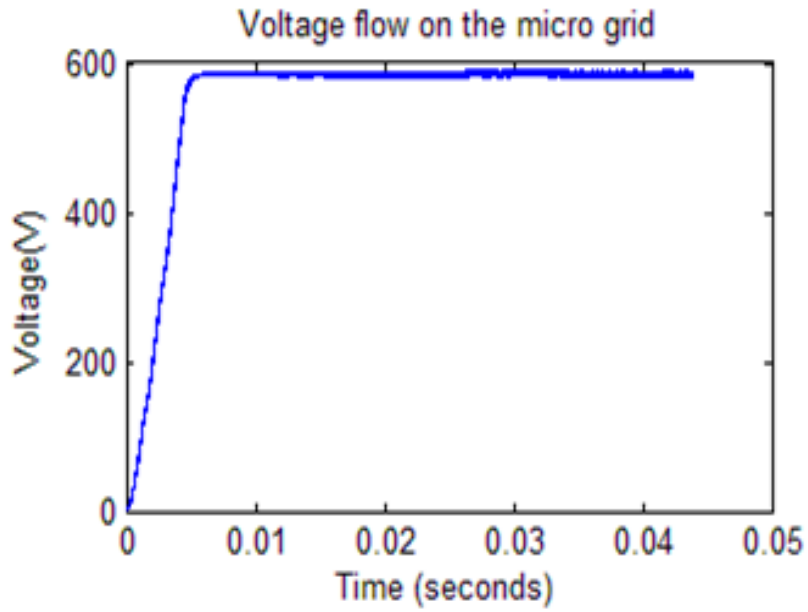
4.4 Voltage flow stability and control comparison with the other methods

Voltage and frequency are the two quantities that need to be controlled in AC power flow. Frequency can be controlled by the rotation of wind turbine and by the increasing and decreasing of apparent power. Voltage can be controlled by stabilising the reactive power. In a DC grid the frequency is equal to zero and there is no reactive power because voltage and current are in phase. It means that the voltage is the only quantity that needs to be stabilised on the DC grid. The voltage on the DC grid can be maintained by supplying the required power to the loads [110]. If the grid is over loaded, then voltage falls will happen on the entire system and energy boost will be required at this point. Thus to maintain the voltage on the DC grid, it is essential to keep an energy balance on the grid at all times i.e. power flowing out of the grid should be equal to power flowing into the grid. Maintaining voltage levels also depends on the number of converters used to control the DC voltage level. Different methods can be applied to maintain the voltage on the DC grid. One common method is the Master/slave drop control. Typically, the DC link system is the section where voltage level can be controlled because it is directly connected to the grid and appropriate voltage level should be achieved [111]. All other converters transmit the voltage at various levels. Some of these converters are operational for converting and controlling the ac power from the wind turbine. All converters should function correctly and dependency should not be

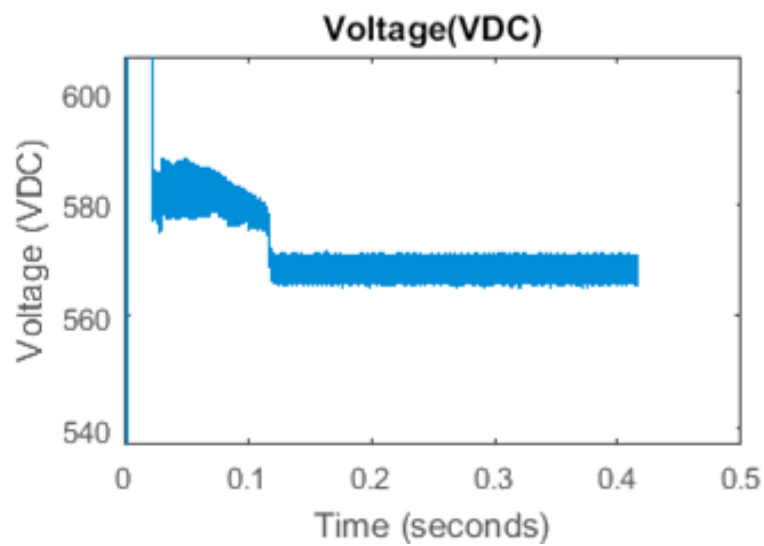
maintained only on the DC link. Communication between the converters is also beneficial to maintain the power flow at the DC grid. The advantage of using the communication system between the controllers is to identify the voltage drops and faults that can happen in the system. If the signals are not transferred to the next converters within a short period of time the DC grid can become unstable. The system should also be protected against unessential communication between the voltage controllers or else it can lead to instability. The Master/slave control method is preferable where one master controller at the DC link is controlling several other devices and converters. Since the DC grid is being fed from the renewable energy resources (which depend on the weather conditions) power is always varying and a complex controller is required which transmits signals at a very fast rate. A battery bank is another source to maintain power at the DC grid during the lower power generation. By monitoring voltage drop in the grid, the battery bank can be used to support the grid to maintain the nominal voltage level. However, batteries cannot regulate the voltage on the grid for a long period of time due to not having enough capacity. There must be a fossil fuel generator which charges up the batteries and supplies power to the loads during the inappropriate circumstances. By regulating the voltage at the DC terminal link, nominal voltage flow can be achieved at the grid.

The system was tested and compared by implementing the following methods reported in the literature. Results of their simulation are shown in Fig.4-7 and compared with the proposed model.

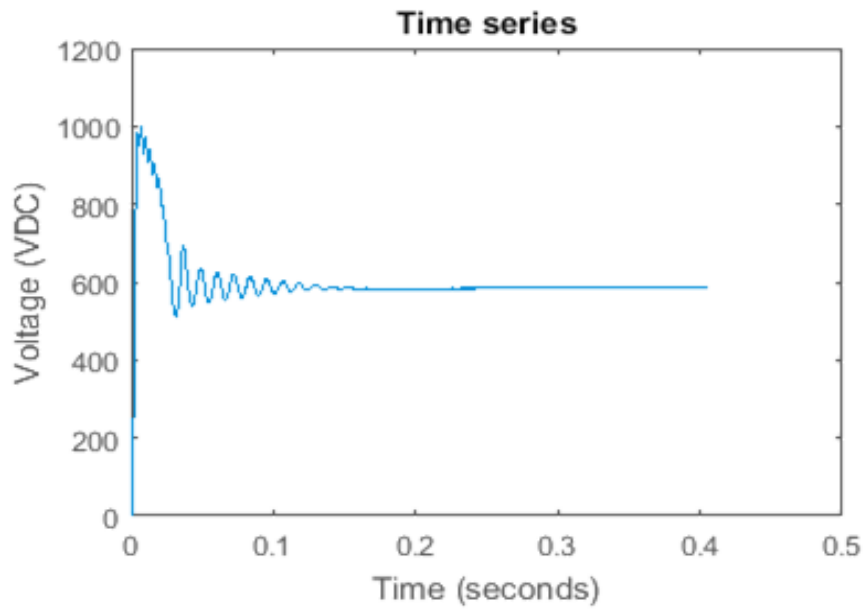
- Perturbs and observed method
- Incremental conductance
- Space vector pulse width modulation



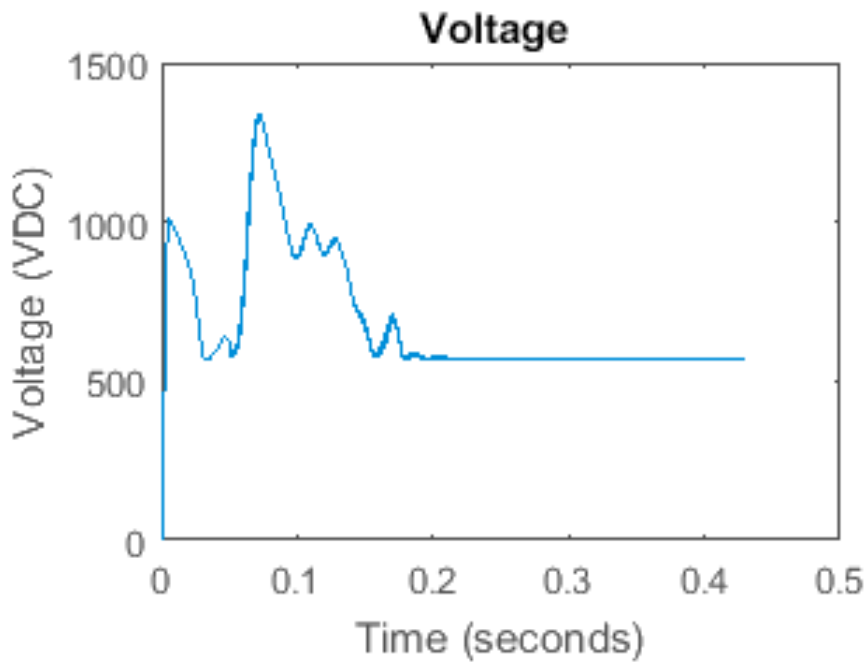
(a) Voltage flow on the micro grid by the implemented proposed control system



(b) The voltage flow on the smart grid with the Perturb and Observe algorithm, which is a part of maximum power point tracking algorithm (MPPT)



(c) Achieving 585VDC on the smart micro grid with the incremental conductance method



(d) Voltage obtained with the space vector pulse width modulation method

Fig.4-7: Grid voltage with several applied control algorithms

4.5 MPPT based Control algorithm

The Maximum power point tracking (MPPT) algorithm makes solar units capable of generating the power at full capacity. It does not move the module towards the sun to extract power. It varies the electrical properties of the PV module to achieve the maximum power and improve the efficiency of the solar panel by maintaining the voltage and current at an appropriate level. The MPPT algorithm is compared with our proposed model to analyse the power flow at the smart micro grid. MPPT calculates the energy values to apply the correct duty cycle to achieve the required results. It is typically suitable for charging up battery banks because it increases the efficiency of battery charging rate. Assume that there is a solar panel which is supplying power of 210W with 18.3V and 11.48A. There is a battery with maximum 150W capacity and needs to be charged up at 12.2VDC. Assume that the battery storage capacity is less than the supplying power of the module. The MPPT controller increases the voltage of the system, closer to the module [112]. It charges up the battery at 18.3V and extracts most of the power from the module. This improves the entire efficiency of the system. Several MPPT algorithms were compared and tested. Fig.4-8 shows the PV system with the MPPT algorithm. Applying the MPPT is essential due to PV dependence on irradiance and temperature. A Boost converter is used to step up the generated voltage for transmitting it at the smart grid.

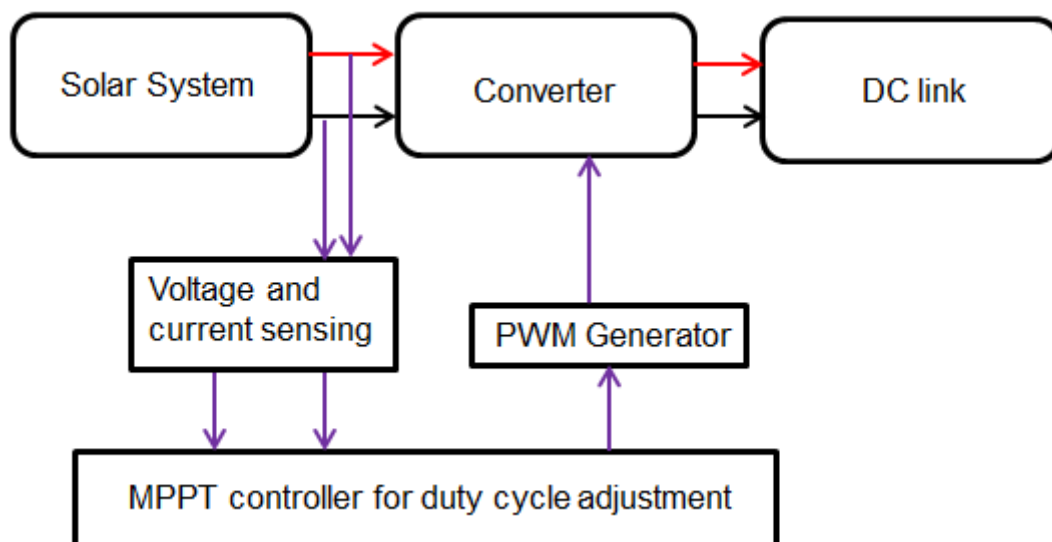


Fig.4-8: Maximum power point to regulate voltage and extract maximum power from the solar system

4.5.1 Perturb and Observe Method control strategy

The system is tested by applying the MPPT based P and O method where the voltage and power are sensed and measured by using sensors as shown in Fig.4-9. This technique is operated by recording the output power by sensing the voltage and regulating it. This process periodically increases and decreases the output voltage of the system and compares the output power of the current cycle with the previous as shown in Fig.4-10. The rate of change is adjusted appropriately to overcome the fluctuations in the steady state. It is found that if this step is taken following the MPPT then better result can be obtained that results in improved efficiency. This is the best method for MPPT but can go to an unbalanced state in very fast variations in atmospheric conditions. During the normal conditions, operation of this method is very feasible.

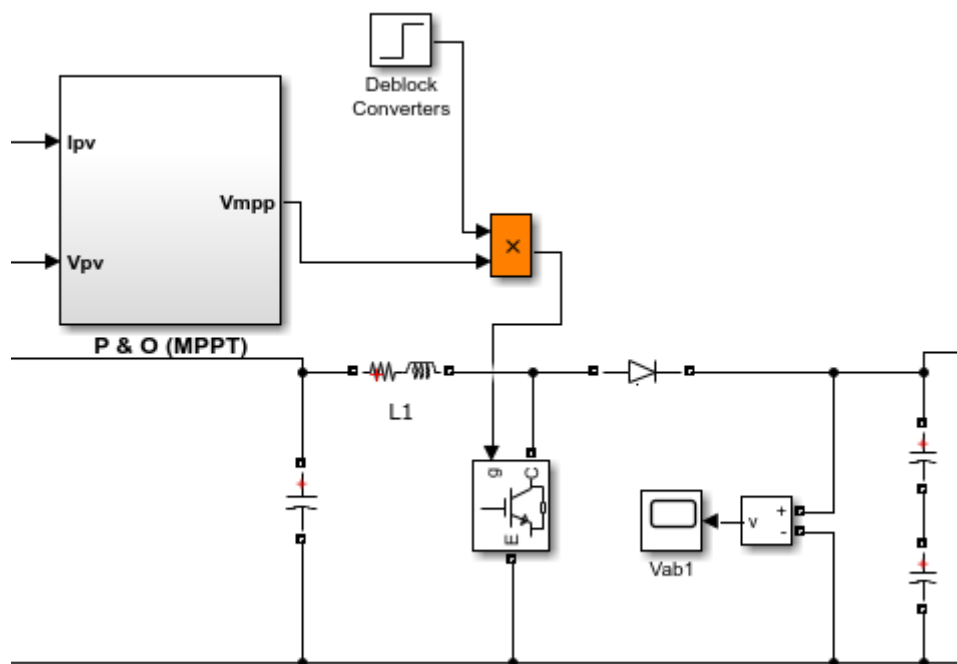


Fig.4-9: Perturb and observe method to regulate the voltage on the microgrid.

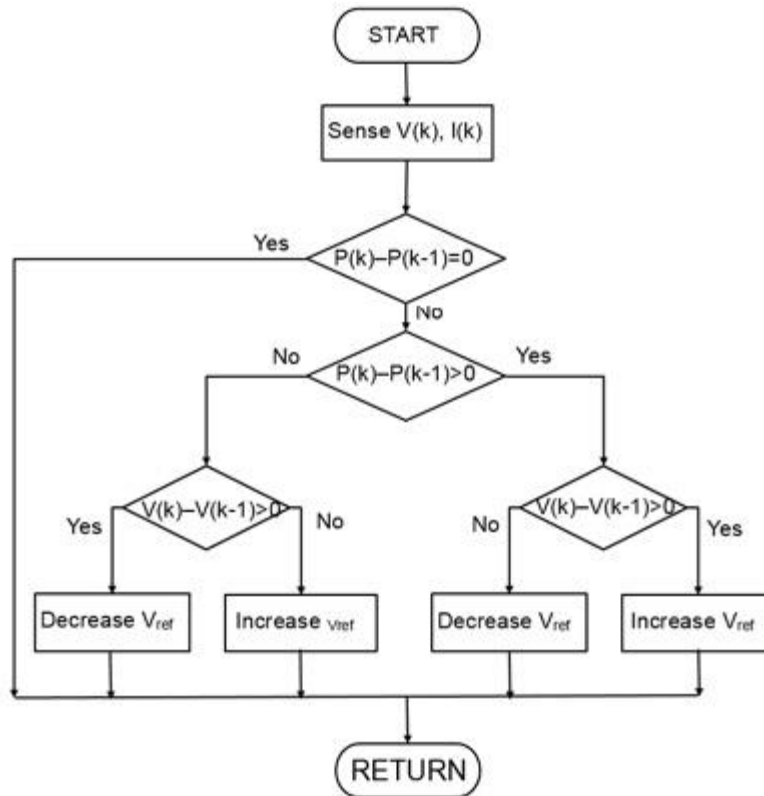


Fig.4-10: Perturb and Observe algorithm

The process can be improved by using the appropriate control system and by applying filters to remove oscillations in the voltage. This method needs less hardware complexity and is better economically. The negative aspect of this method is the oscillations of voltage at the desired point. The output voltage from the wind system is shown in Fig.4-11.

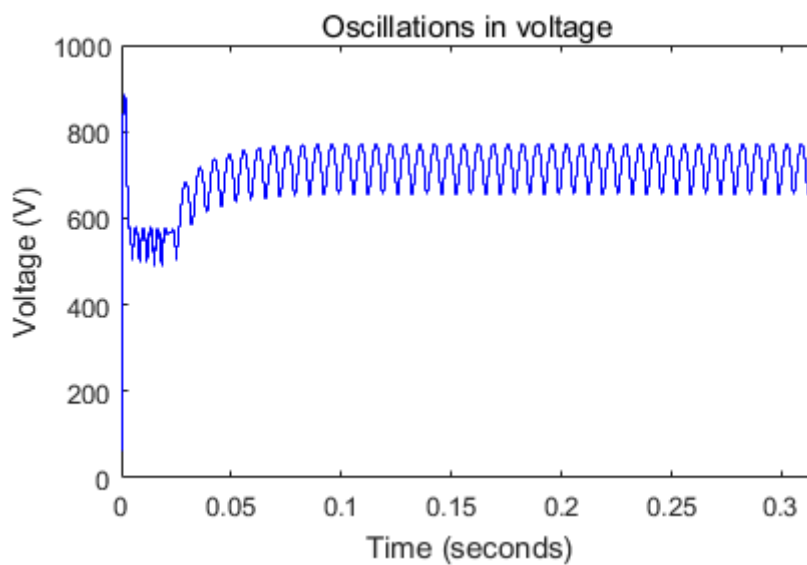


Fig.4-11: Oscillations in voltage observed by implementing P and O method

The voltage transient is observed in the initial 0.03 seconds due to initialization of the system after which the voltage is oscillates around the desired point. The oscillations can be removed by using the fastest control components. This technique is found suitable for areas where little variations happen in the environment. MATLAB tools are used to operate the Perturb and Observe methods to apply the correct duty cycle.

The MPPT temperature method is a useful method for the solar system. In this method, a temperature sensor is used to update the control unit. But for larger PV units, this method is not feasible due to irregular distribution of temperature on PV arrays. This method is found appropriate for smaller PV units and avoids irregularities in the output voltage. This method is the simplest to apply and its equation 4.24 is shown below [113].

$$\mathbf{V_{MPP}} = \mathbf{V_{MPP}(T_{Ref})} + \mathbf{TK_{VOC}(T - T_{REF})} \quad (4.24)$$

Where V_{MPP} is the Maximum power point voltage, T is the PV surface temperature, TK_{VOC} is the temperature coefficient of V_{MPP} , and T_{REF} is the nominal test environment temperature.

The voltage at the smart grid is shown in Fig.4-12. The desired voltage is 585VDC but the oscillations are found in the actual voltage. When the voltage is lower than the desired point then a battery system has to supply power to the system. The batteries are charged up again when the voltage increases to desired point. There is another method, MPP, which relates to principle of maximum power transfer, and where oscillations are used to measure the best point to process. At MPP, the ratio of amplitude of oscillations to the average voltage is constant. It can be implemented by using logic circuits because it only senses the PV voltage level. To apply this method, system oscillation, low frequency ripples or double frequency can be used. A filter needs to be implemented for switching frequencies to prevent incorrect switching orders. If wrong switching is applied, then electromagnetic interference issues can increase. The Ripples Correlations method also relates to principles of maximum power transfer and uses oscillations in power to achieve the required optimal point. By using high frequency filters, high frequency ripples in power and voltage are used to measure $\frac{dP}{dV}$. This method has a fast speed but is limited by the gain of the converter control system.

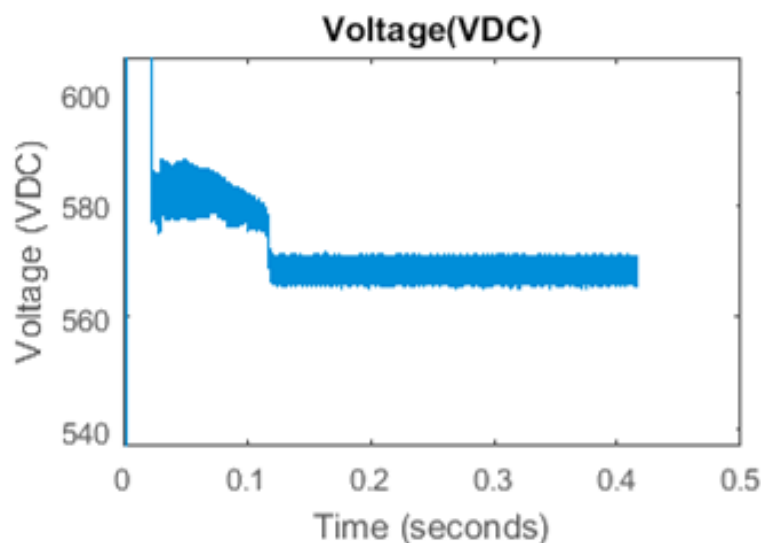


Fig.4-12: Voltage on the smart grid by the implementation of Perturb and Observe method

Maximum Power Point Tracking (MPPT) algorithm based on the Perturb and Observe technique is investigated to analyse energy transmission from the renewable energy system. Voltage and power flow are sensed at different points of the system and this technique is suitable for those regions where environmental variations happen very slowly. Higher oscillations are noticed in the wind system compared to solar system because of fast changing wind speed. The oscillations are even observed in the smart grid. So in this method, power losses increase due to oscillation after the terminal voltage is perturbed.

4.5.2 Incremental Conductance based control system implementation

The system was tested by applying the Incremental Conductance technique to achieve voltage regulation as shown in the SIMULINK model Fig.4-13. The best property of this method is that it does not suffer from fast transient variations due to atmospheric conditions. This method senses both current and voltage and it is not essential to calculate power. The performance of this method is enhanced by the addition of an integrator. It reduces the error by minimising the gap between real values and desired values. It also helps to eliminate the ripples in the steady state [114]. This method is suitable to apply if a larger step size is required for the duty cycle. The digital controller updates the duty cycle to reduce the gap between the MPPT values and the PV values. The Incremental Conductance method has higher efficiency than other methods. It responds rapidly to fast changing environmental conditions. In this method the output voltage is adjusted at the MPP point to extract the maximum power and regulate the PWM signal until desired results are met. It always applies the new duty cycle correctly and replaces the older one. It senses the output voltage and current from the solar panels and generates duty cycle accordingly as shown in Fig.4-14. The DC-DC boost converter is designed to apply the MPPT algorithm. The graphical results are analysed to check the effect of the Incremental Conductance technique for a solar system at fast changing irradiance. Power generated from the solar system is unregulated and requires to be appropriately balanced in order to interface to the grid. Maximum power cannot be extracted if the solar system DC power is directly connected to the load. The converter is placed between the load and the solar system to regulate the output voltage to achieve the maximum output power. It balances the parameters if output power is going up or down. The boost converter operates by varying the switching frequency from applied duty cycle. MPPT controller consists of two inputs (voltage and current) and one output which is the duty cycle. The inputs to the MPPT controller come directly from the solar system and the output is connected to the IGBT switch of the boost converter. The voltage and current variations in the solar system depends on the range of irradiance. Solar panel output voltage is unregulated and is which is boosted to a regulated 585VDC. The power flow in the converters relies on the switching frequency of the IGBT switch. The system is tested with varying irradiance and fixed irradiance. The MPPT balances the output voltage and current to extract the maximum power. Efficiency of the solar system is reduced when the MPPT controller is not used.

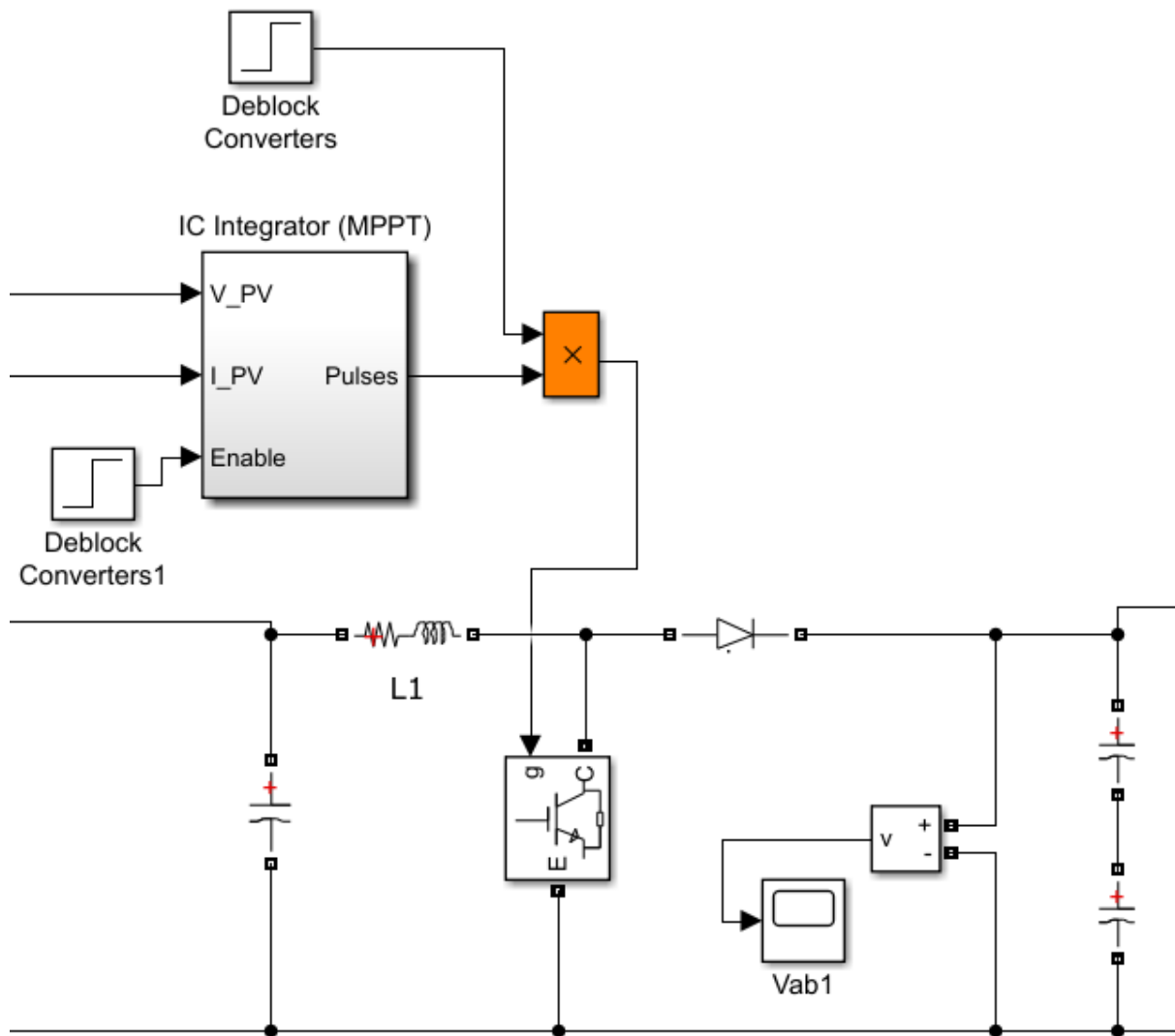


Fig.4-13: Simulation of Incremental Conductance with integrator

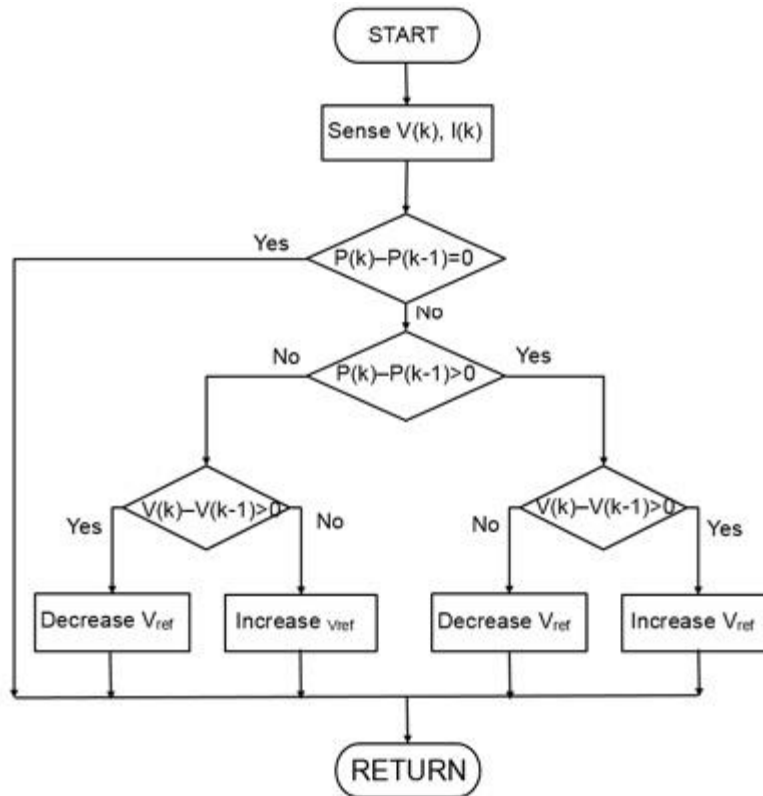


Fig.4-14: Incremental Conductance algorithm.

Fig.4-15 shows the voltage output from the wind system when the Incremental Conductance based MPPT algorithm is applied. For the first 0.3 seconds, unregulated voltage is observed and then constant voltage results due to applying the control for the power flow. This method was found to be more efficient than the other techniques. It increases the system efficiency by extracting maximum power from the energy sources. Less power losses and faster regulation in power flow were observed by implementation of this method.

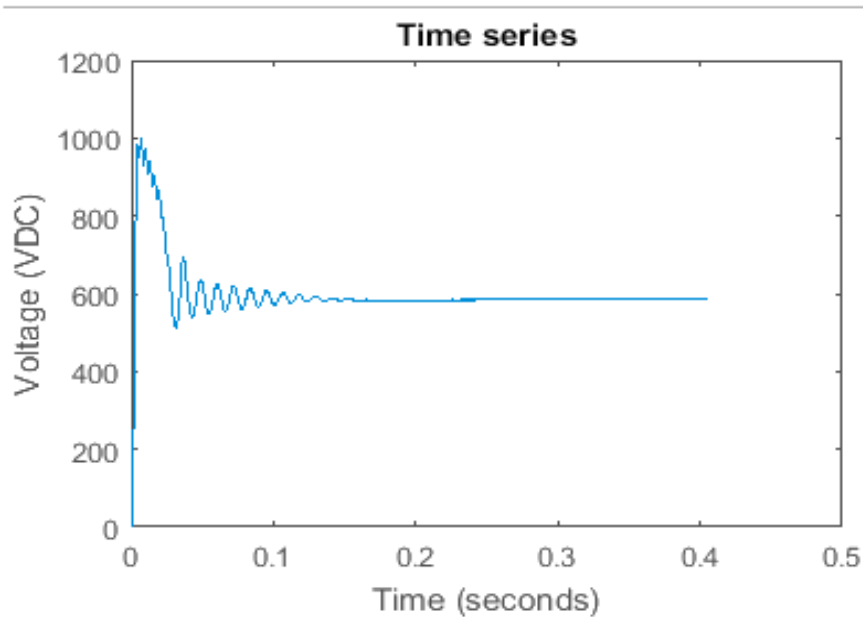


Fig.4-15: Voltage output by using the Incremental Conductance technique

4.5.3 Fix Duty Cycle (FDC) implementation and analysis

System is tested by applying the Fix Duty Cycle (FDC) simulation model as shown in Fig.4-16. This method is found inappropriate as it does not maintain the required voltage at the micro grid during changing environmental conditions. It is suitable in only those regions where temperature varies very little. The positive point of this method is that it is very simple and no complex loops are required. Fig.4-17 shows the voltage at the smart grid. The smart grid requires 585VDC to maintain the correct power flow but it is receiving a severely oscillating voltage. This voltage will damage the smart grid components and is not suitable for transmission or for charging the battery bank which is required to support the smart grid during higher power demands. The voltage is not constant and varies all the time due to varying input and a fixed duty cycle. This voltage is not appropriate for transmitting at the micro grid as it can damage the power equipment.

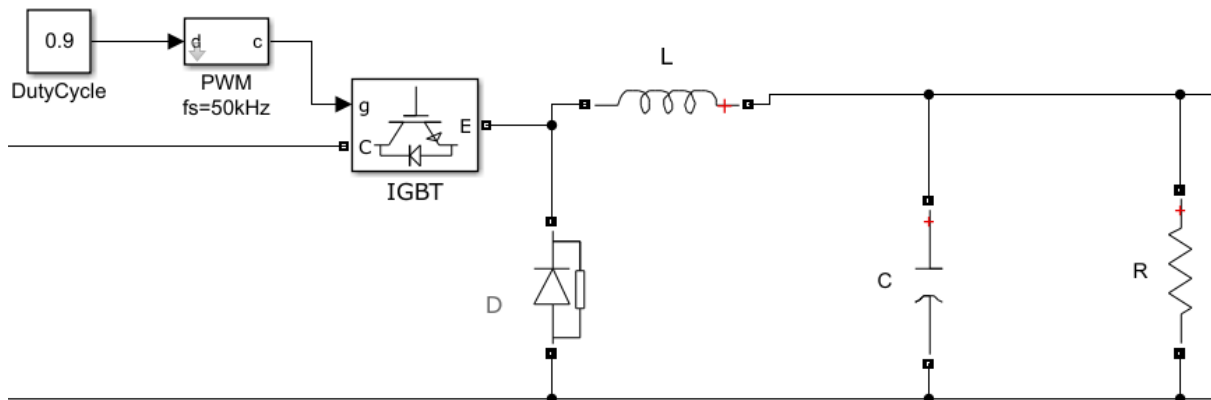


Fig.4-16: Simulation of Fixed Duty Cycle (FDC) applied to the buck converter system.

Fixed duty cycle is applied at different points of the system and transients are observed in the power flow. It reduces the efficiency of the entire system and is not appropriate to maintain constant power flow. It can be applied only in places where variations are small such as at the car charging station terminal or when there is constant voltage at the smart grid. So for varying environmental condition, variations in duty cycle are required to be applied to the entire system.

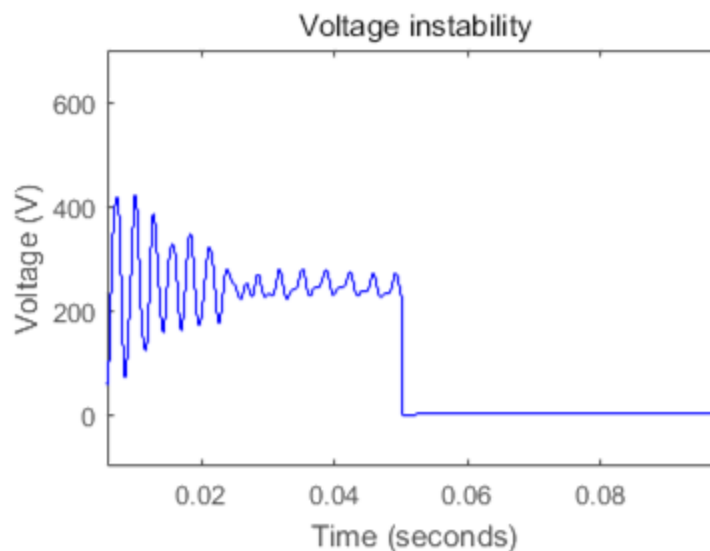


Fig.4-17: Voltage achieved by using the Fixed Duty Cycle.

The aim of applying the MPPT algorithm is to stabilise the power flow when the irradiance is changing fast e.g. in partially shaded solar panels due to fast cloud motion and fast changes in wind speeds. The efficiency of the MPPT algorithm is higher due to the complexity of the

algorithm required to generate the correct duty cycle. MPPT controller was implemented successfully and its correct operation was verified. Output results were verified by using the scopes and the displays available in MATLAB/SIMULINK. The efficiency of the MPPT could not be measured due to time varying time supply of input power. However, by measuring the values of the other equipment's efficiency, the efficiency of the MPPT was measured and to be 96%. Therefore, it can be said that the Incremental Conductance and integrator based algorithm worked efficiently and is suitable for practical applications. The ripples created by using MPPT can be removed by using filters.

4.6 Energy control investigation by using Space Vector Pulse Width Modulation (SVPWM)

The other technique investigated for stabilisation of the power flow is the Space Vector Pulse Width Modulation (SVPWM) technique. This technique is more preferably used now days for AC-DC conversion and DC-AC conversion. It stabilises the output DC voltage and reduces harmonics in the voltage to improve the power flow quality in the system. It stabilises the unregulated voltage from wind turbine or solar panels by applying the correct duty ratio.

The switching frequency of the AC-DC converter is described as [115].

$$f_a = \frac{(2S_a - S_b - S_c)}{3} \quad (4.25)$$

$$f_b = \frac{(2S_b - S_a - S_c)}{3} \quad (4.26)$$

$$f_c = \frac{(2S_c - S_a - S_b)}{3} \quad (4.27)$$

Where S_a , S_b , S_c are the control signals which control the arbitrary phase of the converters and each signal is given a value of 1 or 0. If S_a is 1 then upper switch of the converter turns ON while lower switch remains OFF. If S_a is 0 then lower switch will be ON and upper switch turns OFF. These three control signals can be transformed into two axis vectors:

$$\begin{bmatrix} \mathbf{X}_d \\ \mathbf{X}_q \end{bmatrix} = \frac{2}{3} \begin{bmatrix} \cos\omega t & \cos(\omega t - \frac{2\pi}{3}) & \cos(\omega t + \frac{2\pi}{3}) \\ -\sin\omega t & \sin(\omega t - \frac{2\pi}{3}) & \sin(\omega t + \frac{2\pi}{3}) \end{bmatrix} \cdot \begin{bmatrix} \mathbf{X}_a \\ \mathbf{X}_b \\ \mathbf{X}_c \end{bmatrix} \quad (4.28)$$

In SPVWM the output voltage is described into 8 switching positions and these 8 vectors are represented by V1 –V8 and are called basic space vectors. But only six vectors are

used to provide the active output voltage. These vectors are from V1-V6. The vector V0 and V7 are located on the origin and supply no output voltage. The main reason for using the space vector pulse width modulation is to specify the reference voltage vector in a specific place as shown in Fig.4-18.

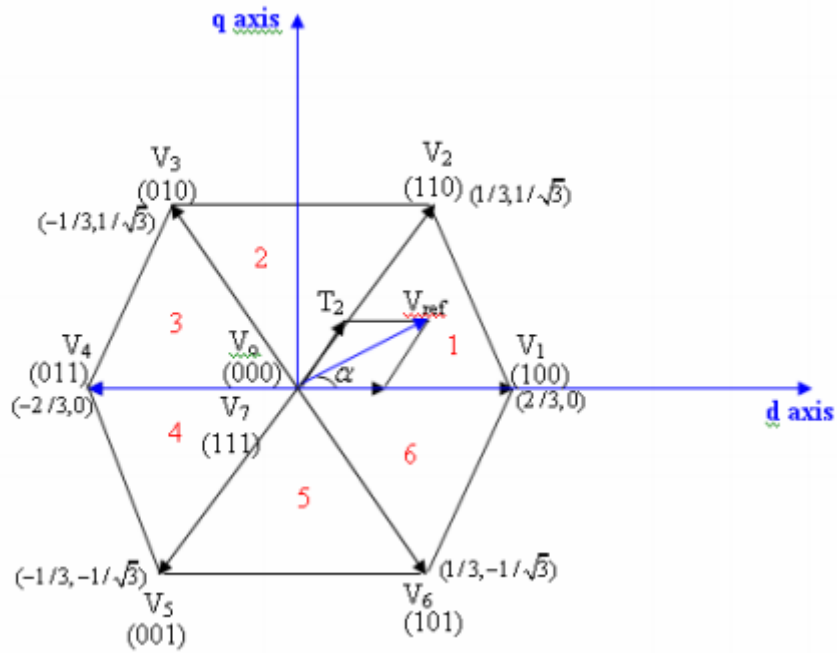


Fig.4-18: Switching Vectors [115]

Tab.4-1: Switching pattern applied by using this table.

NO of Vectors	S_a	S_b	S_c	V_{an}	V_{bn}	V_{cn}
V_0	0	0	0	0	0	0
V_5	0	0	1	$-\frac{V_{DC}}{3}$	$-\frac{V_{DC}}{3}$	$2\frac{V_{DC}}{3}$
V_3	0	1	0	$-\frac{V_{DC}}{3}$	$2\frac{V_{DC}}{3}$	$-\frac{V_{DC}}{3}$
V_4	0	1	1	$-2\frac{V_{DC}}{3}$	$\frac{V_{DC}}{3}$	$\frac{V_{DC}}{3}$
V_1	1	0	0	$2\frac{V_{DC}}{3}$	$-\frac{V_{DC}}{3}$	$-\frac{V_{DC}}{3}$
V_6	1	0	1	$\frac{V_{DC}}{3}$	$-2\frac{V_{DC}}{3}$	$-\frac{V_{DC}}{3}$
V_2	1	1	0	$\frac{V_{DC}}{3}$	$\frac{V_{DC}}{3}$	$-\frac{V_{DC}}{3}$
V_7	1	1	1	0	0	0

The relationship between the voltage and time period T_0 , T_2 , T_1 , is described as [116]:

$$T_0 = \frac{T_s - T_1 - T_2}{2} \quad (4.29)$$

$$T_1 = \frac{2\sqrt{3}}{\pi} M T_s \sin\left(\frac{\pi}{3-\alpha}\right) \quad (4.30)$$

$$T_2 = \frac{2\sqrt{3}}{\pi} M T_s \sin \alpha \quad (4.31)$$

$$T_s = \frac{1}{f_s} \quad (4.32)$$

$$M = \frac{V^*}{V_{sixstep}} = \frac{V^*}{\frac{2}{\pi} V_{DC}} \quad (4.33)$$

The basic idea of space vector pulse width modulation is it sections the 2D plane into six switching states called sectors. Each sector is determined by the four active vectors. By applying these vectors the output voltage is larger than zero. The vectors 0 and 7 are inactive vectors. These two vectors are placed in the centre of circle. The reference voltage rotates in angular velocity which is the same as the frequency of desired AC voltage output. The rotating reference voltage is updated by scanning all sectors following the controller period at which calculation is updated.

IGBT switches are used in the rectification process. The voltage is generated from a wind turbine with varying wind speed. This technique applies the duty cycle to the switches and stabilises the output voltage. The upper switches generate the output voltage while the lower switches remain in the OFF state. Hence eight switching states are used to carry out the switching process. It can be implemented practically by using micro controllers, microprocessor or other digital control methods. The simulation of the space vector pulse width modulation is shown in Fig.4-19. SVPWM has lower switching losses due to varying of one state result in phase to neutral voltage every time. If further reduction is needed to reduce the switching losses then other techniques can be used along with SVPSW. It also shows better performance for higher switching frequency. Extra switching is removed for varying modulation indexes.

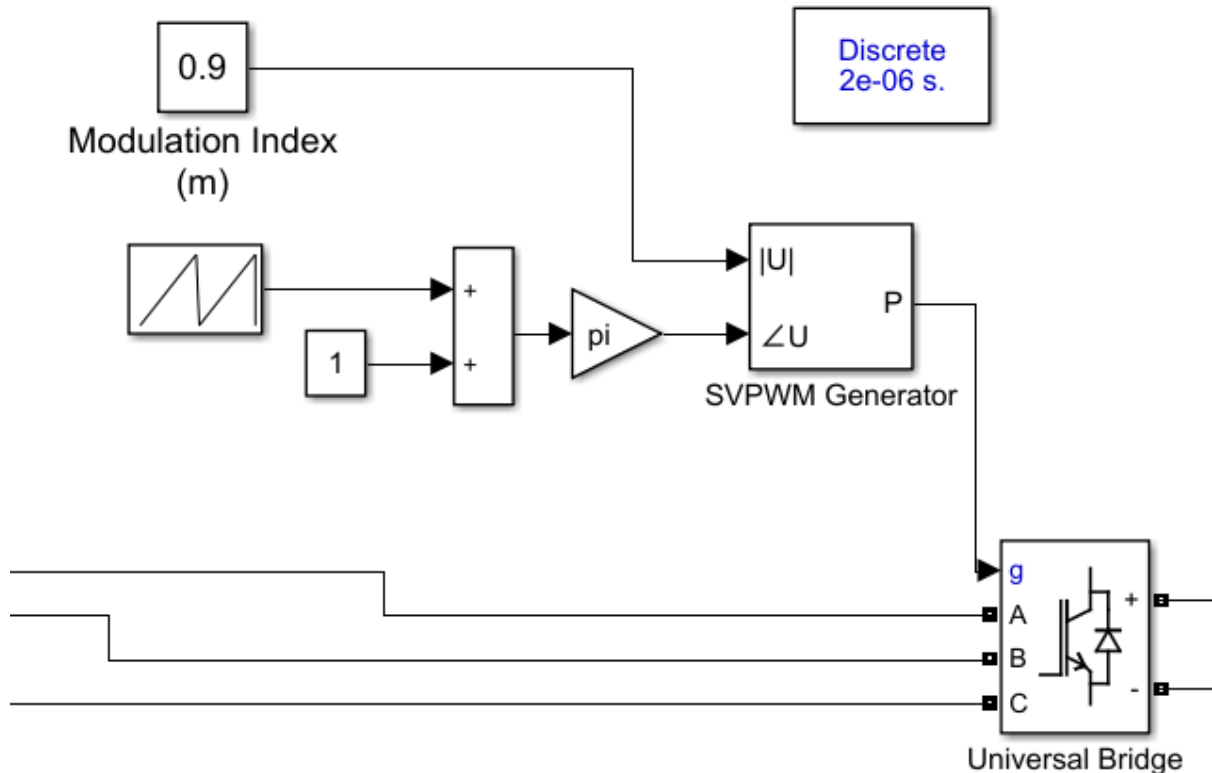


Fig.4-19: Simulation diagram of space vector pulse width modulation

The six step operation for voltage steps is shown in Fig.4-20. Space vector pulse width modulation is more complex than its equivalent sinusoidal pulse width modulation. It requires calculations of switching time period, determination of sector, vector segment calculations and region identification. The input of the rectifier is connected to the three phase permanent magnet source. Then this voltage is balanced by using space vector pulse width modulation. Space vector pulse width modulation is used to generate the pulses for the IGBT switches. By varying the width of the pulses the output voltage is varied. To boost the voltage, it is required to increase the ON time of the pulse. Its switching frequency can be adjusted suitably as it provides constant switching frequencies. Combination of eight ON and OFF states happens. The switching position of the lower section is inverted to the upper one. It can be implemented practically by using a digital signal processing board. But there are many areas that need to be considered to select the controller such as circuit complexity, frequency and speed parameters. The phase voltage is calculated for the combinations of these eight switching pattern and then converted into two phase vectors alpha (α) and beta (β). This transformation results in two zero vectors and six non- zero vectors. The non-zero vectors are V1 to V6. 60degree angle exists between any two non-zero vectors. The other two zero vectors are located at the origin. The circuit only allows positive voltage flow in the

rectification process and eliminates the negative power flow. Only upper switches are used to determine the output voltage which is s1, s3 and s5. Two switches cannot remain ON or OFF simultaneously. Negative voltage are represented as -1 and positive voltages as 1. The 0 represents the states of OFF switches. The switching configuration pattern is shown in the Fig.4-20.

The maximum voltages that can be received are as follows:

$$V_{ph \max} = \frac{V_{dc}}{\sqrt{3}} \quad (4.34)$$

$$V_{11mzx} = V_{dc} \quad (4.35)$$

The r.m.s phase to phase follows as

$$V_{ph \text{ rms}} = \frac{V_{dc}}{\sqrt{6}} \quad (4.36)$$

$$V_{11 \text{ rms}} = \frac{V_{dc}}{\sqrt{2}} \quad (4.37)$$

The eight switching pattern is shown in Fig.4-20.

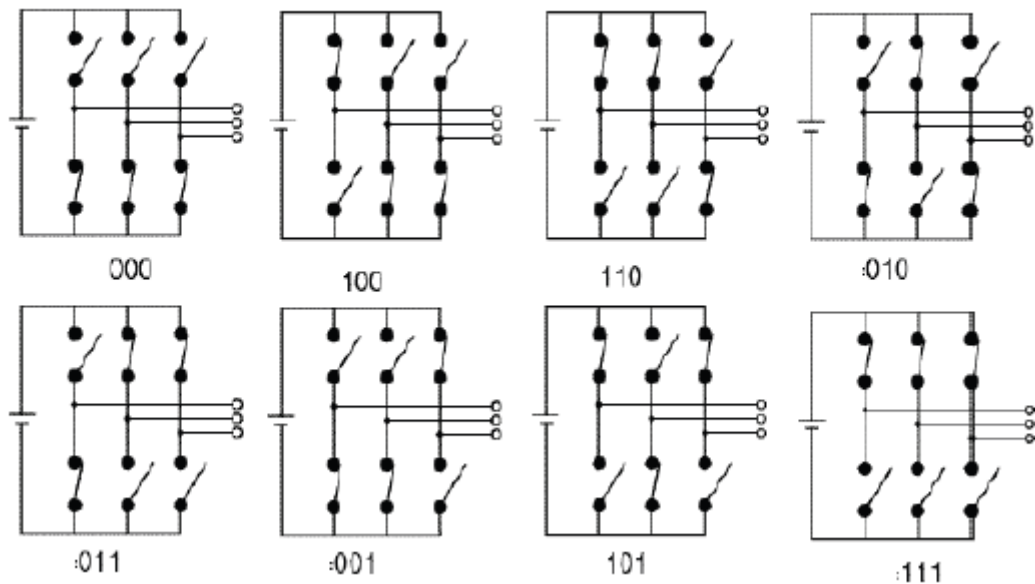


Fig.4-20: Vector rotation for space vector pulse width modulation [117]

The vector which rotates across the space is called the reference voltage vector. It rotates with angular velocity = $2\pi f$. Switches turn ON and OFF when the reference vector passes through each sector. One cycle completes after the reference voltage vector completes one revolution. The other zero and non-zero vectors are stationary vectors and do not rotate in space.

4.7 Simulation Results and analysis

Power flow on the micro grid is investigated by performing simulations of the proposed smart control system in MATLAB/SIMULINK as shown in Fig.4-21. The aim of implementing the control algorithm is to stabilise the power flow in fast changing environmental conditions such as varying irradiance, temperature and wind speeds, and the changing number of electric vehicles/type of batteries.

It is verified that the proposed control algorithm is operating correctly; that it increases the efficiency of the system by reducing the losses and by extracting maximum power from the solar/wind energy sources. The required energy is available on the micro grid constantly irrespective of variations in wind/solar energy. It has the capability to supply the required power to the EV charging station for the full 24 hour period. The controller senses the input voltage and current to generate the duty cycles to regulate voltage. The voltage flow recorded on the grid is 585VDC, as shown in Fig.4-22 (a-d). Oscillations are observed because of energy fluctuations in the inductance and capacitance in the converters/line and on the load side. It is observed that different inductors provide different load response. Higher inductance creates lower peak currents and reduces losses and improves the efficiency as shown in Fig.4-23. Secondly, the switching frequency of the IGBT switches affects the current flow on the micro grid. Higher switching frequency creates lower ripples in current and vice versa. The amount of power flow depends on the numbers of cars and type of batteries. The losses on the micro grid are recorded negligible due to short operation times and limited power flow. A spike in power flow is observed when charging up of converter components. Power flow on this grid is available constantly irrespective of variations in wind/solar energy. To remove the transients and harmonics from the micro grid transmission system; low pass filters are implemented which regulate the voltage and maintain the current level by reducing the voltage spikes. A bidirectional converter with control is placed between the DC micro grid and the battery bank which charges up and discharges the batteries by monitoring the power flow at the grid. Measurement tools are connected at every section of the micro grid to measure the power flow. The grid includes circuit breakers which are used

to protect the grid during short circuits and any other types of faults. This grid enables plug in electric vehicles to be directly connected to the micro grid. The main parameters are calculated by using typical sizes and types of conductor. If the rate of change of current is double or inductance increases to double than the induced e.m.f. also doubles in the line.

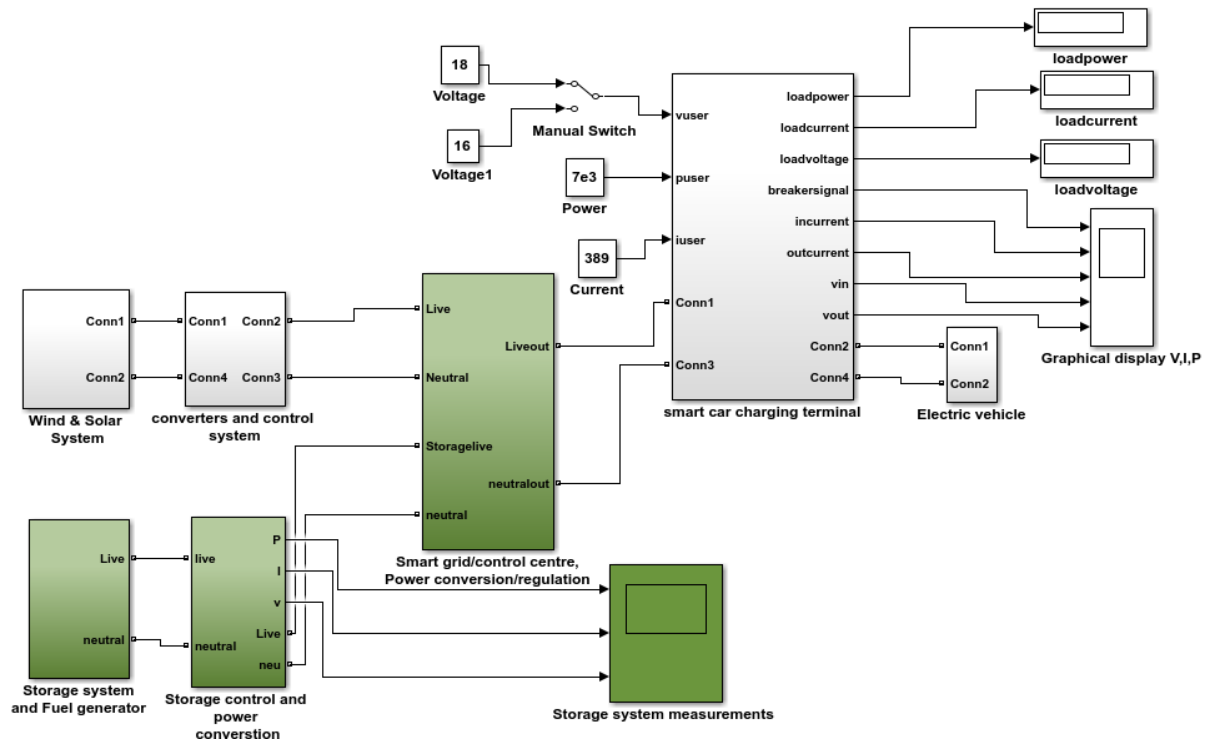
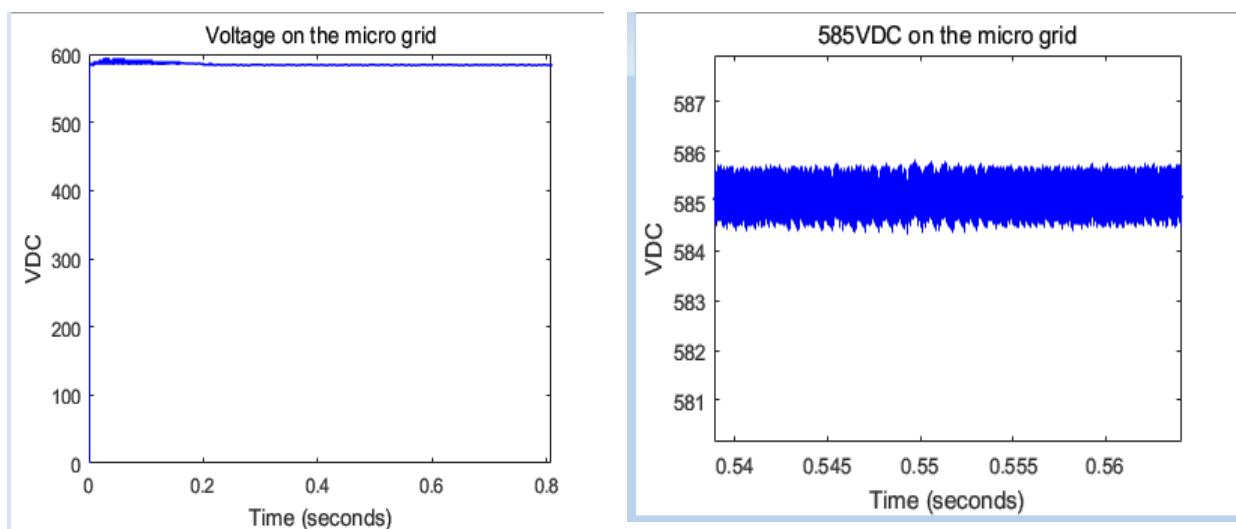
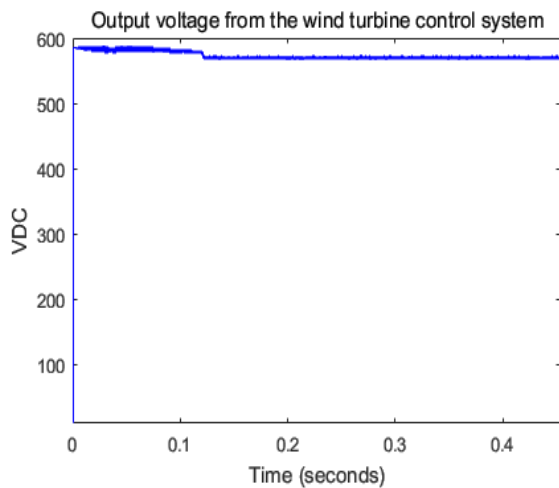


Fig.4-21. Simulation model to investigate control of the smart grid that connects wind/solar sources to the EV charging station.

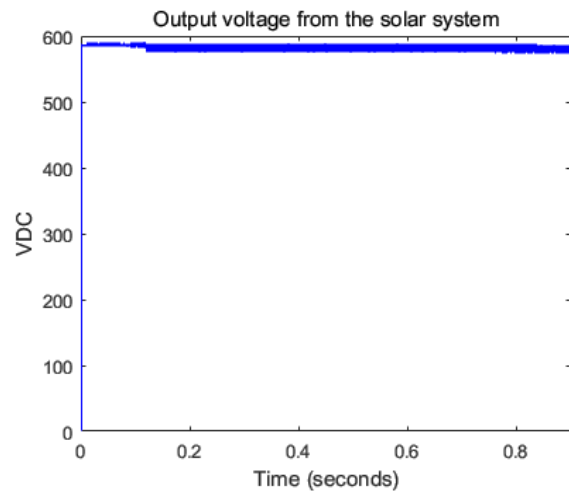


(a)

(b)

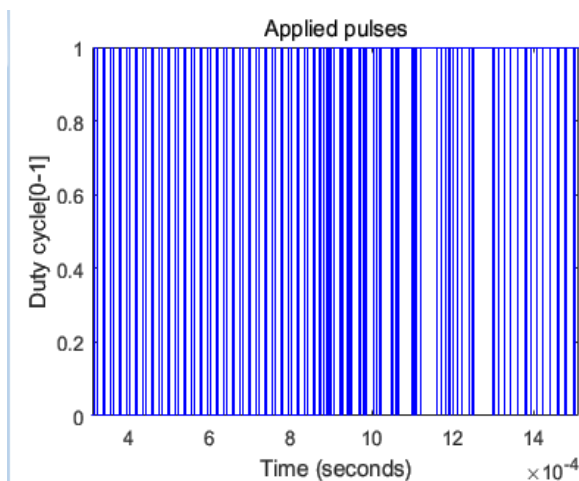


(c)

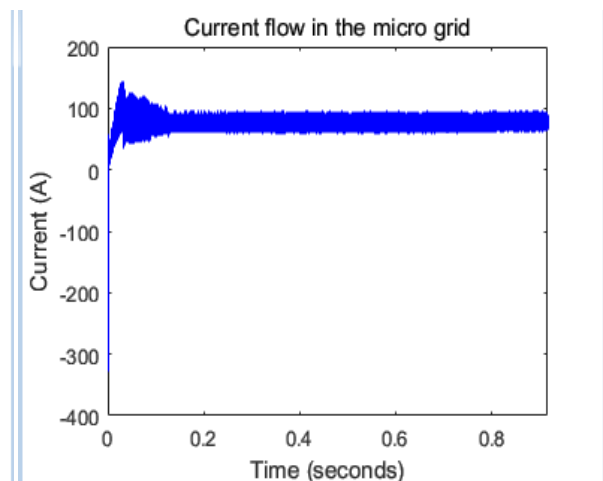


(d)

Fig.4-22: (a) Illustrates voltage regulation on the micro grid (b) Voltage output from the solar system (c) minor oscillations in the desired voltage on the micro grid (d) regulated DC voltage achieved at AC/DC power conversion station from the wind turbines



(a)



(b)

Fig.4-23: (a) Applied duty cycle to stabilise the fluctuating voltage from the wind and solar farms (b) Regulation of current flow in the micro grid

Summary

The aim of implementing the electrical control algorithm is to stabilise the power flow in the faster changing environmental conditions such as rapidly varying irradiance and wind speed. The efficiency of the control algorithm needs to be higher due to complexity of the algorithm for generating the correct duty cycle. It was verified that the proposed control algorithm was operating correctly. It increases the system efficiency by extracting maximum power from the energy resources. Less power losses and faster regulation in power flow was observed by

implementation of this method. For the first 0.03 seconds no power flow is observed and then constant power is flowing due to applying the control for the power flow. The controller senses the input voltage and current to generate the correct duty cycles to regulate voltage. The implementation of the Perturb and Observe method created oscillations in the desired voltage. The results were then analysed to check the effectiveness of the Incremental Conductance technique for the system. This method was found appropriate and more efficient than the MPPT algorithm but took longer to settle down to a constant level.

The Space Vector Pulse Width Modulation (SVPWM) technique was investigated to stabilise the power flow. It stabilises the output DC voltage and reduces harmonics to improve the power flow quality in the system. It successfully stabilises the unregulated voltage from wind turbine or solar panels by applying the correct duty ratio. The algorithm is more complex to implement than the method proposed in this chapter.

Chapter 5 Connection of Electric Vehicle Charging Station and Battery Storage to Smart Grid

Power flow in a grid is intermittent due to energy generation from the renewable energy solar/wind sources and varying loads at electric vehicle charging stations. A smart micro grid system and controller to regulate grid voltage and power flow has been proposed and investigated in earlier chapters. The algorithm to manage and control power is shown in Fig.5-1. The electric-vehicle charging station is considered to be fully operational. Four charging points with the total capacity of 103.50 kWh are connected to the micro grid terminal which is extracting energy from the wind/solar system. These representative charging points are commonly found in most EV charging stations in London. The proposed system has the capability to run the electric-vehicle charging station from wind/solar and storage system/fuel generators.

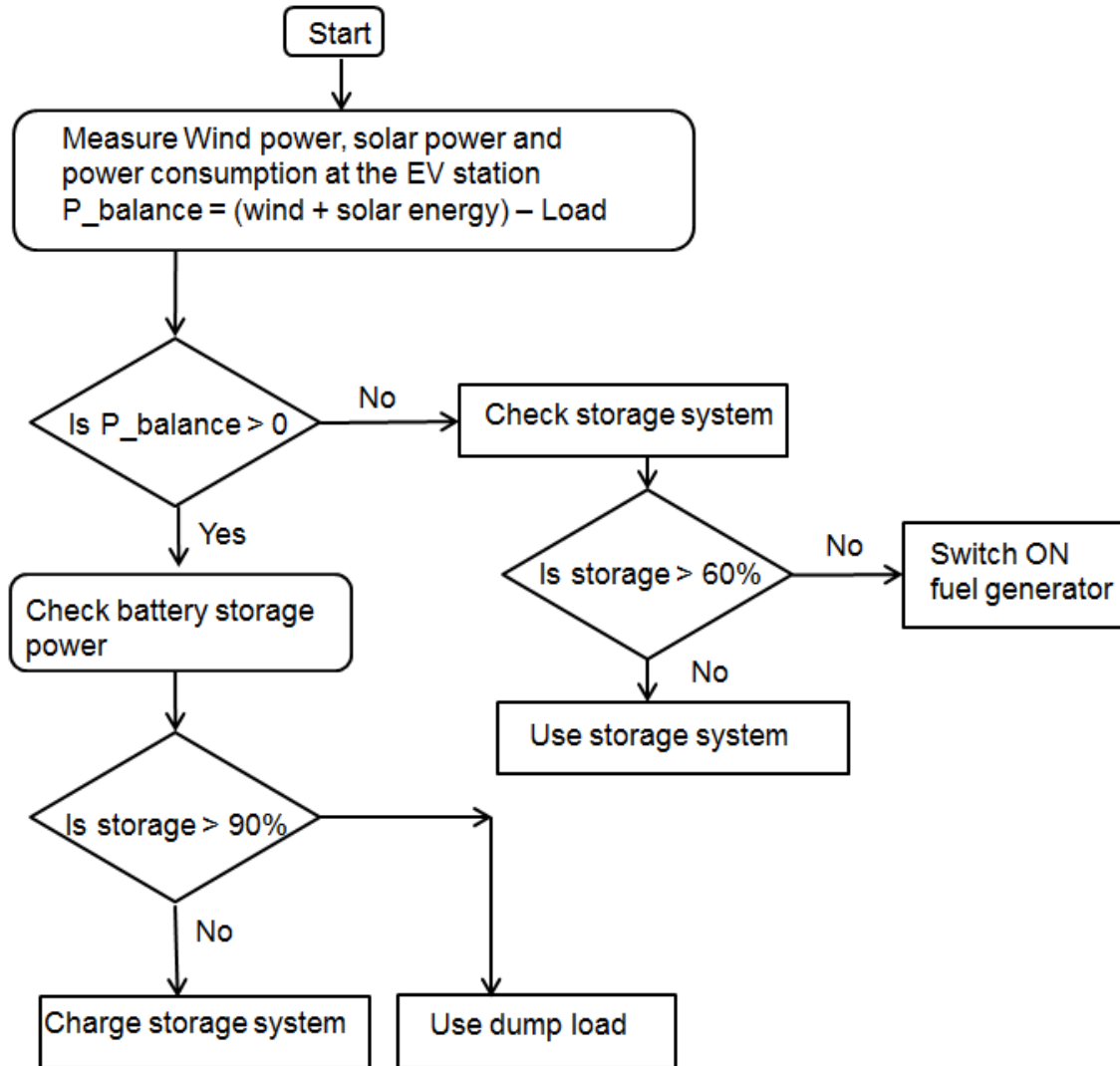


Fig.5-1: The system energy management algorithm.

Investigations are performed by comparing the energy generated by the wind turbines and solar units with the EV station and the losses in the converters/grid. The controller located at the micro grid and control centre measures the generated energy from the wind and solar system to compare with the load side. If the combined energy from the wind and solar system is more than the total energy consumption at the load side and the losses in the system, then it checks the charging of the storage system. If the storage system is less than 90% of the full capacity than it charges the storage units. The storage system is not charged if the wind/solar generated energy is less than or equal with the load on the micro grid. If the load on the micro grid is more than the total generated energy by the wind/solar system, then the storage system will be used to supply power to the micro grid. The nominal power generation capacity of the wind/solar energy sources are shown in Fig.5-2.

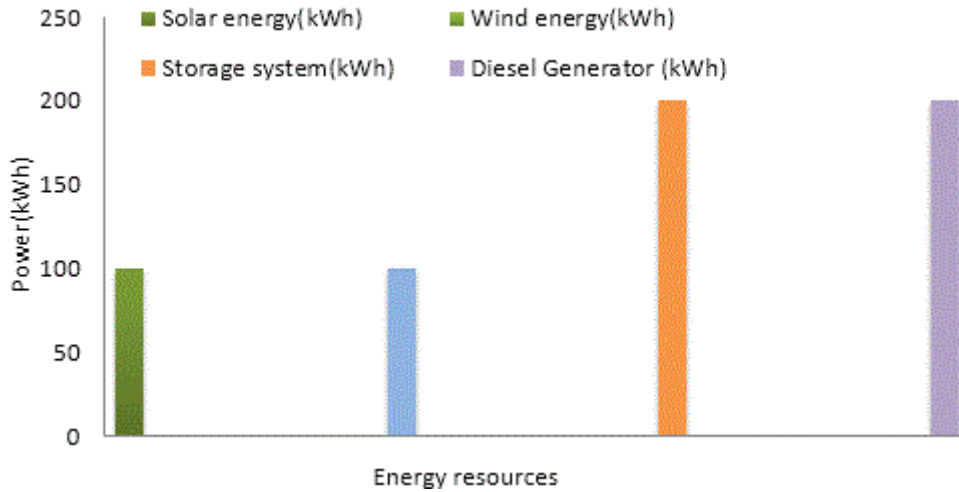


Fig.5-2: The energy sources connected to the micro grid

A 24-hour analysis is carried out to maintain the power flow on the micro grid. The energy generation pattern for a 24-hour period is shown in Fig.5-3 where the effects of temperature, irradiation and wind flow are illustrated. From 12am to 9pm, the energy generated is close to the nominal values. The fewer losses are due to temperature effects on the solar system and wind flow. From 9pm-5am, there is no solar energy generation due to irradiation effects on the solar system, but the wind units are still operational and generating the electrical energy. At this point (9pm-5am), the combined solar and wind energy is not enough to run the EV station during the peak times.

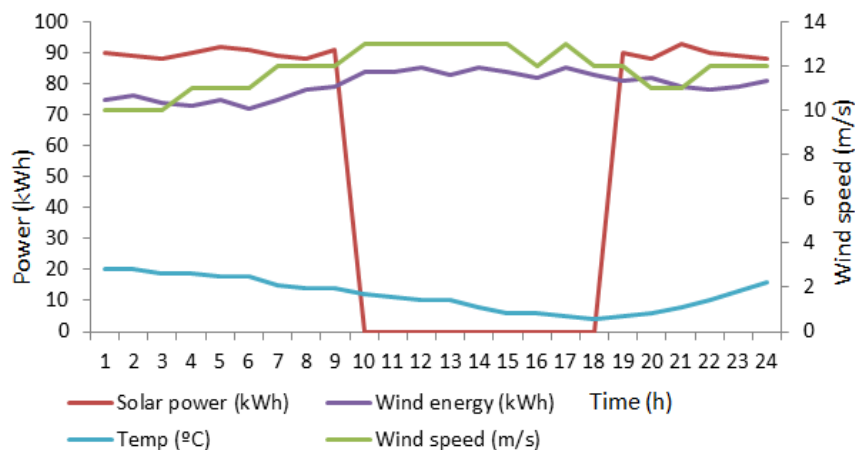


Fig.5-3: Energy generated by the solar/wind farms for a 24 hours' period

The battery storage system will be required to be operational from 9pm to 5am to balance the power on the micro grid because no energy is being generated by the solar system during this period. The storage system is connected to the DC micro grid by DC/DC bi-directional

converters and an electrical control system as shown in Fig.5-4. The storage system should have the capability to meet the energy demand at the electric-vehicle charging station during this scenario. The power is supplied by the storage system; initially the storage system is 200kW (fully charged) and then the storage energy reduces at 10pm when it is supplying power to electric-vehicle charging station. The fuel generator is switched ON from 2pm to 6pm to charge up the storage system after its storage capacity falls to 60%.

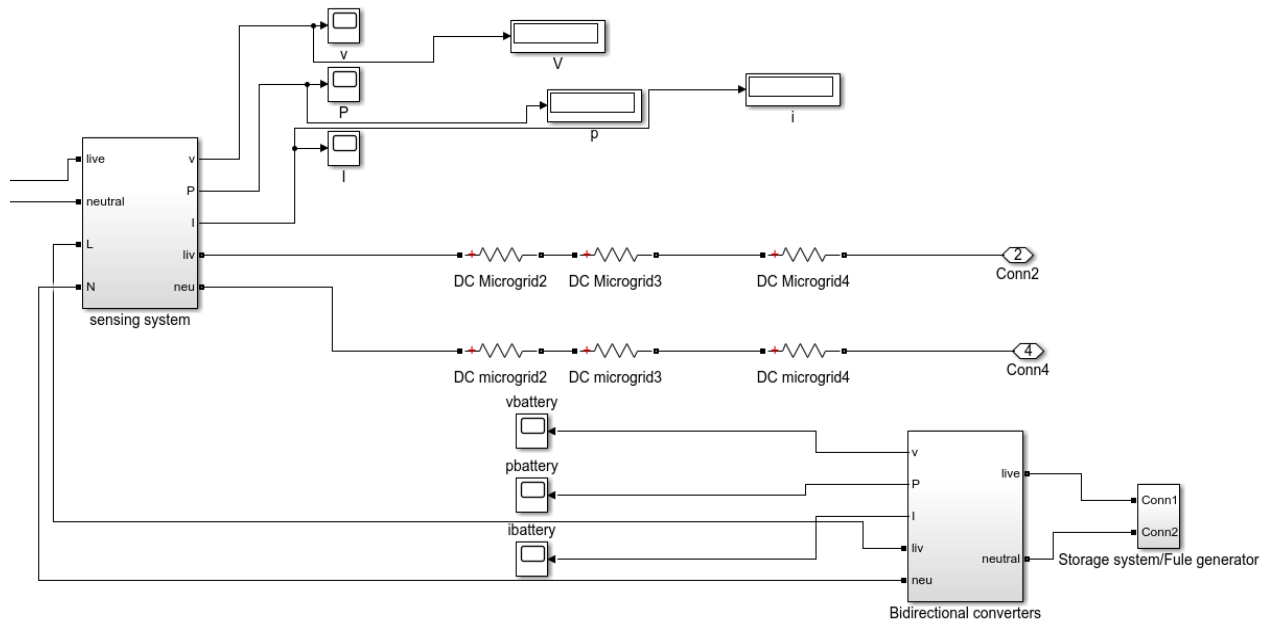


Figure 5-4: Microgrid connection with the storage system

The equation used to calculate the terminal voltage V_i at the storage system is given by [118].

$$V_i = V_0 + R_i \cdot I_3 - K \frac{Q}{Q_f i_3 dt} + A \cdot \exp\left(\int_0^t i_i dt\right) \quad (5-1)$$

Where, V_0 is the terminal voltage during open circuits, R_i is the storage system internal resistance, I_3 is the storage current, Q is the rated capacity of the storage system, and K is the polarisation resistance, and A is the exponential voltage. The controller is used to detect the voltage/power flow on the micro grid and then supply power from the storage system during power shortages as shown in Fig.5.5.

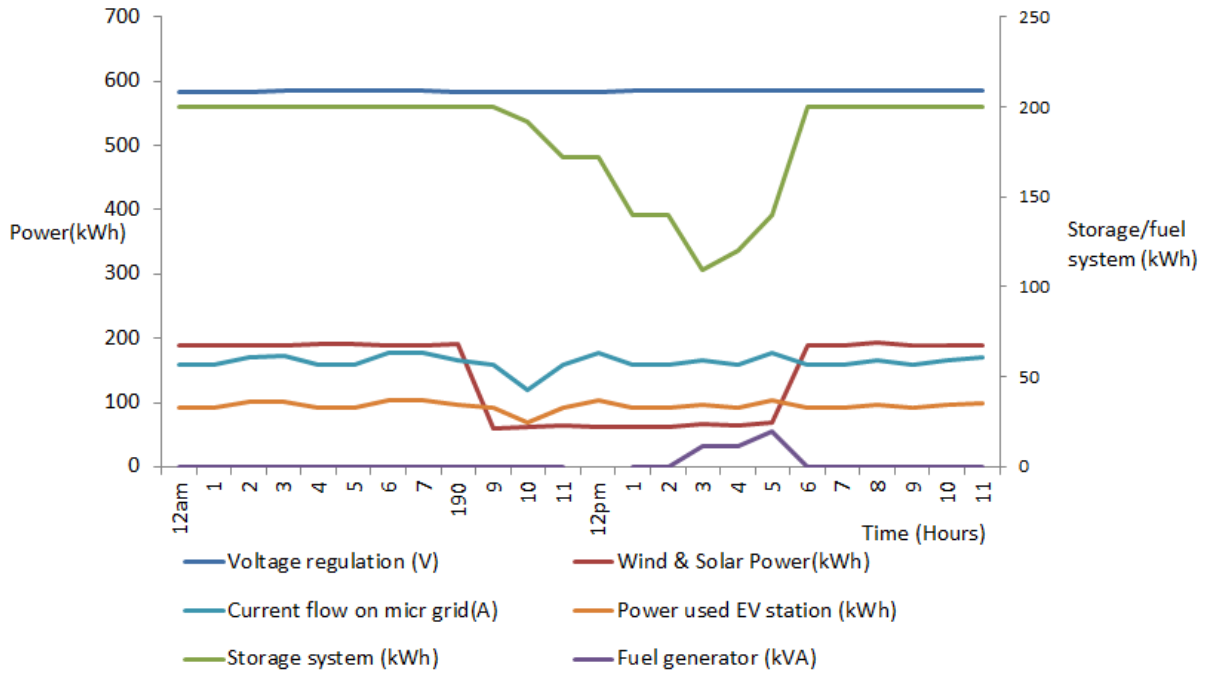


Fig.5-5: Energy management when EV is charging during the 24 hour period.

During the operational hours from 5am-9pm; the transmitted energy is received from the renewable energy resources (wind/solar) and the storage system is in standby mode at this point. The solar unit is fully operational and generating the maximum energy during this period and meeting the energy demands at the EV charging station. The comparison of the combined energy from the wind/solar with the EV charging station is shown in Fig.5-6 and at this stage several charging points are considered operational.

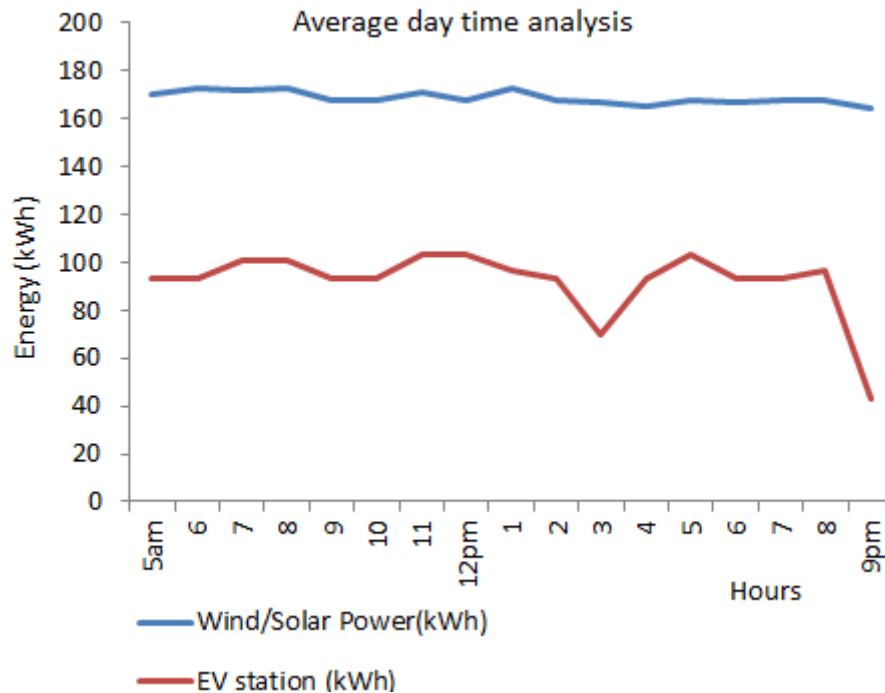


Fig.5-6: Graph showing that the wind/solar energy generation is capable of running the EV station independently from 5am-9pm.

5.1 Features of implemented electric-vehicle charging terminal

The machines in the electric vehicles are powered up by batteries but currently batteries take longer to charge up so an engine needs to be running to store power at the batteries and support the vehicles in the hills and to maintain speed [119]. To meet these requirements demands of the new technology investigated earlier and DC power flow is found most reliable and efficient for this task because it charges up batteries in very short time [120]. The energy can be stored quickly in the vehicle batteries at the car charging station and by means of regenerative breaking when the vehicles stop. DC power charging up also improves the efficiency of the power flow in electric cars by supplying the required power to the AC electric machines being used in electric or hybrid cars by means of converters

To investigate the power flow two scenarios are considered.

The simulation of electric-vehicle charging terminal that supplies controlled power to the electric vehicle is shown in Fig.5-7. Various voltage levels and nominal power can be attained at this terminal. It also makes the electric vehicle capable of charging up in a very short time. There are 15 charging points in the station as shown in Fig.5-8, with the total

power consuming capacity of 13.5kWh during the peak times. The total power consuming capacity of the individuals charging points is 3.5kWh, 7kWh, 43kWh, 50kWh.

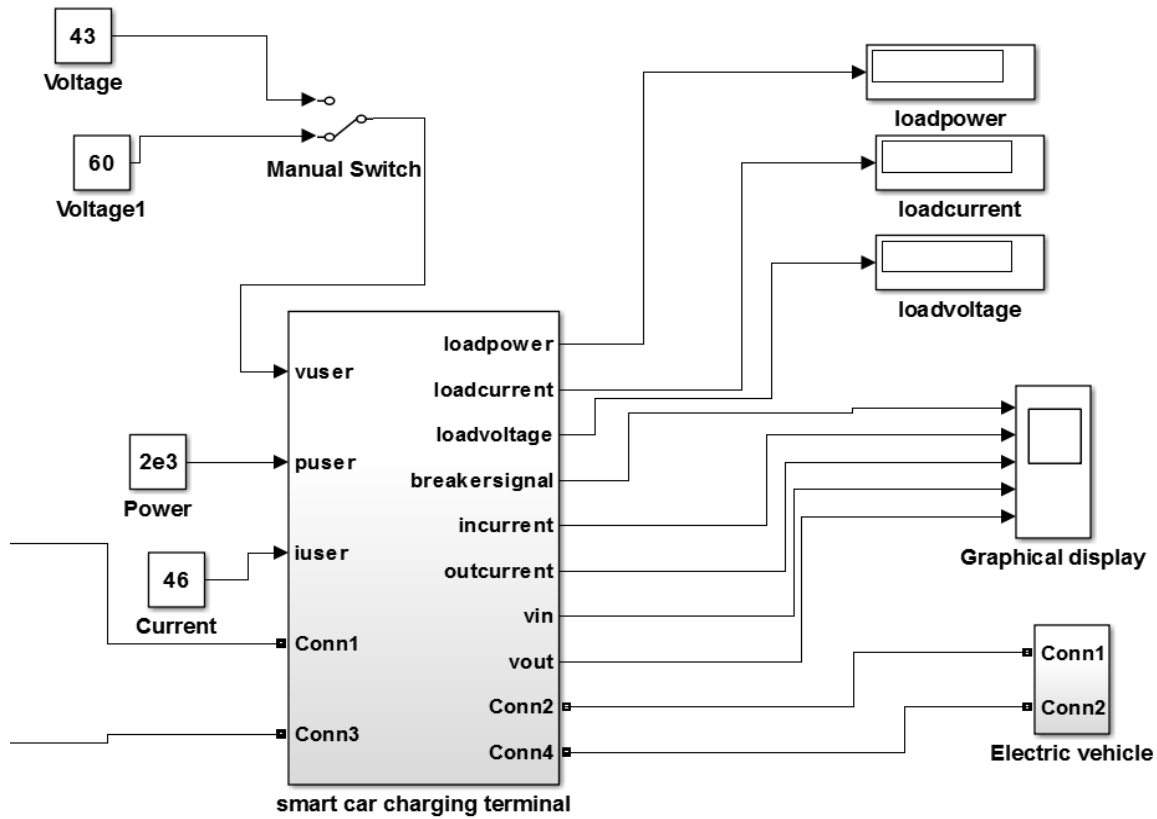


Fig.5-7: The smart vehicle-charging terminal where an electric vehicle is charging up and showing the smart measurement display

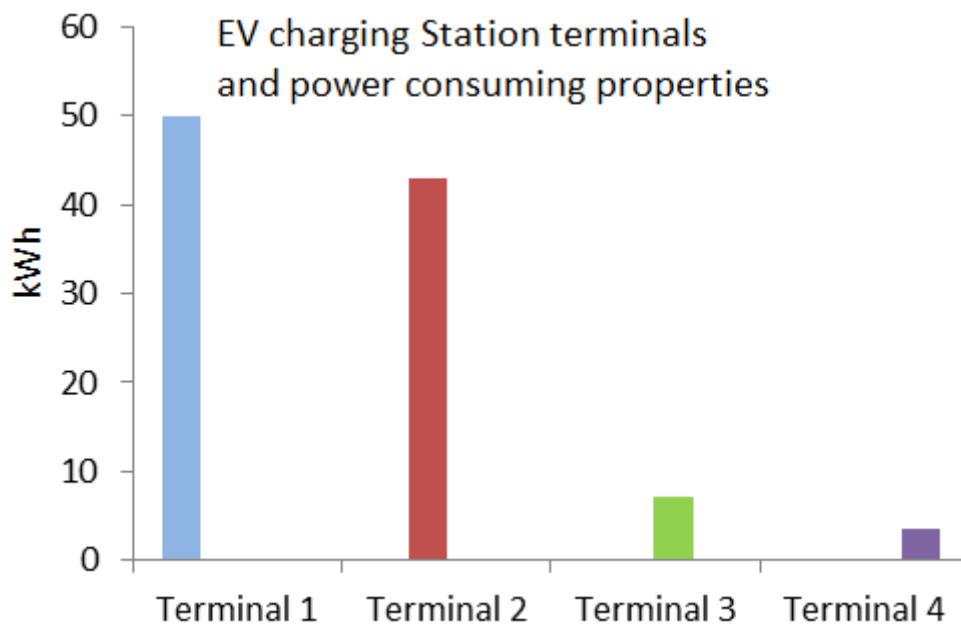


Fig.5-8: Operating features of the Electric-vehicle charging station

5.2 Optimal design and energy management at the electric-vehicle charging station

1. Renewable energy units are operating at full capacity (Best case scenario)
2. Renewable energy units are not operational and batteries are supplying power to the load (Worst case scenario).

5.2.1 Condition 1 best case scenario

Wind and solar farm are generating the electrical energy at the full capacity of 200kW and supplying it to electric-vehicle charging station. At this stage, micro grid is drawing no power from the storage system. This is the best scenario as transmitted energy is received from the renewable energy resources and the storage system is fully charged up at this point. Power flow varies due to variations of charging vehicles at the load side and the power flow is available constantly. The power losses on the grid in this case are very small due to the short length of conductors and full range of power availability on the grid. The power management on the micro grid is shown in Fig.5-9. It shows the power drawn by the electric-vehicle during the peak times and included the losses in the system are supplied by the renewable energy resources. In this case electric-vehicle charging station is considered fully operational and all the charging points are connected to the electric-vehicles. This scenario is more efficient than the other techniques because it increases the system efficiency by extracting maximum power from the wind and solar energy. Less power losses and faster regulation in power flow is detected by implementation of this scenario.

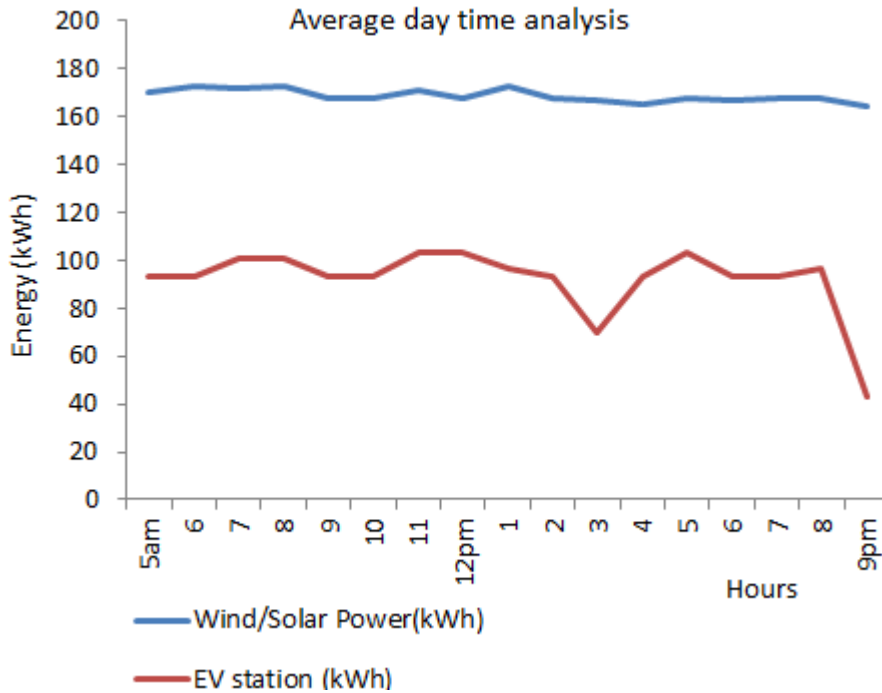


Fig.5-9: The wind/solar energy generation is capable of running the EV station independently from 5am-9pm.

Tab.5-1: The operating features for the electric-vehicle charging station.

Electric-vehicle charging point capacity	Voltage at the grid side(DC)	Voltage at the load side	Maximum current flow on the grid
3kW	585V	12V	5.1Ah
7kW	585V	12V	12Ah
43kW	585V	16V	73.5Ah
50kW	585V	16V	85Ah
Fully operational	585V	Variable	320Ah

5.2.2 Condition 2 worst case Scenario

In this case storage system is supplying power to the loads where wind and solar system are not considered to be generating any power. The battery storage system has the capability to meet the energy demands at the electric-vehicle charging station during the worst case scenario. A fuel generator is connected to the storage system, which turns ON by detecting the voltage and power storage capacity from the batteries. The generator is switched ON after storage system capacity falls below 60%. The electric-vehicle load is considered variable which means that only a few charging terminals are operational at a time. The parameters of the storage system are stated as [121].

$$V_3 = V_0 + R_{P3} \cdot I_{P3} - K \frac{Q}{Q_f i_{P3} dt} + A \cdot \exp \left(\int_0^t i_{P3} dt \right) \dots \dots \dots (5-2)$$

Where V_3 is the terminal voltage of the storage system during functioning, V_0 is the terminal voltage during open circuits, R_{P3} is the storage system internal resistance, I_{P3} is the storage current, Q is the rated capacity of the storage system, and K is the polarisation resistance and A is the exponential voltage. The storage system is connected to the DC micro grid by DC/DC bi directional converters and an electrical control system. The controller is used to detect the voltage and the power flow on the grid and then supply power to the grid from the storage system during power shortages and charge up from the grid according to the requirements. The storage system regulates the power flow when the charging station is operated from the storage system and no power is received from the wind/solar energy units. The power availability on the EV charging station is shown in Fig.5-10.

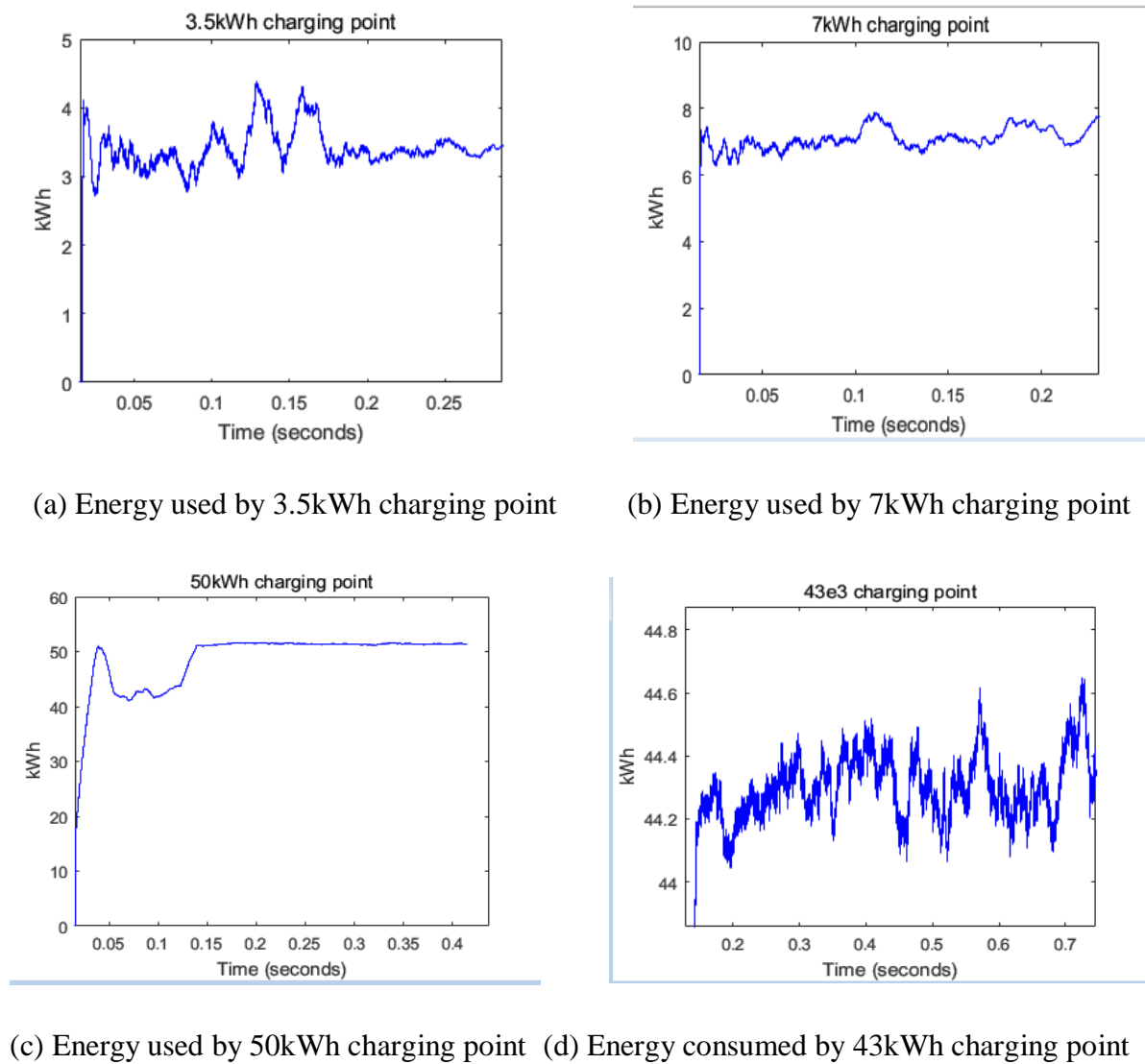


Fig.5-10: Power consumption at the electric-vehicle charging station

5.3 Electric-vehicles charging station characteristics

There are four EV charging points connected for this system. These charging points are associated with faster charging because of their connection with the higher DC voltage of 585VDC. The charging points consume 50kWh, 43kWh, 7kWh, 3.5kWh. The proportion is selected based on the charging points being installed in several places in the UK such as 2×50kWh and 1×43 in Toddington Dunstable on the M1 motorway and similar systems are installed in China town in London, Charter street Leicester and many other places in the UK [122]. Electric vehicle batteries take a long time to charge up. To obtain faster charging of EV batteries, a new high voltage DC power supply is investigated and found to be more appropriate to solve this issue. The investigated system has the features to supply the energy during peak/off-peak times at the EV charging station by means of solar and storage system connected as shown in Fig.5-11.

With the rapid increase in power consumption at the EV charging terminal, there are three issues linked with the storage/solar system:

- Quick energy supply from the storage system into the EV charging terminal
- Quick energy injection from the solar system to the charging station.
- Dynamic behaviour instead of long term serving capacity of the storage system

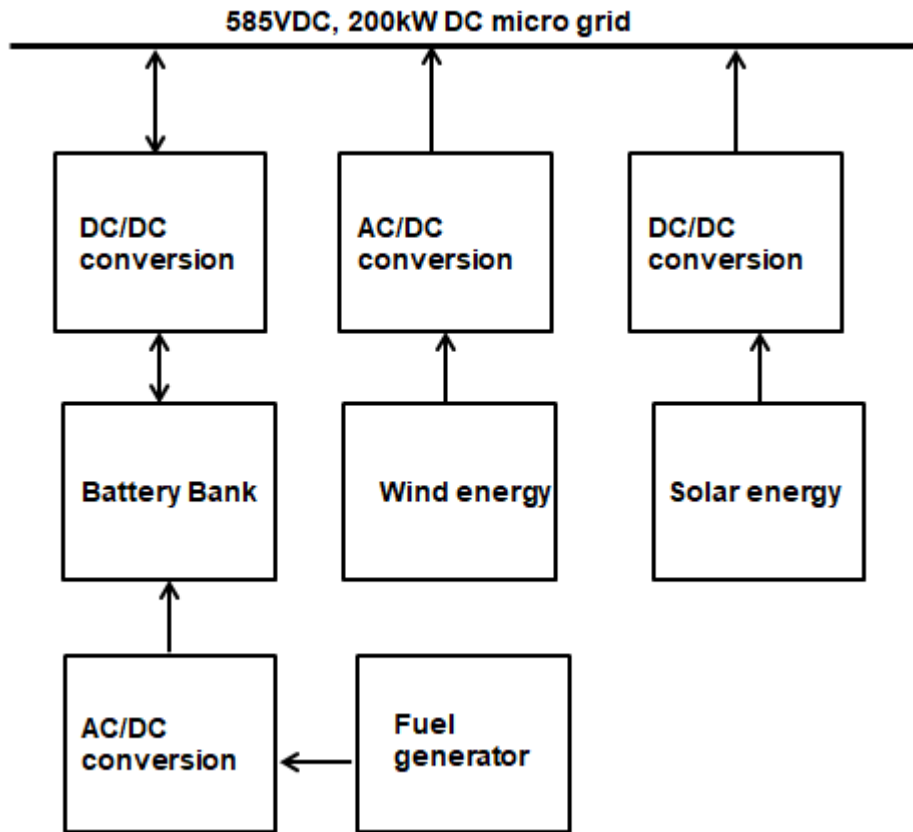


Fig.5-11: Energy sources connected to the micro grid by using power conversion system

5.4 Future implementaiton of ultra/super capacitors in Electric/hybrid vehicles

Super capacitors are more beneficial than standard storage batteries due to less weight, no harmful chemicals and can charge and discharge in seconds. Energy storage in capacitors depends on the size of metal plates and quality of material used for dielectric materials. By using better materials for the dielectric and larger metal plates, the energy storage capacity in capacitors can be increased. Super capacitors have two plates that are separated by a thin insulator made up of paper, carbon or plastic. Super capacitors are also called ultra-capacitors and are different from ordinary capacitors because their plates are much larger and very small dielectric distance exists between them. There plates are made of metal coated with a powdery charcoal substance which increases the charge storage capacity. They store larger energy in a short period of time as well. These are used as equivalent to energy reservoirs or flywheels. Super capacitors can also be used to regulate the power supply from the batteries. They can also smooth the power supply generated by solar or wind power braking in cars

when they stop. But super capacitors are limited to only a few volts, while ordinary capacitors are operational to higher voltages. The super capacitor was charged up from the car charging station terminal. Various voltage levels and nominal power were selected to view the effect of charging up on the micro grid. Capacitors improve the efficiency of the power flow in electric cars by supplying the required reactive power to the AC electric machines being used in electric or hybrid cars. In future super capacitors can replace lithium-ion batteries mostly used in electric or hybrid cars because lithium ion batteries store limited power and consume longer time for recharging.

Summary

It is noted when the solar/wind system is independently supplying power to the EV charging terminal then the storage system stays in off-mode. This is the best feature as energy demand is completely achieved by the renewable energy/solar system. This scenario has the capacity to meet the energy demands at the EV station during the Peak and off-peak times. In other case, the generated energy from the solar/wind system is charging up the storage system in peak times. In this case, the EV charging terminal is consuming the energy at full capacity. Then the storage system and fuel generator are meeting the energy demands at the EV charging station. At this point, the solar system is in off-mode and not generating any power. Fuel generator charges up the storages when energy level falls below 60%. Storage system degradation is normally measured by three main features, such as depth of discharge, temperature, and the conditions of charge. These three factors affect the performance of batteries used in the storage system.

Chapter 6 Conclusion and Future Work

The aim of this work was to develop an isolated smart micro grid connecting renewable energy sources and storage devices/ electric cars by stabilizing and controlling power flow in the grid to obtain an efficient power transmission flow. The power is to be transmitted to electric car charging stations where hybrid and electric car batteries charge up. The aim was achieved by simulating the proposed model on MATLAB and SIMULINK. The simulation results were compared with the mathematical formulation to examine the power efficiency.

A literature review has been performed in the renewable energy sector to discover a gap in the power transmission to the EV charging station. It was found that AC power transmission is not effective for charging up electric-vehicles because it takes long due to usage of high power electronic components. The grid based connections introduce harmonics, voltage transients and inrush rush in the National grid transmission system. A standalone DC microgrid was proposed to reduce the charging time for the electric-vehicles. In the DC microgrid system; several ranges of voltage were examined to find the suitable voltage for power transmission to the EV charging station. But the transmission of renewable energy for the standalone microgrid was challenging due to intermittent and randomness of energy generation and usage of power electronics components such as DC/DC converters.

Renewable energy interactions in smart grid ensure energy security, reduce carbon emissions and promote energy savings. For the renewable energy sector, wind and solar sources were chosen to generate electrical energy. A wind energy system was simulated with SIMULINK. In the wind energy system, electric power generation was not constant due to variable wind speed. This effect was minimised by using the doubly fed induction generator that gives constant voltage amplitude and frequency at varying wind speeds. In this generator only 30% of electric power was transmitted through the stator and was regulated by using power electronic components. Instability issues were investigated such as frequency issues, voltage transients and variations in rotor angle. Three methods were proposed to overcome the fluctuations and maintain stability in the wind energy generation unit. These are (a) the time domain method, (b) the equal criterion method and (c) the direct method.. A solar system was simulated to examine the efficiency of the PV module during the summer and winter season. Several parameters were investigated such as dust, temperature, and irradiation that impacted the energy generation from the solar system. It was noticed that the lower irradiation reduced the PV modules efficiency . The PV module showed better performance in the winters

compared to summer seasons showing the effect of heat in lowering efficiency. Dust on the PV module impacted the efficiency due to not receiving the required irradiation.

Architecture of a proposed smart DC microgrid was simulated to transmit the power in an efficient way. A master controller was included in the microgrid that created a communication network between power electronic converters, renewable energy system, storage system and the EV charging station. The controller has the features to predict minute-ahead, hour-ahead and day-ahead energy flow on the smart grid. A simulated sensing system enabled measurements from the simulation environment. The proposed smart grid manages the electric power during energy shortages by drawing power from a battery storage system and fuel generators.

Then an electrical power control system was included to regulate voltage from the DC/DC converters. The efficiency of the applied control algorithm was closer to nominal valuations. It regulated the output voltage and extracted maximum power from the solar system. It minimised power losses by removing the transients, harmonics and inrush current at the DC/DC converter station. Different types of electrical control algorithms were applied to investigate the voltage regulation such as maximum power point tracking algorithm and space vector pulse width modulation. In the maximum power point tracking algorithm; several sub-algorithms were tested such as incremental conductance, perturb and observe method, fix duty cycle and temperature methods. Incremental conductance was the best method for the stand alone wind/solar system because it operated at faster changing environmental conditions such as fluctuating wind speed/irradiation. Space vector pulse width modulation is also feasible but it takes longer to remove the transients from the system.

Conclusion

A smart DC micro grid has been proposed that connects fluctuating renewable energy sources such as wind and solar to electric vehicle charging stations on a grid that is separate from the national distribution grid. It avoids power flow issues such as transients, voltage reductions, harmonics and losses at the existing UK national transmission system. The smart grid includes energy storage systems to supply power to the grid during higher energy demands and when the renewable sources are not producing enough energy. The advantages of an independent DC micro grid are that it reduces charging time for electric and hybrid vehicles, has lower line losses due to shorter lengths and requires fewer power converters. Voltage regulation on the grid is achieved by measuring power flow at different points, implementing

a smart communication system to provide feedback signals to a control system. The control system applies the correct duty cycle to converter switches at a higher switching frequency at the buck converter station. Power fluctuations are minimised by applying filters following the mathematical modelling and simulation results. The proposed micro grid was analysed mathematically and simulated over a twenty-four-hour period to assess its voltage regulation capability with simulation performed with standard Simulink toolboxes. The desired voltage level of 585 VDC was attained at the car charging station and findings indicate an improvement of the voltage regulation efficiency to 99% and reduction of electrical power losses in the micro grid to 1%.

FUTURE WORK

- Several power system models have been investigated and tested to examine the results. The obtained research finding enhances the discussions by providing the initial findings to some aspects that requires further investigations. The direction of future work is to incorporate the communication system that should include a fast signal processing unit at the electric-vehicle charging station/smart grid to examine the energy flow from the renewable energy and storage system. This communication should be linked with the smart sensors that are implemented at several points such as DC/DC solar converter, DC/DC storage converters and at the grid. This will improve the protection for the EV charging terminal during the disturbances from solar/storage or at the converters.
- The smart grid uses digital components and communication so a cyber-security system is also an important aspect and needs to be investigated.
- The future work should be performed on the large scale of 100% renewable transmission.
- The standardization of the 100% renewable energy to the electric-vehicle charging station and vehicle-grid policies should also be incorporated.
- The electricity pricing for the electric vehicles in a time-varying pricing policy has to be implemented that allows the users to manage the use of electric power according to electricity prices.
- The vehicle-grid pricing also has to be set by taking the response from the consumers to achieve the better energy flow in the system.

References

- [1]. M. Sheng, D. Zhai, X. Wang, Y. Li, Y. Shi and J. Li, "Intelligent Energy and Traffic Coordination for Green Cellular Networks With Hybrid Energy Supply", IEEE Transactions on Vehicular Technology, 2017, vol-66, pp.1631-1646.
- [2]. C. Edwards, "The 100 per cent solution", Journal of Engineering & Technology, The IET, 2016, vol-11, pp.38-41.
- [3]. G. Parkes, C. Spataru, "Integrating the views and perceptions of UK energy professionals in future energy scenarios to inform policymakers", Energy policy, 2017, vol-104, pp.155-170.
- [4]. S. J. G. Cooper, G. P. Hammond, M. C. McManus and D. Pudjianto, "Detailed simulation of electrical demands due to nationwide adoption of heat pumps, taking account of renewable generation and mitigation", Journal of IET Renewable Power Generation, 2016, vol-10, pp.380-387.
- [5]. Y. V. Pavan Kumar, Ravikumar Bhimasingu, "Electrical machines based DC/AC energy conversion schemes for the improvement of power quality and resiliency in renewable energy microgrids", International Journal of Electrical Power & Energy Systems, 2017, vol-90, pp.10–26.
- [6]. M. Dubarry, A. Devie, K. McKenzie, "Durability and reliability of electric vehicle batteries under electric utility grid operations: Bidirectional charging impact analysis", Journal of Power Sources. 2017, Vol-358, pp- 39–49.
- [7]. Y. Shi, R. Li, Y. Xue and H. Li, "High-Frequency-Link-Based Grid-Tied PV System With Small DC-Link Capacitor and Low-Frequency Ripple-Free Maximum Power Point Tracking", IEEE Transactions on Power Electronics, 2016, vol-31, pp-328-339.
- [8]. K. Sarmila Har Beagam , R. Jayashree, M. Abdullah Khan, "A New DC Power Flow Model for Q Flow Analysis for use in Reactive Power Market", International Journal of Engineering Science and Technology, 2017, vol-20, pp.721-729.
- [9]. S. Kazemlou and S. Mehraeen, "Decentralized Discrete-Time Adaptive Neural Network Control of Interconnected DC Distribution System", IEEE Transactions on Smart Grid, 2014, vol-5, pp.2496-2507.
- [10]. M. Nijhuis, M. Gibescu and J. F. G. Cobben, "Application of resilience enhancing smart grid technologies to obtain differentiated reliability", IEEE 16th International Conference on Environment and Electrical Engineering (EEEIC), Florence, 2016, pp. 1-6.
- [11]. E. Jiménez, M. J. Carrizosa, A. Benchaib, G. Dammd, F. Lamnabhi-Lagarrigueb, "A new generalized power flow method for multi connected DC grids", International Journal of Electrical Power & Energy Systems, 2016, vol-74, pp.329–337.
- [12]. H. Liu and J. Sun, "Voltage Stability and Control of Offshore Wind Farms With AC Collection and HVDC Transmission", IEEE Journal of Emerging and Selected Topics in Power Electronics, 2014, vol-2, pp.1181-1189.
- [13]. A. Mohantya , M. Viswavandyaa, S. Mohantyb, P. K. Rayc, S. Patrad, "A New DC Power Flow Model for Q Flow Analysis for use in Reactive Power Market", International Journal of Electrical Power & Energy Systems, 2016, vol-20, pp.444–458.

- [14]. P. B. Kitworawut, D. T. Azuatalam and A. J. Collin, "An investigation into the technical impacts of microgeneration on UK-type LV distribution networks," 2016 Australasian Universities Power Engineering Conference (AUPEC), Brisbane, Australia, 2016, pp. 1-5.
- [15]. Statically press release by UK GOVT (UK energy statics), department of energy and climate change, Q130 June 2016, <https://www.gov.uk/government/statistics/energy-trends-june-2016>
- [16]. Utilising locally generated energy from renewable sources to fuel electrically powered vehicles, Berkshire Economic Strategy Board, Page 12, https://2Freport-for-berkshire-economic-strategy-board.pdf&usg=AOvVaw1hTz-ehGs7-Wkf9i1y_aCc
- [17]. EON Electro-mobility On the move with electricity, http://www.eon.com/content/dam/eoncom/en/downloads/e/EON_Elektromobil_ENG_final.pdf
- [18]. M. Nijhuis, M. Gibescu and J. F. G. Cobben, "Application of resilience enhancing smart grid technologies to obtain differentiated reliability," 2016 IEEE 16th International Conference on Environment and Electrical Engineering (EEEIC), Florence, 2016, pp. 1-6.
- [19]. Kenneth E. Okedu, Enhancing DFIG wind turbine during three-phase fault using parallel interleaved converters and dynamic resistor, IET Renewable Power Generation, pp 1211 – 1219, September 2016
- [20]. T. Mannen and H. Fujita, "A DC Capacitor Voltage Control Method for Active Power Filters Using Modified Reference Including the Theoretically Derived Voltage Ripple," in IEEE Transactions on Industry Applications, vol. 52, no. 5, pp. 4179-4187, Sept.-Oct. 2016
- [21]. J.Guan, B. Chen "Adaptive Power Management Strategy for a Four-Mode Hybrid Electric Vehicle". J.Energy Procedia. 2017, Volume 105, pp. 2403-2408.
- [22]. Y. Cao, Ryan C. Kroeze, Philip T. Krein "Multi-timescale Parametric Electrical Battery Model for Use in Dynamic Electric Vehicle Simulations", IEEE Transactions on Transportation Electrification, 2016, Vol.2, pp. 432 - 442
- [23]. WuShengjun, XuQingshan, YuanXiaodong , ChenBing " Optimal EV Charging Control Strategy Based on DC Microgrid", Journal of Energy Procedia, Vol 100, 2016, pp. 243-247
- [24]. L. Tan., B. Wu, S. Rivera, V. Yaramasu "Comprehensive DC Power Balance Management in High-Power Three-Level DC–DC Converter for Electric Vehicle Fast Charging". IEEE Transaction on Power Electronics. 2016, vol-31, pp-89-100.
- [25]. R. Salas-Cabrera, "On the real time estimation of the wind speed for wind energy conversion systems", IEEE international conference on electronics, communication and computers, Colula, Feb 2010, pp 237-241
- [26]. Shichao Liu, Peter X. Liu, Abdulmotaleb El Saddik, "Modeling and Stability Analysis of Automatic Generation Control Over Cognitive Radio Networks in Smart Grids" IEEE Transactions on Systems, Man, and Cybernetics: Systems, 2015, Vol-45, pp- 223 – 234.

- [27]. N.Phuangpornpitak, S.Tia, "Opportunities and Challenges of Integrating Renewable Energy in Smart Grid System", *Energy Procedia*, 2013, Volume 34, pp- 282-290
- [28]. Quang-ThoTran, Anh VietTruong , Phuong MinhLe "Reduction of harmonics in grid-connected inverters using variable switching frequency", *International Journal of Electrical Power & Energy Systems*, 2016, Vol-82, Pages 242-251
- [29]. J. Guan, B.Chen "Adaptive Power Management Strategy for a Four-Mode Hybrid Electric Vehicle". *J.Energy Procedia*. 2017, Volume 105, pp. 2403-2408.
- [30]. Yue Cao, Ryan C. Kroeze, Philip T. Krein "Multi-timescale Parametric Electrical Battery Model for Use in Dynamic Electric Vehicle Simulations", *IEEE Transactions on Transportation Electrification*, 2016, Vol.2, pp. 432 - 442
- [31]. WuShengjun, XuQingshan, YuanXiaodong , ChenBing " Optimal EV Charging Control Strategy Based on DC Microgrid", *Journal of Energy Procedia*, Vol 100, 2016, pp. 243-247
- [32]. L. Tan., B. Wu, S. Rivera, V. Yaramasu "Comprehensive DC Power Balance Management in High-Power Three-Level DC–DC Converter for Electric Vehicle Fast Charging". *IEEE Transaction on Power Electronics*. 2016, vol-31, pp-89-100.
- [33]. M. R. Miyazaki, A. J. Sørensen and B. J. Vartdal, "Reduction of Fuel Consumption on Hybrid Marine Power Plants by Strategic Loading With Energy Storage Devices," in *IEEE Power and Energy Technology Systems Journal*, vol. 3, no. 4, pp. 207-217, Dec. 2016.
- [34]. M.H. Mehdiabadi, J.Zhang, W. Hedman, "Wind Power Dispatch Margin for Flexible Energy and Reserve Scheduling With Increased Wind Generation" *IEEE Transactions on Sustainable Energy*, 2015, Vol-6, pp- 1543 – 1552
- [35]. D.Hdidouan, I.Staffell, "The impact of climate change on the levelised cost of wind energy" *Renewable energy Journal*, 2017, Vol-101, Pages 575-592.
- [36]. Rita T. Aljadiri, "Electrostatic harvester for wind energy harvesting and wind speed remote sensing", *IEEE conference on electrical and computer engineering*, Halifax NS, Feb 2015, pp 412-417
- [37]. S.Akdağ, Ö.Güler, "Alternative Moment Method for wind energy potential and turbine energy output estimation", *Renewable energy Journal*, 2018, Volume 120, pp- 69-77.
- [38]. M.Capellaro, "Prediction of site specific wind energy value factors", *Renewable energy, Renewable energy journal*, 2016, Vol-87, pp-430-436
- [39]. J.Pahasa, "Model predictive control-based wind turbine blade pitch angle control for alleviation of frequency fluctuation in a smart grid", *IEEE international conference on electrical engineering congress*, Chonburi, March 2014, pp 1-4
- [40]. S.Roy, "Maximum Likelihood Output Curve and Modal Bounds for Active Pitch-Regulated Wind Turbine" 2016, *IEEE Transactions on Sustainable Energy*, Volume-7, pp: 554 – 561
- [41]. A. C. Smith, R. Todd, M. Barnes and P. J. Tavner, "Improved Energy Conversion for Doubly Fed Wind Generators," in *IEEE Transactions on Industry Applications*, vol. 42, no. 6, pp. 1421-1428, Nov.-dec. 2006.

- [42]. B.Liu, F.Zhuo, Y.Zhu, H.Yi, System Operation and Energy Management of a Renewable Energy-Based DC Micro-Grid for High Penetration Depth Application, IEEE Transactions on Smart Grid, pp 1147 – 1155, December 2014
- [43]. Y.Errami, M.Ouassaid, M.Maaroufi, “Control of a PMSG based Wind Energy Generation System for Power Maximization and Grid Fault Conditions” Energy Procedia, 2013, Vol-42, pp-220-229
- [44]. R. Melício, “Behaviour of PMSG wind turbines with fractional controllers to a voltage decrease in the grid”, IEEE conference on power electronics machines and drives, Bristol, March 2012, pp 1-5
- [45]. A.Mudholker, P.M.Menghal, A.JayaLaxmi, “SVPWM Based Converter for PMSG Based Wind Energy Conversion System”, Procedia Computer Science, 2015, Vol-70, 2015, pp- 676-682
- [46]. V.Yaramasu, “A New Power Conversion System for Megawatt PMSG Wind Turbines Using Four-Level Converters and a Simple Control Scheme Based on Two-Step Model Predictive Strategy—Part II: Simulation and Experimental Analysis”, IEEE Journal of Emerging and Selected Topics in Power Electronics, January 2014, pp 3-13
- [47]. E. Okedu, Enhancing DFIG wind turbine during three-phase fault using parallel interleaved converters and dynamic resistor, IET Renewable Power Generation, pp 1211 – 1219, September 2016
- [48]. J. Usaola, “Transient stability studies in grids with great wind power penetration. Modelling issues and operation requirements”, Power Engineering Society General Meeting, IEEE, July 2003
- [49]. CFurlan, CMortarino, “Forecasting the impact of renewable energies in competition with non-renewable sources”, Renewable and Sustainable Energy Reviews, 2018, Volume 81, Pages 1879-1886
- [50]. S.Wang, “Virtual Synchronous Control for Grid-Connected DFIG-Based Wind Turbines”, IEEE Journal of Emerging and Selected Topics in Power Electronics, October 2015, pp 932-944
- [51]. S.Yang, “Unbalanced control system design for DFIG-based wind turbines”, IEEE conference power engineering and automation conference, Wuhan, Sept 2012, pp 1-4
- [52]. S.Lamichhane, “Influence of wind energy integration on low frequency oscillatory instability of power system”, IEEE conference on power engineering, September 2014, pp 1-5
- [53]. J. Xu, P.Kairu, Kanyingi, K.Wang, “Probabilistic small signal stability analysis with large scale integration of wind power considering dependence” Renewable and Sustainable Energy Reviews, 2017, Vol 69, pp- 1258-1270
- [54]. A.Rygg Årdal, T. Undeland, K. Sharifabadi, “Voltage and Frequency Control in Offshore Wind Turbines Connected to Isolated Oil Platform Power Systems”, Energy Procedia, 2012, Vol-24, pp 229-236
- [55]. T.Weckesser, Real-Time Remedial Action Against Aperiodic Small Signal Rotor Angle Instability, IEEE Transactions on Power Systems, January 2016, pp387-396

- [56]. F.Díaz-González, M.Hau, A.Sumper, “Coordinated operation of wind turbines and flywheel storage for primary frequency control support”, *International Journal of Electrical Power & Energy Systems*, 2015, Vol 68, pp- 313-326
- [57]. G. Kanabar, “Evaluation of Rotor Speed Stability Margin of a Constant Speed Wind Turbine Generator”, *IEEE conference on power system technology*, New Delhi, Oct 2008, pp 1-6
- [58]. J.Wang, D.Ahmadi, R.Wang, “Optimal PWM method based on harmonics injection and equal area criteria”, *IEEE Energy Conversion Congress and Exposition*, 2009, DOI: 10.1109/ECCE.2009.5316105
- [59]. Y. Liu, H. Hong, and A. Q. Huang, “Real-time calculation of switching angles minimizing THD for multilevel inverters with Step modulation”, *IEEE Trans on Ind. Elect.* vol. 56, no. 2, Feb 2009, pp. 285-293.
- [60]. Y.Zhao, W.Zhang, R.Liu, “A direct method to determine the stability of power systems during transients”, *Power and Energy Engineering Conference (APPEEC)*, 2016 *IEEE PES Asia-Pacific*, DOI: 10.1109/APPEEC.2016.7779889
- [61]. P.Kaya, C.K.Chanda, “Placement of wind and solar based DGs in distribution system for power loss minimization and voltage stability improvement”, *International Journal of Electrical Power & Energy Systems*, 2013, Volume 53, Pages 795-809
- [62]. H.Terzioglu, “A New Approach to the Installation of Solar Panels”, *IEEE conference information science and control engineering*, Shanghai, April 2015, pp 573-577
- [63]. D. Sinha, A. B. Das, D. K. Dhak and P. K. Sadhu, "Equivalent circuit configuration for solar PV cell," 2014 1st International Conference on Non-Conventional Energy (ICONCE 2014), Kalyani, 2014, pp. 58-60.
- [64]. Javid,M., Qayyum, A. (2014). Electricity consumption-GDP nexus in Pakistan: A structural time series analysis. *Energy Journal*, 64, 811-817.
- [65]. Ahmad,A., Saqib,A. M., Kashif, S . Yaqoob Javed, M., Hameed, A., Khan,U.M. (2016). Impact of wide-spread use of uninterruptible power supplies on Pakistan's power system. *Energy Policy*, 2016, Volume 98, pp 629-636
- [66]. Raza, A.S., Shahbaz,M., Nguyen, C.D. (2015). Energy conservation policies, growth and trade performance: Evidence of feedback hypothesis in Pakistan. *Energy Policy*, 80, 1-10
- [67]. Pickard, W. (2014). Smart Grids Versus the Achilles ‘ heel of Renewable Energy: Can the Needed Storage Infrastructure Be Constructed Before the Fossil Fuel Runs Out. *Proceedings of the IEEE*, 102(7)7, 1094-1105.
- [68]. Farrokhhabadi, M., et al. (2015). Energy Storage in Microgrids: Compensating for Generation and Demand Fluctuations While Providing Ancillary Services. *IEEE Power and Energy Magazine*, 15(5), 81-91.
- [69]. Das,I., Bhattacharya, K and Cañizares, C. (2017). Optimal Incentive Design for Targeted Penetration of Renewable Energy Sources. *IEEE Transactions on Sustainable Energy*, 5(4), 1213-1225.
- [70]. Sampaio, P., Orestes,M., González, A. (2017) Photovoltaic solar energy: Conceptual framework. 74, 590-60.

- [71]. Umrani. Z. (2017). Solar Energy: Challenges and opportunities in Pakistan. International Conference on Innovations in Electrical Engineering and Computational Technologies (ICIEECT). 1-1.
- [72]. Wakeel, M., Chen, B., Jahangir, S. (2016). Overview of Energy Portfolio in Pakistan. Energy Procedia, 88, 71-75.
- [73]. Rehman,W., Sajjad, I., Malik, T., L. Martirano., Manganelli, M. (2017). Economic analysis of net metering regulations for residential consumers in Pakistan. IEEE International Conference on Environment and Electrical Engineering and 2017 IEEE Industrial and Commercial Power Systems Europe (EEEIC / I&CPS Europe). 1-6.
- [74]. Qureshi, T., KafaitUllah., Arentsen,J. (2017). Factors responsible for solar PV adoption at household level: A case of Lahore, Pakistan. Renewable and Sustainable Energy Reviews. 78, 754-763
- [75]. Khaliq, A., Ikram A.,M. Salman.(2015) .Quaid-e-Azam Solar Power park: Prospects and challenges. Power Generation System and Renewable Energy Technologies (PGSRET). 1-6.
- [76]. Hussain, A., Rahman, M., Memon, J., (2016) . Forecasting electricity consumption in Pakistan: the way forward. Energy Policy, 90, 73-80.
- [77]. Abdullah., Zhou, D., Shah, T., Jebran, K., Ali, S., Ali, A. (2017). Acceptance and willingness to pay for solar home system: Survey evidence from northern area of Pakistan. Energy reports, 3, 54-60.
- [78]. Adnan,S., Khan,H., Haider,S., Mahmood,R. (2012). Solar energy potential in Pakistan, Journal of Renewable and Sustainable Energy. 4, 1–7.
- [79]. Farooqui, S. (2014). Prospects of renewables penetration in the energy mix of Pakistan. Renewable and Sustainable Energy Reviews, 29, 693-700
- [80]. Amer,M., Tugrul,U., Daim. (2011). Selection of renewable energy technologies for a developing county. Energy for Sustainable Development, 420-435
- [81]. Ahmed, A., Ahmed, F., Akhtar, W. (2009). Estimation of global and diffuse solar radiation for Hyderabad, Sindh, Pakistan. Journal of Basic and Applied Sciences. 5,73–79
- [82]. Ahmed, A., Ahmed, F., Akhtar,W., (2010). Distribution of total and diffuse solar radiation at Lahore, Pakistan. Journal of Scientific Research.37–43
- [83]. Mirza, K., Ahmed, N., Majeed,T., Harijan,K. (2007). Wind energy development in Pakistan. Renewable and Sustainable Energy Reviews. 2179–2190.
- [84]. Hara. S., Kasu.M., and Matsui, N. (2016). Estimation Method of Solar Cell Temperature Using Meteorological Data in Mega Solar Power Plant. IEEE Journal of Photovoltaics, 6(5), 1255-1260.
- [85]. Ilahi,T., Abid,M. (2015). Design and analysis of thermoelectric material based roof top energy harvesting system for Pakistan. Power Generation System and Renewable Energy Technologies (PGSRET), 1-3.
- [86]. Kaushik.S.C., Ranjan.K.R.,Panwar.N.L. (2013). Optimum exergy efficiency of single-effect ideal passive solar stills. Energy efficiency 6(3), 595–606

- [87]. Shaker, H., Zareipour, H and Wood, D. (2016). Estimating Power Generation of Invisible Solar Sites Using Publicly Available Data. *IEEE Transactions on Smart Grid*. 7(5), 2456-2465.
- [88]. Vadiiee, A., Yaghoubi, M., Martin, V., Bazargan-Lar, Y. (2016). Energy analysis of solar blind system concept using energy system modelling. *Solar Energy*.139, 297-308
- [89]. Villalba, A., Correa, E., Pattini, A. et al. (2017). Hot-cool box calorimetric determination of the solar heat gain coefficient and the U-value of internal shading devices. *Energy efficiency*, 10(6), 1553–1571.
- [90]. He, G., Chen, Q., Kang, C., and Xia, Q. (2016). Optimal Offering Strategy for Concentrating Solar Power Plants in Joint Energy, Reserve and Regulation Markets. *IEEE Transactions on Sustainable Energy*. 7(3), 1245-1254.
- [91]. Žandeckis, A., Kirsanovs, V., Dzikēvičs, M. et al. (2017). Performance simulation of a solar- and pellet-based thermal system with low temperature heating solutions. *Energy Efficiency*, 10(3), 729-741.
- [92]. Sultan, S., Ali, M., Waqas,A., Raza, H., Aziz, F., and Haq,S.(2016). Modelling of a solar energy driven water desalination system using TRNSYS. 19th International Multi-Topic Conference (INMIC) IEEE, 1-6
- [93]. Vivar, M., Fuentes,M., Castro, J., Pachec, G. (2015). Effect of common rooftop materials as support base for solar disinfection (SODIS) in rural areas under temperate climates. *Solar Energy*,115, 204-216.
- [94]. Ruoyang Du, Paul Robertson, “Cost-Effective Grid-Connected Inverter for a Micro Combined Heat and Power System”, *IEEE Transactions on Industrial Electronics*, 2017, Vol-64, pp-5360 – 5367.
- [95]. Y. T. Quek, W. L. Woo, T. Logenthiran “Smart Sensing of Loads in an Extra Low Voltage DC Pico-Grid Using Machine Learning Techniques”, *IEEE Sensors Journal*, 2017, Vol-17, pp-7775 – 7783
- [96]. N. Eghtedarpour and E. Farjah, "Distributed charge/discharge control of energy storages in a renewable-energy-based DC micro-grid," in *IET Renewable Power Generation*, 2014, vol. 8, no. 1, pp. 45-57, January 2014. doi: 10.1049/iet-rpg.2012.0112
- [97]. A. M. Nobrega, M. L. B. Martinez and A. A. A. de Queiroz, "Investigation and analysis of electrical aging of XLPE insulation for medium voltage covered conductors manufactured in Brazil," in *IEEE Transactions on Dielectrics and Electrical Insulation*, vol. 20, no. 2, pp. 628-640, April 2013.
- [98]. M.K.Kim, “Multi-objective optimization operation with corrective control actions for meshed AC/DC grids including multi-terminal VSC-HVDC, 2017”, *International Journal of Electrical Power & Energy Systems*, Volume 93, Pages 178-193.
- [99]. Yew MingYeap, NageshGeddada, AbhisekUkil, “Capacitive discharge based transient analysis with fault detection methodology in DC system”, *International Journal of Electrical Power & Energy Systems*, 2018, Vol-97, pp-127-137
- [100]. P Wang, XP Zhang, PF Coventry, R Zhang, “Control and protection sequence for recovery and reconfiguration of an offshore integrated MMC multi-terminal HVDC system under DC faults”, *International Journal of Electrical Power & Energy Systems*, 2017Volume 86, pp-81-92.

- [101]. Y. Wang, M. Yu and Y. Li, "Self-adaptive inertia control of DC microgrid based on fast predictive converter regulation," in *IET Renewable Power Generation*, 2017, vol. 11, no. 8, pp. 1295-1303.doi: 10.1049/iet-rpg.2016.0463.
- [102]. P. J. Liu, Y. M. Lai, P. C. Lee and H. S. Chen, "Fast-transient DC–DC converter with hysteresis prediction voltage control," in *IET Power Electronics*, 2017, vol. 10, no. 3, pp. 271-278.doi: 10.1049/iet-pel.2016.0382
- [103]. K. Ali, R. K. Surapaneni, P. Das and S. K. Panda, "An SiC-MOSFET-Based Nine-Switch Single-Stage Three-Phase AC–DC Isolated Converter," in *IEEE Transactions on Industrial Electronics*, vol. 64, no. 11, pp. 9083-9093, Nov. 2017.doi: 10.1109/TIE.2017.2701764
- [104]. N Rocha, CB Jacobina, EC dos Santos Jr, "Parallel single-phase ac–dc–ac shared-leg converters: Modelling, control and analysis", *International Journal of Electrical Power & Energy Systems*, vol- 61, pp-27-38, 2014
- [105]. Weerachat Khadmun, Wanchai Subsingha, "High Voltage Gain Interleaved DC Boost Converter Application for Photovoltaic Generation System", *Energy Procedia*, vol 34, pp-390-398, 2013
- [106]. X. Liu, P. K. T. Mok, J. Jiang and W. H. Ki, "Analysis and Design Considerations of Integrated 3-Level Buck Converters," in *IEEE Transactions on Circuits and Systems I: Regular Papers*, vol. 63, no. 5, pp. 671-682, May 2016.doi: 10.1109/TCSI.2016.2556098
- [107]. H.Mashinchi, E.Babaei, "Mathematical modeling of buck–boost dc–dc converter and investigation of converter elements on transient and steady state responses", *International Journal of Electrical Power & Energy Systems*vol-44, Issue 1, Pages 949-963,2013.
- [108]. Vahid Samavatian, Ahmad Radan, "A high efficiency input/output magnetically coupled interleaved buck–boost converter with low internal oscillation for fuel-cell applications: Small signal modeling and dynamic analysis", *International Journal of Electrical Power & Energy Systems*, vol-67, pp-261-271, 2015
- [109]. H. Yuan, X. Yuan and J. Hu, "Modeling of Grid-Connected VSCs for Power System Small-Signal Stability Analysis in DC-Link Voltage Control Timescale," in *IEEE Transactions on Power Systems*, vol. 32, no. 5, pp. 3981-3991, Sept. 2017.doi: 10.1109/TPWRS.2017.2653939
- [110]. C. Sun, J. Zhang, X. Cai and G. Shi, "Voltage balancing control of isolated modular multilevel dc–dc converter for use in dc grids with zero voltage switching," in *IET Power Electronics*, vol. 9, no. 2, pp. 270-280, 2 10 2016. doi: 10.1049/iet-pel.2015.0409
- [111]. H Bounechba, A Bouzid, H Snani, A Lashab, "Real time simulation of MPPT algorithms for PV energy system", *International Journal of Electrical Power & Energy Systems*vol-83, pp-67-78, 2016
- [112]. T. Selmi, M. Abdul-Niby, L. Devis and A. Davis, "P&O MPPT implementation using MATLAB/Simulink," 2014 Ninth International Conference on Ecological Vehicles and Renewable Energies (EVER), Monte-Carlo, 2014, pp. 1-4. doi: 10.1109/EVER.2014.6844065

- [113]. F. Pulvirenti, A. La Scala, D. Ragonese, K. D'Souza, G. M. Tina and S. Pennisi, "4-Phase Interleaved Boost Converter With IC Controller for Distributed Photovoltaic Systems," in *IEEE Transactions on Circuits and Systems I: Regular Papers*, vol. 60, no. 11, pp. 3090-3102, Nov. 2013
- [114]. M.Valan Rajkumar, P.S.Manoharan, A.Ravi, "Simulation and an experimental investigation of SVPWM technique on a multilevel voltage source inverter for photovoltaic systems", *International Journal of Electrical Power & Energy Systems*, vol- 52, pp-116-131, 2013.
- [115]. W. Wang, B. Zhang and F. Xie, "A Novel SVPWM for Three-Level NPC Inverter Based on m-Modes Controllability," in *IEEE Transactions on Industrial Electronics*, vol. PP, no. 99, pp. 1-1.doi: 10.1109/TIE.2017.2787583
- [116]. L. Liu, X. Deng, J. Lu, J. Sun and F. Yuan, "Constant frequency hysteresis-SVPWM current control method for active power filter," *IECON 2017 - 43rd Annual Conference of the IEEE Industrial Electronics Society, Beijing, China, 2017*, pp. 158-163.doi: 10.1109/IECON.2017.8216031
- [117]. T. Mesbahi, N. Rizoug, F. Khenfri, P. Bartholomeüs and P. Le Moigne, "Dynamical modelling and emulation of Li-ion batteries–supercapacitors hybrid power supply for electric vehicle applications," in *IET Electrical Systems in Transportation*, vol. 7, no. 2, pp. 161-169, 2017. doi: 10.1049/iet-est.2016.0040
- [118]. S. R. Pulikanti and V. G. Agelidis, "Hybrid Flying-Capacitor-Based Active-Neutral-Point-Clamped Five-Level Converter Operated With SHE-PWM," in *IEEE Transactions on Industrial Electronics*, vol. 58, no. 10, pp. 4643-4653, Oct. 2011.doi: 10.1109/TIE.2011.2106098
- [119]. J Y Yong, VK Ramchandaramurthy, KM Tan, "Bi-directional electric vehicle fast charging station with novel reactive power compensation for voltage regulation", *International Journal of Electrical Power & Energy Systems*, vol- 64, pp-300-310, 2015.
- [120]. P. Fan, B. Sainbayar and S. Ren, "Operation Analysis of Fast Charging Stations With Energy Demand Control of Electric Vehicles," in *IEEE Transactions on Smart Grid*, vol. 6, no. 4, pp. 1819-1826, July 2015.doi: 10.1109/TSG.2015.2397439
- [121]. F. Machado, J. P. F. Trovão and C. H. Antunes, "Effectiveness of Supercapacitors in Pure Electric Vehicles Using a Hybrid Metaheuristic Approach," in *IEEE Transactions on Vehicular Technology*, vol. 65, no. 1, pp. 29-36, Jan. 2016.doi: 10.1109/TVT.2015.2390919
- [122]. F. Machado, J. P. F. Trovão and C. H. Antunes, "Effectiveness of Supercapacitors in Pure Electric Vehicles Using a Hybrid Metaheuristic Approach," in *IEEE Transactions on Vehicular Technology*, vol. 65, no. 1, pp. 29-36, Jan. 2016. doi: 10.1109/TVT.2015.2390919